URBAN INFRASTRUCTURE NETWORKS:

FUNCTIONAL TOPOLOGY AND INTERDEPENDENCE

A Dissertation

Submitted to the Faculty

of

Purdue University

by

Christopher Klinkhamer

In Partial Fulfillment of the

Requirements for the Degree

of

Doctor of Philosophy

May 2019

Purdue University

West Lafayette, Indiana

THE PURDUE UNIVERSITY GRADUATE SCHOOL
STATEMENT OF DISSERTATION APPROVAL

Dr. Suresh Rao, Chair

Lyles School of Civil Engineering and Department of Agronomy

Dr. Daniel DeLaurentis

School of Aeronautics and Astronautics

Dr. Larry Nies

Lyles School of Civil Engineering

Dr. Satish Ukkusuri

Lyles School of Civil Engineering

Approved by:

Dr. Linda S. Lee

Head of the School Graduate Program

TABLE OF CONTENTS

Page

LIST OF TABLES

LIST OF FIGURES

Figure Page

Figure Page

ABSTRACT

Klinkhamer, Christopher Ph.D., Purdue University, May 2019. Urban Infrastructure Networks: Functional Topology and Interdependence. Major Professor: Suresh Rao.

Cities are composed of multiple interconnected, interdependent infrastructure networks. These networks are expected to continuously operate at near 100% of their designed service capacities. When the operation of just one of these networks is disrupted the effects are often not contained to a single network. How these networks function and interact is critically important in increasing urban community resilience when subjected to stochastic disruptions. Despite apparent differences in the physical qualities of both infrastructure and cities this work, uses principles of complex network analysis to reveal stunning similarities in the functional topology of infrastructure networks around the globe. Network based models are used to demonstrate how failures cascade between infrastructure networks. The severity of these cascades is shown to be influenced by population, design decisions, and localized variance within the larger infrastructure networks. These results are important for all design, maintenance, retrofitting, and resilience aspects of urban communities.

1. CITIES, SCALING, AND SELF-SIMILARITY

1.1 Introduction

Cities are dominant features of modern life, influencing how we live, how we move, how we interact, and our health [1–3]. The diversity of cities is evident, influencing our culture and imaginations [4]. In turn, cities themselves reflect design features influenced by disparate cultural, historical, governmental, regulatory, and climatic backgrounds [5–7]. The increased social and economic opportunities provided by means of economies of scale inherent to cities have driven a global migration of people from rural areas to urban [2, 8]. As the Rural-to-Urban migration continues and the unpredictable effects of global climate change begin to intensify throughout the next century, understanding how cities are composed, function, and are made to be sustainable and resilient will become ever more important [8].

Within cities in developed countries nearly every aspect of our lives and livelihoods depend upon the uninterrupted operation of multiple social, ecological, and technological systems (SETS) [9]. Each of these SETS are themselves comprised of an enormous number of discrete, independently managed networks [10]. The operation, or function, of these infrastructure networks is typically to facilitate flows of services, goods, people, or information. These networks are expected to continuously operate at near 100% of their designed service capacities and are so seamlessly interwoven and interdependent that we often fail to marvel at their complexity [11].

For example, the ability of road networks, designed to facilitate bidirectional flow of goods and people to and from all destinations, to properly function, they are dependent on a properly functioning electric grid to power the traffic signals controlling network flow. Pressure driven Water Distribution Networks (WDNs) are similarly dependent on the grid to power pumps that supply the pressure gradients necessary to drive the flow of water, in a mostly directed manner, from one (or a few) sources to all destinations, and the pow-

erplants generating the energy flowing on the grid are themselves dependent on properly functioning WDNs to provide cooling [10–12]. That these networks, so interconnected and interdependent, operate so consistently is simply astounding.

When the operation of just one of these networks is disrupted the effects are often not contained to a single network and the consequences may be far reaching or even catastrophic. In Florence Italy, 2016 a crowded thoroughfare collapsed rendering dozens of cars immobilized, trapped in a gaping hole in the earth, tourists seeking to visit popular attractions in the area were unable, and workers were incapable of getting to their places of business. The collapse was caused not by a deficiency in the roads construction, but by a leaking water distribution line below it. The flowing, unconfined water simply washed the roads foundation away. One year after the incident, the road was still not fully repaired, water was still being delivered through temporary pipelines constructed on the sidewalk, and total financial losses were estimated to exceed 30,000,000 USD [13]. These losses however pale in comparison to those faced as a result of disruptions often caused pursuant to extreme events.

In March 2011 a 9.0 magnitude earthquake in the Pacific Ocean sent a 15-meter tsunami racing toward the Fukushima Daiichi nuclear powerplant. Robust safety precautions allowed the plant to withstand the earthquake without any damage the resulting tsunami, however, breached existing countermeasures, severing the plants connection to the electrical power grid was lost, and rendering backup generators inoperable. With external electrical power unavailable cooling systems in three reactors were unable to run and prevent the cores from melting [14]. The result was one of the worst nuclear disasters in history, and the repercussions were felt around the globe. The financial, environmental, and social impacts were staggering. To prevent exposure radiation, over 100,000 Japanese citizens were displaced from their homes, although no lives have yet been lost due to radiation sickness, this prolonged displacement of local residents has resulted in over 1,000 deaths; the Japanese government estimated that the total economic costs of the disaster will exceed 180,000,000,000 USD; and as a result of public scrutiny following the disaster, planned nuclear expansions in multiple other countries were halted, fundamentally altering global energy supply portfolios and trade networks [15, 16].

Fig. 1.1. Collapse of a Florence, Italy road as a result of co-location induced spatial dependence of WDN and road networks. Photo: Washington Post, 2016 [13]

Understanding how SETS, and the networks they are comprised of, function and interact, the dependencies and interdependencies that exist within and between these networks, and how disruptions propagate from one network to another is a truly complex problem, characterized by unpredictability, and is not fully knowable [9–11, 17]. And yet the flawless operation of these networks is so vital that we term them critical infrastructure (CI). So im-

portant are these CI that we guard details of their construction, operation and management as matters of national security [18–20].

1.2 Scale-Invariant and Self-Similar Cities

Almost immediately upon entering downtown Manhattan, it is plainly obvious that the city, its buildings, its people, and their customs are all vastly different than what one would expect to find in West Lafayette, Indiana. Subject to, among others, constraints placed by topography, climate, and local regulations, cities take on very different structural and cultural identifies [5, 7, 17, 21, 22]. In addition to the variance existing between cities, they also change and evolve internally over time [1, 6, 7, 17]. a Londoner falling into a Rip Van Winkle-esque slumber in 1830 and awaking in the present day would be hard-pressed to describe what had become of her city. Reflecting design decisions influenced by new and evolving tastes, regulations, technologies and other factors, the city she knew when she went to bed would bare little resemblance to present experience. The manifold differences in the physical form and structure between cities in both time and place are obvious. They are so obvious that they barely deserve mentioning. And yet, in some ways, starkly disparate and highly complex cities can be remarkably similar and even predictable.

1.2.1 Scale-Invariance

Despite the apparent differences between and within cities, multiple structural and functional aspects of cities and city life have been shown to follow nonlinear scaling patterns [1, 2, 23–25]. Based on the assumption that the most important variable necessary to describe a city is its population, Bettencourt et al examine correlations between population size and multiple physical, economic and social attributes of cities and city residents [2,25]. Their analyses revealed universal relationships that could be used to model multiple attributes of the city and its residents based solely on population size. Importantly, these correlations were found found to be scale-invariant, following a relationship of the form:

$$Y(X) = Y_0 X^{\beta}, \tag{1.1}$$

Where Y is the city attribute of interest, Y_0 is a normalized constant, X is population and β is the scaling exponent, describing the relationship between Y and X. When arbitrarily scaling Equation 1.1 by factor Υ, such as:

$$Y(\Upsilon, X) = Z(\Upsilon, X)Y(X), \tag{1.2}$$

When Z in Equation (1.2) is dependent only on the value of Υ, such that:

$$Z(\Upsilon, X) = Z(\Upsilon), \tag{1.3}$$

Then equation (1.1) can be solved as:

$$Z(\Upsilon) = (\Upsilon^{\beta}), \tag{1.4}$$

Thus, $\beta = Y(\Upsilon X)/Y(X)$, becoming a dimensionless parameter, indicating that ratio between population and the attribute of interest, $\mathrm{Y}(\Upsilon, X)/Y(X)$ remains invariant with changes in population, X, being dependent only on the value of Υ. If the value of $\beta > 1$ the scaling relationship is said to be super-linear, indicating that the variable increases at a rate greater than would be expected by linear correlation. If the value $\beta < 1$ the relationship is said to be sub-linear, indicating that the variable grows at a slower rate than would be expected by linear correlation, this concept is commonly known as an economy of scale [2,25].

The idea sparked a wave of related research leading Bettencourt et al and others to show that given population alone one could with reasonable accuracy predict multiple attributes related to the city and its residents. Attributes such as the availability of super-creative employment, average wages, incidence of serious crime and the time spent stuck in traffic were found to increase super-linearly with increasing population [1,2,23,25]. Average walking pace was found to increase nearly linearly with population suggesting that small, slow cities grow-up to be large, bustling cities [25]. These studies cut through the inherent complexity and multitude of interacting, physical constraints, social norms and policy variables responsible

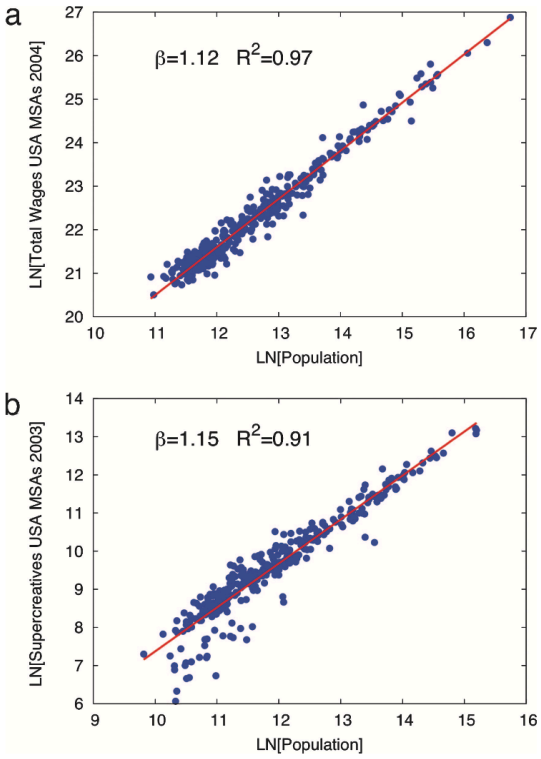

Fig. 1.2. Examples of scaling relationships for (A) Total Wages and (B) Super Creative Employment and city population. Figure from Bettencourt et al [25]

for producing these behaviors, revealing the beautifully simple universal relationships shown in Figure 1.2.

1.2.2 Self-Similarity

Self-similarity is a term describing the scale-invariance present in the structure (or function) of objects (or networks) when analyzed at different scales or hierarchies, a famous example of this concept being the structure of broccoli [26, 27]. As a head of broccoli grows it develops a hierarchical, branching structure. At all stages of growth new terminal nodes, possessing nearly identical properties, are generated, grow, and split into branches at regular intervals. New branches eventually fill the spaces between existing branches resulting in the familiar shape of a head of broccoli. Because the broccoli grew following a consistent, space-filling generative mechanism, characterized by the production of similar terminal nodes that grow and split at regular intervals, the structure of broccoli appears similar at all hierarchies. So a picture of a piece of broccoli broken off of a head would appear nearly identical to a picture of the head when printed at the same resolution, so too would the pictures of smaller and smaller pieces of broccoli until the head was broken down so small that the backbone of the network is destroyed and the structure is no longer recognizable [27]. Objects possessing these space-filling, self-similar, and scale-invariant properties are commonly referred to as fractals.

The scale-invariant and self-similar properties of fractals were famously extended to geographic objects by Mandelbrot through the thought experiment of measuring the coastline of Britain [28]. The basic concept being that if one were to measure a coastline with a ruler the obtained result would be entirely dependent on the chosen length of the ruler. A shorter ruler would be able to fit into smaller nooks and crannies of the rocks and land formations around the coast and the overall length would increase at a fixed ratio, following the same scaling relationship as Equations 1.4. Mandelbrot contended that real-world objects, possessing fractal properties, cannot be accurately described by smooth lines [28, 29]. They are irregular and the irregularity they exhibit is the same at any scale used to measure them.

The measure of this irregularity is referred to as its fractal dimension. A mostly smooth fractal object would have few irregularities and could nearly be described by a line, thus giving it a dimension near one, while a highly irregular object would nearly fill the two-dimensional plane it is measured in, and would thus have a fractal dimension near two [28].

In a similar vein, Batty and Longley utilized principals of fractal geometry to explore the spatial structure of cities, identifying universal, self-similar patterns among cities in their structure and boundaries. They found city structures and functions possess repeating hierarchical structures that were similar at neighborhood, district, and regional scales [5]. Batty further showed that as cities grow in time they exhibit space-filling properties consistent with the growth of fractal objects [6, 7]. They and others further extended this line of thought showing that infrastructure networks, such as the transportation networks, that form the backbone of cites are themselves fractal in nature [**?**, 1, 24, 30–33]. Following these initial contributions to the field multiple other studies have confirmed the scale-invariance of road networks around the world [23, 34] (See Appendices A, B, C, and E). Not only have road networks been shown to possess fractal properties, correlation of the fractal dimension of road networks (i.e. the area covered by roads) and population in the United States has been shown to be scale-variant [35]. Indeed, it has been well established that road networks exhibit fractal properties at all scales both in their form and in their function.

1.3 Networks: Form and Function

In recent years principles of graph theory and network science have emerged as a powerful tools for describing complex systems. Although the concept of describing physical and social systems and their dynamics (i.e. their function) as networks, comprised of nodes and links, has existed for centuries, the exponential increases in data access and computing power of the digital-age have facilitated the application of network science principles to a great many disciplines [17, 27, 36–41]. Today it is possible to analyze not only large networks, but also realistic, complex networks.

Watts and Strogatz are widely credited with expanding the application of network science principles to real-world networks by describing several important concepts [42]. Their 1998 publication introduced the concept of The Small World Phenomenon. Their work showed that multiple real-world networks are characterized by short average path lengths (i.e. one can travel between two nodes in the network by passing through a small number of links) and a high clustering coefficient (i.e. if a given node is connected to two others then those two nodes are very likely connected to each other as well), thus even very large networks can be traversed in very few steps (i.e. they are effectively small). Furthermore, Watts and Strogatz showed that common, existing network models, those of completely random graphs and regular lattices, were insufficient for describing real-networks.

A universal model that could describe most real-world networks was soon introduced by Barabasi and Albert [43]. They showed that the node-degree distribution (i.e. the statistical distribution of the number of links attached to each node in a network) typically followed a power-law distribution of the form:

$$p(k) = \alpha k^{\gamma} \tag{1.5}$$

Where k is the node degree, α is a normalized constant, and γ is the scaling parameter. Networks following this sort of regime are commonly referred to as scale-free, meaning scale-invariant. Scale-free networks are a special case of the Small World Phenomenon identified by Watts and Strogatz. Barabasi and Albert found that most real-world networks not only possess scale-free node-degree distributions, but also the scaling parameter, γ, was typically found to be in the range of $2 < \gamma < 3$. In addition, networks of this type could be created through a simple generative mechanism known as preferential attachment, wherein new nodes added to a network preferentially attach (i.e. form links) to existing high-degree nodes. Following the introduction of the Scale-Free Network Model, a plethora of real-world networks have been shown to possess heavy-tailed node-degree distributions approximating those of scale-free networks, though the statistical rigor necessary to make such characterizations has been a matter of frequent debate [17, 27, 34, 36–41, 44–48] (See Appendices A, B, C, E, and G).

Spatial networks, such as infrastructure networks however typically lack the broad range of node-degrees necessary to produce power-law node-degree distributions [44, 49, 50]. Physical constraints such as, in the case of road networks, the complexity of navigating an intersection of more than five or six roads and the amount space available to the network in cities, limit the quantity and types of links that can be made to a single node. The typical road network for instance has an average node-degree, $< k >$, of about four. Other infrastructure networks are similarly constrained. As a result, the maximum node-degree of infrastructure networks is typically in the single digits, resulting in peaked node-degree distributions [17, 49].

However, the subject of interest in analyzing infrastructure networks is typically how the network is used (i.e. its function). Functional aspects of a network can be introduced to the analysis by considering a dual representation of the network [51]. The dual representation of a network introduces the functional aspects of the infrastructure network by reclassifying how nodes and links are assigned. To that end the dual representation is simply an alternate construction of the network wherein nodes are defined as a set of continuous network features sharing similar attributes. For example, the ordinary, or primal, representation of a road network would consider each intersection as a node and each road segment as a link, but if we instead group together road segments based on some common attribute related to how we navigate through the city, such as road name or how sharply the road bends, and consider these grouped segments as nodes and each intersection as links, we introduce functional aspects of the network to its analysis [32, 32, 51, 52]. In this functional topology, the node-degree distributions of infrastructure networks may become much more broad.

1.4 Functional Topology of Urban Infrastructure

In the case of a road network the dual-representation represents mobility patterns and describes the knowledge necessary for one to traverse it [32, 32, 51, 52]. The dual representation, thus constructed introduces function to network analysis and has been referred to as the information space of the network [32]. In the in the dual-representation, high-

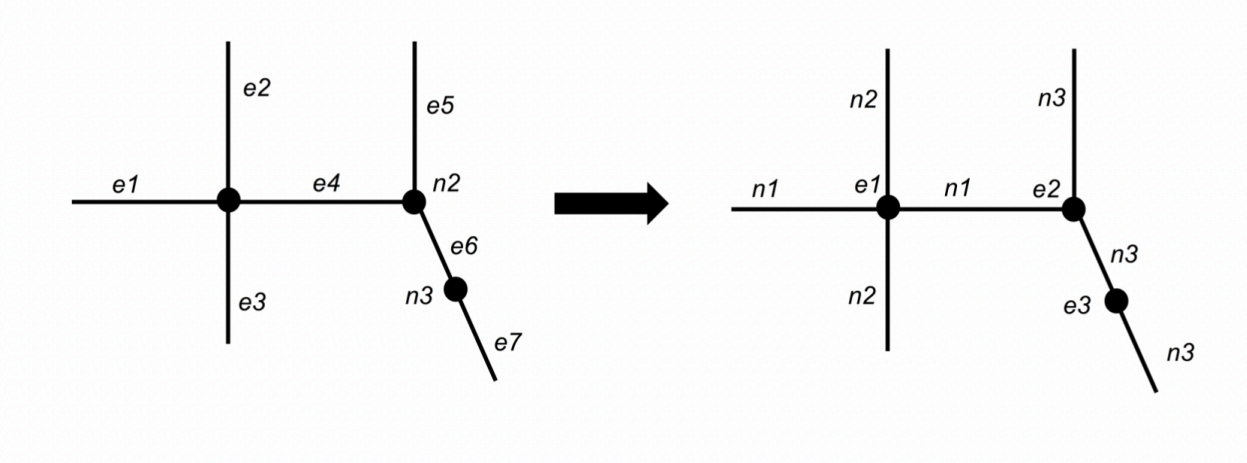

Fig. 1.3. In this example two network representations are produced from hypothetical road segments intersecting at three junctions. In traditional road network analyses (left) the junctions would be considered as nodes and each segment as a link. Here, the dual representation (right) is produced by the method intersection continuity negotiation (ICN) method, wherein segments are joined as continuous stretches of road if the angle between segments does not exceed some threshold value (45) and are considered as nodes, each junction is then considered as an edge.

degree nodes represent highly connected streets that can facilitate travel to a large number of destinations. In a Dual-UDN or Dual-WDN the node-degree distribution of the dual-representation, based on pipe diameter, describes the flow of water through the network with high-degree nodes representing collector pipes that drain or distribute water from/to large areas of the city [34, 46, 48, 53](See Appendices A and C). An example of the dual representation process is shown in Figure 1.3. Utilizing the dual representation, multiple studies have shown the functional topology of road networks around the world to possess broad node-degree distributions approximating those of scale-free networks [24, 32, 34, 48, 53] (See Appendices A and C).

1.4.1 Analysis of Sparse Networks

Klinkhamer and Segovia investigated the scale-invariance of highly aggregated WDN data for each of the 27 Brazillian state capitals [54]. WDN data for each capital were sourced from spatially-anonymous network flow diagrams, from the Brazilian ATLAS database . Network data available in infrastructure diagrams sources consisted of critical network components such as pumping stations, sources, reservoirs, and distribution zones aggregated to individual "super-nodes", with links representing all of the infrastructure necessary to connect these critical components. These aggregated data were used to construct the dual-representation of each WDN. The consistent aggregation of network features based on common criteria serving as the method of deriving the function-based dual-representation. Their analysis of the functional topology of these WDNs revealed heavy-tailed node-degree distributions with scaling components, γ, similar to those of roads. However due to the high level of aggregation, the average network contained fewer than 50 nodes. As a result statistically significant γ values could only be obtained for three larger WDNs shown in Table 1.1.

1.4.2 Convergence of Functional Topology

Other recent studies have utilized higher resolution infrastructure networks to investigate variance in the functional topology of WDNs and UDNs within cities. The first such study

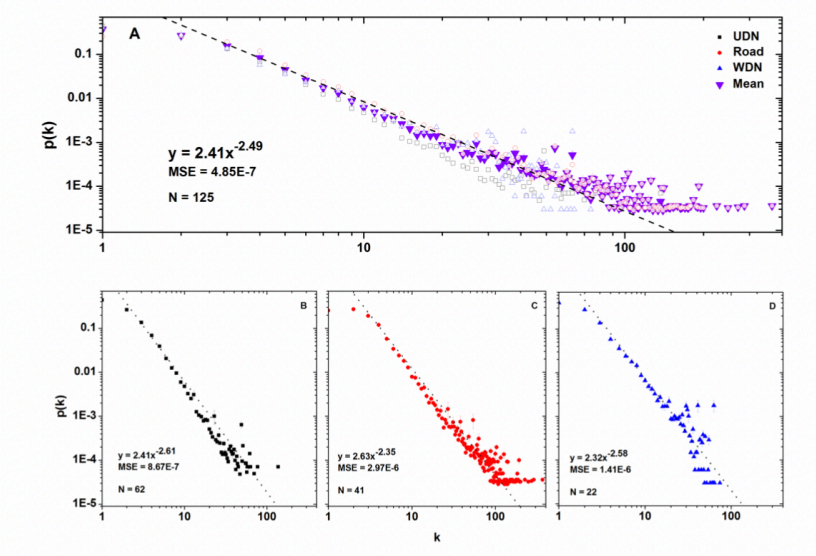

Fig. 1.4. (A) Mean p(k) (purple triangle; n = 125) of node-degree distributions (dual representation; n = 62) for all UDN (black square; n = 41) RN (red circle; n = 22), and WDNs (blue triangle (B) Mean p(k) of UDNs ; (C) Mean p(k) of RNs; (D) Mean p(k) of WDNs. Regression lines are shown for fits to Pareto probability density functions, $p(k) = \alpha k^{-\gamma}$, $k > 2$, with (A): $\alpha = 2.41$; $\gamma = 2.49$; $MSE = 4.85E-7$ (B): $\alpha = 2.41$; $\gamma = 2.61$; $MSE = 8.67E-7$ (C): $\alpha = 2.63$; $\gamma = 2.35$; $MSE = 2.97E-6$ (D): $\alpha = 2.32$; $\gamma = 2.58$; $MSE = 1.41E-6$. Tempering at the tails of the distributions is thought to be a rusult of averaging multiple distributions together and remains whether arithmetic or harmonic mean is used. Figure taken from Klinkhamer et al [34](See Appendix A)

Table 1.1.
Observed γ Values for Brazilian Selected Brazillian State Capital WDNs

City	**Nodes**	**Gamma**	**p-value**
Recife	131	2.59	0.05
Curitiba	52	2.55	0.05
Fortaleza	70	3.21	0.05

by Kruger et al showed that portions of the WDN and UDN of a large Asian city followed broad node-degree distributions resembling scale-free networks, and could be characterized by double-Pareto distributions, the tail of which converged to that of the trunk with increasing network size [48]. Klinkhamer et al subsequently found similar results for a large city in the Midwest, United States, showing that both the UDN as a whole and randomly selected subsections displayed broad node-degree distributions and could also be characterized by double-Pareto distributions [**?**].

Another recent study by Klinkhamer et al (See Appendix A) went further, investigating 125 UDN, WDN and road networks for 52 global cities with populations ranging from 5,000 to over 8,000,000 [34]. Klinkhamer et al showed that not only do Roads, UDNs, and WDNs display broad node-degree distributions resembling scale-free networks, but also that the scaling parameter, γ, of these networks converged to a single, universal value $\gamma = 2.49$ as network size, defined as the number of nodes in the network, increased. In addition the evolution of three urban infrastructure networks where shown to follow a generative mechanism termed spatially constrained partial preferential attachment. These findings suggest the existence of a universal scaling of functional topology for at least these three urban infrastructure network types [34].

2. FACTORS DRIVING CONVERGENCE OF FUNCTIONAL TOPOLOGY

2.1 Infrastructure Network Types

Just as individual cities are clearly different in multiple ways, so too do manifest differences exist between infrastructure network types. WDNs and UDNs facilitate the transport of water, while roads facilitate vehicular travel, the materials used to construct the network and the internal forces they experience differ, and their structures range from tree-like (UDNs) to nearly fully looped designs with multiple, redundant flow pathways (roads). These and other differences existing between infrastructure network types are summarized in Table 1. Despite these differences however, Klinkhamer et al, and others, have shown the functional topology of these disparate infrastructure networks to converge, following universal scaling-patterns [34, 48, 53, 55] (See Appendecies A, C, and E). This chapter discusses several contributing factors driving the convergence of the functional topology of infrastructure networks.

Table 2.1.: General Characteristics of Infrastructure Network Types. Modified from Klinkhamer et al [34]. (See Appendix A)

Attribute	**Road**	**Water Distribution**	**Urban Drainage**
Structure	Highly looped, cyclic graphs	Less looped, cyclic graphs	Typically branching, acyclic graphs

continued on next page

Table 2.1.: *continued*

Attribute	**Road**	**Water Distribution**	**Urban Drainage**
Evolution	Driven by demands for mobility. Constrained by availability of space and resource.s	Driven by increasing service demands. Placement constrained by road and building placement.	
Function	Full, bidirectional connectivity to all origins and destinations	Transport from one or few sources to all destinations. Loops for redundancy; valves for reliability	Branching/gravity driven from from multiple inputs to one or few destinations. Similar to rivers, but less space-filling.
Management / Maintenance	Disrupts flow of traffic	Requires closing valves or diversions, disrupting water or wastewater transport; may also result in traffic disruptions on roads due to co-location	

continued on next page

Table 2.1.: *continued*

Attribute	**Road**	**Water Distribution**	**Urban Drainage**
Reliability	Highly reliable but locally vulnerable to failures	Highly reliable, Isolation of network segments for repair means population impacted by disruption may be higher than roads	Reliable, high-tolerance to failures; Overcapacity conditions result in urban flooding

2.2 Infrastructure Network Evolution

Infrastructure networks evolve to meet the demands of the populations dependent upon them. Multiple studies have shown that the general pattern of road network evolution can be characterized by initial periods of expansion dictated by high-level concerns such as the need to expand services or connect to other, distant cities, after which continued network growth is dominated by densification of the network through self-organized local optimization strategies [1, 5–7, 17, 21]. The specifics of how this process plays out and the eventual physical form of a given city and infrastructure network are subject to the competing demands of bottom-up, local optimization, and top-down, centrally controlled, engineering design strategies. Such a pattern was observed by Klinkhamer et al for the city of Melbourne, Australia. Over a fifty year period service are expands significantly only during a ten year period coinciding with historical infrastructure projects, while the total length of the network expand linearly throughout the fifty year study period [34].

Barrington-Leigh and Millard-Ball analyzed the evolution of the United States road network over a 100-year period [56]. Their analysis showed a general trend of road network

and densification.pdf

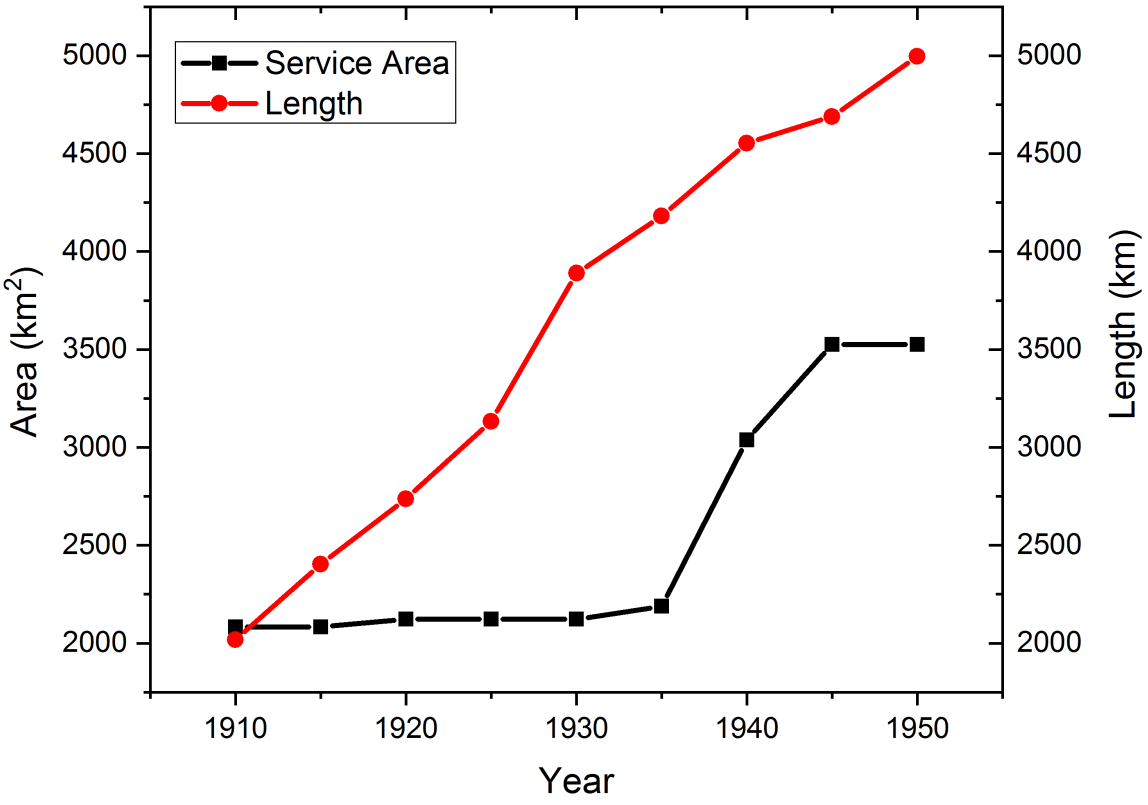

Fig. 2.1. The total length of Melbourne, Australia's UDN is shown to grow approximately linearly while expansion of service area grows rapidly only over an approximately ten year period. This reflects the densification of the network in response to local demands.

expansion, or sprawl, fueled by the rapid rise of the automobile ownership and low gasoline prices throughout the twentieth century with peak sprawl occurring in 1994. Since that time the road network nationwide has entered a phase of densification. This trend has been most prominent in areas with policies that actively promote public-transport and new urban design concepts such as walk-able cities, however the effect is noticeable even where such policies are not in effect, reflecting self-organized local-optimization of travel decisions and

road designs. The convergent effects of locally-optimized self-organization in the topologies of road networks is so persistent that Barthelemy has suggested that top-down road design decisions may be thought of as stochastic shocks that are eventually overridden through self-organization, reflecting how the networks are actually used locally [17].

2.2.1 Hysteric Effects of City Growth

Several studies have shown that early on in the initial periods of network expansion, major structural components forming the backbone of infrastructure networks are set in place and remain largely unchanged, even when subsequent expansionary periods occur in response to rising population or the incorporation of nearby settlements [17, 22, 55] (See Appendix E). Yang et al, Krueger et al, Zischg et al, and Klinkhamer et al (See Appendices A, B, and E) all showed that the scaling parameter of growing infrastructure networks rapidly converge to those of their fully developed, modern-day counterparts [34, 46, 48, 55]. Massuci et al had previously found similar results for the London road network. Showing the scaling parameter of the networks dual representation to exhibit little variance throughout a nearly 200-year period of growth from 1830 - 2010 [32, 33]. Thus, even though the hypothetical London time traveler described in the first chapter may not recognize her new, drastically altered surroundings the functional topology of the city's infrastructures would be largely unchanged from her previous experience.

City features such as buildings and infrastructure persist over long time-horizons, dictating the basic form of the city and its infrastructure networks, limiting the placement of new infrastructure [1]. Densification of the network through self-organized local optimization over time leads to convergence of topological metrics to universal values, but is incapable of substantively altering the spatial distribution of topological metrics [17]. Altering the backbone structure of the network and the spatial distribution of key topological metrics such as betweenness centrality (a measure describing the percentage of all possible network paths that pass-through a given node or link) can only be achieved through sweeping central control strategies [21]. A famous case study illustrating the challenge of altering the spatial

distribution of topological metrics being the redesign of the Paris road network during the reign of Napoleon III.

Eager to modernize what he felt was an outdated urban design Napoleon III commissioned Baron Haussmann to completely redesign large portions of the city by demolishing outdated housing, broaden roadways into grand boulevards, create new gardens and public spaces, install new WDNs, new UDNs, and increase connectivity by building several new bridges. Analysis of the Paris road network before and after Haussmanns sweeping redesign surprisingly showed no significant changes in the statistical distributions of topological metrics such as node-degree, shortest path lengths, or betweenness centrality [21]. However, Hausmann was successful in altering the spatial distribution of these topological metrics likely reducing congestion in the city center. Since the completion of Haussmanns work 1888 no other redevelopment projects of this magnitude have occurred, and the effects of the top-down design principles Haussmann enacted are still present in the analysis of the modern Paris road network [17].

2.2.2 Geospatial Co-Location of Urban Infrastructure

In modern cities, lacking dictatorial rule, the majority of available land is often privately owned and unavailable for the construction of new infrastructure at the scale of Haussmanns redevelopment. Gaining the ability to develop private lands for public works thus requires the acquisition of such rights either through the purchase of large amounts of property or claims of eminent domain. The difficulty of acquiring land within cities also influences the placement of subterranean infrastructure networks, such as UDNs and WDNs. Blumensaat et al, Mair et al, and Klinkhamer et al have all assessed the geospatial co-location of UDNs and WDNs with road networks, finding that the majority of the length of a given UDN or WDN is very likely to be found within 15-meters of the centerline of an overlying road, as shown in Figure 4 [34, 53, 57, 58] (See Appendices A and C). Variability in the percentage of UDNs and WDNs co-located with road networks was largely explained by Blumensaat to

be influence by local factors such as topography, with mountainous cities preferring to route pipes directly down steep slopes than to follow winding road networks [59].

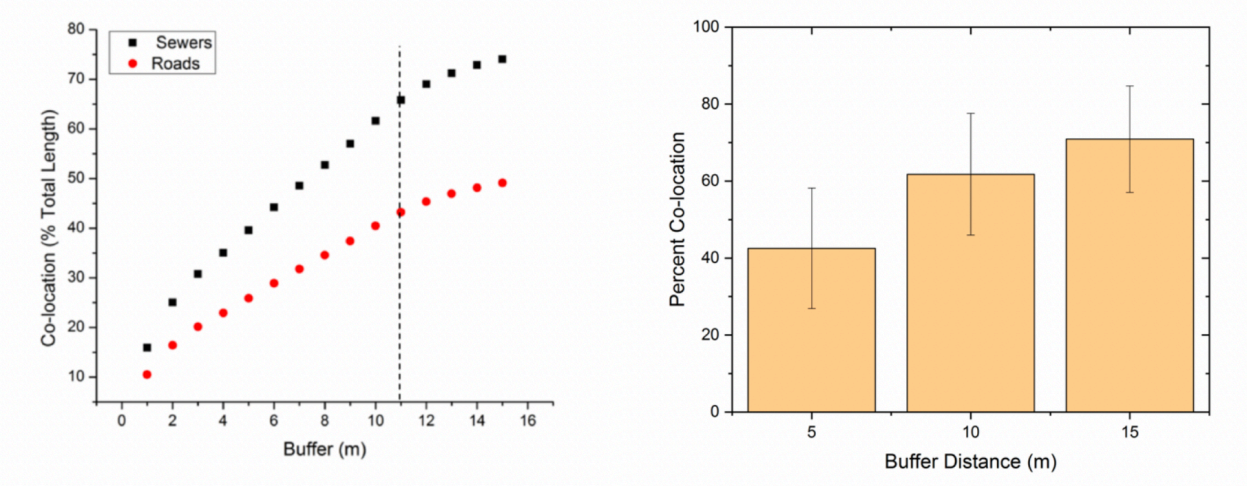

Fig. 2.2. Left: Percent of road and UDN geospatially co-located in a Midwest US city. The length of both the road and UDN co-located is shown to increase as the distance from the road centerline is expanded. Dashed line represents typical US right-of-way distance. Panel taken from Klinkhamer et al [53] (See Appendix C). Right: Mean percent co-location of UDN components with roads for 40 global cities. Buffering distances of 5, 10, and 15 meters were applied to road centerlines. Error bars indicate one standard deviation from the mean.

The expense and difficulty of obtaining the land area required to affect the spatial distribution of topological metrics, both the statistical and spatial distribution of these metrics

remain relatively stable in time. Changes to the distribution of topological metrics can only occur over long-time horizons, a reality holding major implications to engineering design and urban planning, a topic of ongoing research that will be discussed in Chapter.

2.2.3 Spatially Constrained Partial-Preferential Attachment

One of the primary factors leading to the scale-invariant networks is the presence of a consistent, hierarchical generative mechanism [27]. Klinkhamer et al (See Appendix A)studied the growth of three large subterranean infrastructure networks (2 UDNs; 1 WDN) [34]. Their analysis showed that each of these networks shared a similar generative mechanism, wherein new additions to the network preferentially attached to existing features with node-degrees within the second quintile (20-39th percentile) or higher of the node-degree distribution. New additions to the network were also shown to be averse to attachment to existing features within the first quintile (0-19th percentile) of the node-degree distribution, as shown in Figure 2.2. This partial-preferential attachment strategy was consistently observed at all time steps in each of the networks.

As described by Barabasi and Albert, following a preferential attachment generative growth mechanism will result in networks exhibiting heavy-tailed, scale-free node-degree distributions [43]. In addition, Carletti et al show that imperfect preferential attachment (i.e. that occurring when new network additions prefer to attach to the highest existing node-degree but lack full information of the network topology and thus attach to the highest known existing node-degree feature) results in tempered node-degree distributions that approach zero probability faster than would be expected of a truly scale-free distribution, such as those observed for infrastructure networks [60].

Engineering design principles and spatial constrains limit placement of new network features. To ensure reliability of the network, new pipes added to UDNs or WDNs must attach to existing features capable of accepting, or distributing, additional flow. Zisch et al have shown a positive correlation between the node-degree of diameter-based Dual-WDNs and Dual-UDNs with pipe diameter [61] (See Appendix B). Suggesting that existing features in

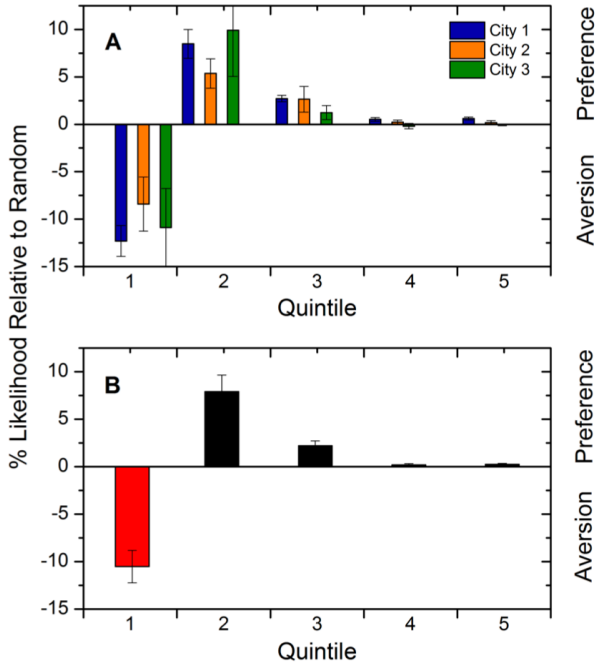

Fig. 2.3. Average attachment of of new network components for individual cities (A) and for all cities (B). In all cases there is an observed aversion for new network components to attach to existing components in the first quintile (lowest 20%) of node-degree and a preference for attachment to second quintile (21st - 40th%) and third quintile (41st - 60th%) of node-degree. Figure taken from Klinkhamer et al [34] (See Appendix A)

the 2nd - 5th quintile (20 - 99th percentile) are typically of larger diameter and greater capacity than existing features in the 1st quintile (0-20th percentile), and are thus more likely to be capable of handling increased service demands. Physical, spatial constraints and

financial considerations, such as the material and labor costs associated with installing new subterranean infrastructure, further prohibit linking new network components to all but the nearest existing components of sufficient capacity.

3. DISRUPTION AND INTERDEPENDENCE

Infrastructure networks do not operate independently. Increasing urbanization and the introduction of new technologies, such as Wi-Fi enabled thermostats, lighting, appliances, and the resulting internet of things, have led to ever greater connectivity, dependencies (and interdependencies) [10, 11]. The list of interconnections, interactions, and interdependencies occurring within and between Infrastructure networks alone is nearly endless, simultaneously providing certain stability enhancing advantages and introducing potential vulnerabilities [10, 31, 62–64].

Interdependencies between infrastructure networks may be physical in nature or indirectly occur as the result of spatial proximity or socio-economic drivers, as described in Table 3.1. Frequently these Interdependencies provide synergistic benefits. D'Souza et al found that the number of interconnections between grid sections could be optimized so as to minimize service loss initiated both internal and external causes [65]. Similiar optimization opportunities have been found between interdependent transportation networks. Strano et al analyzed the traffic volume of the London road and tube networks finding that lowering the speed of trains in the tube would lead to reduced congestion in both the tube and road networks [12]. Eventually however, whether due to chronic stresses and lack of maintenance or stochastic shocks, infrastructure components will fail, often leading to a temporary loss of service. The effects of these disruptions may extend to multiple other dependent and interdependent networks leading to their own service losses. These chain of events type failures are known as cascading failure [66]. These cascades may be initiated in multiple ways, as described in Table 3.2, and may have far reaching, widespread consequences.

Given the complexity of interconnections, dependencies, inter-dependencies, and emergent threats present in infrastructure networks, there is an urgent need to understand how networks operate and interact, especially when faced with disruptions. Current state-of-the-art approaches to monitoring and modeling interactions and the spread of failure between

multiple infrastructure networks involve federated modeling, simulation, and analysis (Federated Models), wherein individual, specialized models for individual infrastructure, social, and supervisory networks are modeled simultaneously using common data structure and sharing protocols [67]. However, while such models are considered to be invaluable resources, building, running, and interpreting their results is so demanding in terms of financial cost, technical expertise, data requirements, and computational power, that examining them has become its own field of study, and only those with the highest levels of access to data and resources are capable of producing these types of models. To illustrate this point, the United States operates a Federated Model, the National Infrastructure Simulation and Analysis Center (NISAC), originally developed as a battlefield analysis tool by DARPA and now run by Sandia National Laboratory. The European Union despite a decade of efforts has been unsuccessful in developing an equivalent model. Additionally, these types of models are limited in their usefulness in responding to disruptions in real-time as a single minute of simulation may take hours or days to process [67].

Network based approaches present a more tractable solution to modeling and analyzing both single network and cascading failures, as only statistical properties of the networks are often sufficient for conducting simulations. Several studies have been conducted, using both theoretical and empirical approaches, illustrating the effects of network topology, inter-connectivity, and spatial distribution, to the stability of both individual and coupled, interdependent networks [31, 62, 63, 65, 68, 69].

3.1 Network Disruption

Methods for modeling network disruptions, failures, and fragmentation have generally involved either node or link removal or percolation strategies [36]. Percolation characterizes network robustness by the value of the critical percolation threshold, the probability that any given node or link will be removed, beyond which additional removal of network components leads to rapid fragmentation of the largest connected component, as well as other properties describing how the size of this cluster changes as the network is increasingly fragmented.

Node or link-removal strategies involve either the random removal of node or links, or rank-order removal of important components such as, high degree or centrality nodes or links. Several of these studies have shown that individual scale-free networks are highly resilient to random failures, but are, never the less, vulnerable to the targeted removal of high-degree nodes, hubs. The removal of hubs from the network quickly fragmenting it, isolating large sections [70]. Until recently most network fragmentation studies of both types had been conducted using virtually generated independent networks [11].

Table 3.1.: Classification and Examples of Infrastructure Network Dependencies. Modified from Kroger and Nan [10]

Classification	Description
Physical	Network function depends on the performance of another. Examples include a water distribution networks dependence on electrical power to run pumps and distribute potable water to individual households
Geospatial	Close physical proximity of multiple infrastructure networks means that disruptions may affect several or all infrastructure in the area. Examples of disruptions producing interdependencies of this type include natural disasters such as fires, floods, or hurricanes, and may also include human-influenced disturbances such as vehicular crashes

continued on next page

Table 3.1.: *continued*

Classification	Description
Informational	Informational links such as Supervisory Control and Data Acquisition (SCADA) systems monitor and control the function and maintenance of multiple infrastructure networks. These types of informational interconnections are vital for the maintenance of infrastructure networks such as the electrical grid, transportation networks, and water distribution networks. In disaster response scenarios, mitigation of cascading failures may depend on direct communication with field workers providing real-time updates of changing conditions
Social	Network function is dependent on social factors such as public confidence, cultural background, or malicious acts such as vandalism or terroristic activity
Policy / Procedural	Governmental, regulatory or organizational shifts may promote or discourage the utilization of certain infrastructure networks. For example, strict parking fees may discourage the use of private vehicles in favor of public transport, or government regulation may shift primary energy production away from fossil fuels in favor of renewable sources leading to changes in the operation of the electrical grid

continued on next page

Table 3.1.: *continued*

Classification	Description
Financial	Infrastructure networks may be affected by financial disruptions such as the bankruptcy of a major network operator, or new entrants to the market. For example, the rapid rise in availability and convenience of ride hailing services such as Uber or Lyft have precipitated major disruptions in the mobility patterns of commuters in cities all over the world, altering the traffic flows of transportation networks of all types.

Table 3.2.: Classification of Failures Events Resulting from Dependencies. Modified from Kroger and Nan [10]

Common Cause	A single event such as an earthquake or flood causes failures in multiple infrastructure networks
Escalating	Consequences of failure in one infrastructure network are exacerbated because of failure in another. For example, and electrical blackout means that the electronic SCADA system cannot be run resulting in a prolonged blackout
Cascade Initiating or Resulting	Failure in one infrastructure network (a leaking pipe, initiating event) causes failure in another (pothole or collapsed road, resulting event)

However, coupling multiple networks, through the creation of interdependent links, has been shown to introduce very different behavior in terms of how individual networks within

the network of networks respond to disruptions and how those disruptions cascades within and between networks. Percolation based analyses of interdependent networks have found coupled scale-free networks to be far more vulnerable to disruptions than equivalent independent networks [62]. Specifically, studies have found that increasing interconnections and dependencies alters the nature of percolation across networks by shifting the percolation from a continuous, second-order transition to a discontinuous first-order transition, sometimes referred to as explosive percolation, wherein the network fragments very rapidly, once a critical percolation threshold, that is much lower than that of second-order transition is reached. Baxter et al found the percolation threshold of individual scale-free networks to transition from continuous, second-order, percolation to discontinuous, second-order, percolation. The transition occurring when the the scaling parameter of the node-degree distribution γ meets the condition $\gamma > 3$ [62].

Before phase transition occurs, as Baxter et al showed, the percolation threshold of equally-sized, virtual scale-free networks with γ in the typical range of $2 < \gamma < 3$ diminishes as γ approaches $\gamma = 3$. Additionally, the ratio of the size of the largest component to total network size, S, a key factor describing network connectivity, of such virtual networks with $\gamma = 2.1$ did not approach zero until components were removed with probability $p = .8$, where as for networks with $\gamma = 2.8$, S rapidly approached zero when components were removed with probability $p < .3$ [62]. Klinkhamer et al also showed that as γ approaches $\gamma = 3$ real UDN and road networks fragment much more quickly in response to random disruptions [34].

3.1.1 Infrastructure Network Disruptions

Although the scale-free network model introduced by Barabasi and Albert lead to an abundance of studies characterizing the scale-invariant characteristics of real-world networks, the statistical rigor of many of these assertions has been called into question [44,45,71]. Spatial networks, existing in physical space often possess heavy-tailed node-degree distributions that are sharply truncated at finite limits as the networks fill all available space [49]. In fact, most spatial networks, including infrastructure networks in their primal form follow

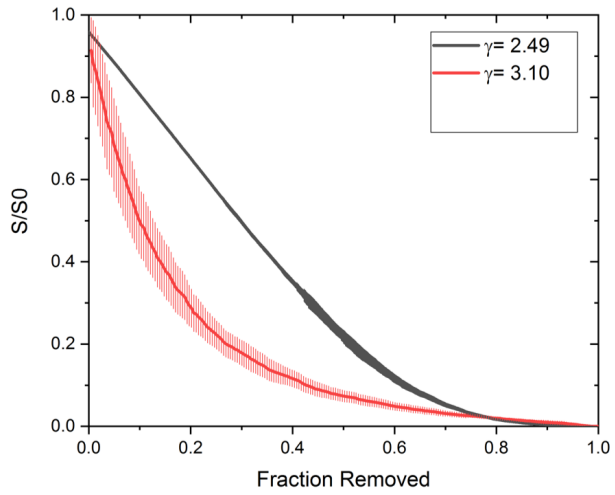

Fig. 3.1. The response of the size of the largest connected component to removal of random nodes for two infrastructure networks with different γ are shown.

peaked node-degree distributions that are not at all heavy-tailed [21, 44]. Even the scaling relationships of the largest spatial networks, such as rivers, are characterized by heavy-tailed distributions that are truncated as a result of the finite size of continental river basins. Smaller networks such as infrastructure networks frequently lack the size necessary to meet the statistical definition of a scale-free network [72].

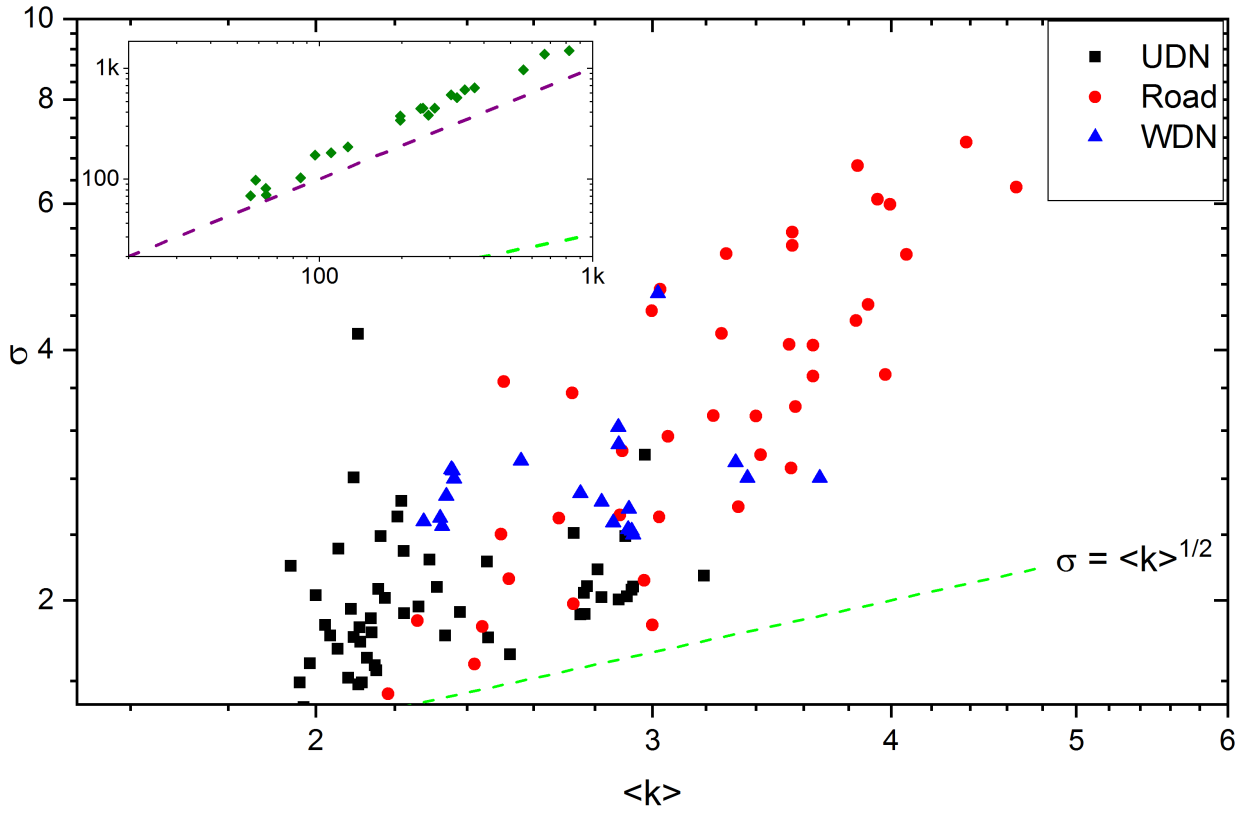

Fig. 3.2. $< k >$ vs σ for 125 infrastructure networks and 18 river networks (inset). all of the infrastructure networks and river networks are shown to have greater variance in node-degree than expected of a Poisson random graph. (dashed green line $\sigma =< k >^{1/2}$)

The utility of applying such statistical rigor for the purpose of modeling network disruptions is itself a subject of debate, Barabasi has himself voiced support for considering the relative value of such statistical methods [71]. The work of Watts and Strogatz indicates that any network with sufficient variability in its node-degree distribution, such that node-degree variance, σ, is greater than that of a Poisson random graph of with equal $< k >$, will exhibit network fragmentation dynamics approximating those typical of scale-free network [42] So, the failure and disruption characteristics of both scale-free and other sufficiently variable heavy-tailed distributions are likely to behave in a similar manner .

Klinkhamer et al (See Appendix A) used this concept to show that functional topologies of each of 125 infrastructure networks (Roads, UDNS, and WDNs) in 52 global cities all possess node-degree distributions with variability greater than that expected of a Poisson random graph, as shown in Figure 3.1 [34] (See Appendix A). The difference between the observed σ continues increasing with average node-degree all the way up to the largest networks, river networks, as demonstrated by the variance in the Strahler order distribution of 18 German rivers.

Additional analysis by Klinkhamer, using the same 125 networks, measured the size of the largest connected component following random and rank order node-removal strategies. Each of the networks were found to display fragmentation characteristics similar to those that would be expected of scale-free networks. An example of 1000 simulations of targeted and random node-removal conducted on the UDN of one case-study Canadian city is shown in Figure 3.2.

Other Network Disruption Models

Although node-removal and percolation based strategies for modeling network fragmentation have proven useful for describing the effects of disruptions, they are most directly applicable to disruptions that affect structural components of infrastructure networks. A closed road or burst pipe for instance are structural disruptions affecting physical components of the networks. However, other types of disruptions, such as traffic jams, merely

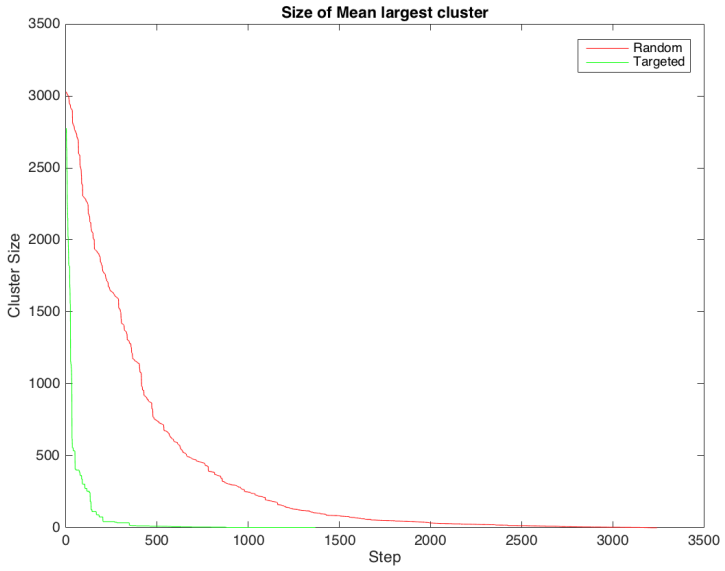

Fig. 3.3. Mean size of the largest connected component of Canadian UDN (n=1000 simulations). A rapid reduction in the size of the largest connected component when subjected to targeted removal of high-degree nodes relative to the random removal strategy is observed at all node-removal steps.

reduce the service capacity of network components though they are still structurally intact. Zhan et al investigated these types of functional failures by examining the traffic patterns in large Chinese cities [73].

Zhan et al measured the functional state of network components by monitoring the the speed of traffic on individual components of the dual-road networks of Beijing and Shanghai. If the speed of traffic fell below a critical threshold, the affected component was split at that point into two separate nodes. When the speed of traffic recovered, the two nodes were rejoined. Changes in the functional topology of the networks produced following this method were used to identify identify archetype cascading failures as a result of traffic, self-splitting (a result of city-scale traffic loads), Self-Contagion (a result of traffic backing up on one road), and neighbor contagion (a result of vehicles seeking alternate routes, leading to congestion of nearby road segments). The authors were able to relate the type and frequency of these failure types to structural differences in the road networks that could either amplify or mitigate the effects of congestion during times of heavy travel [73].

3.1.2 Disruption of Interdependent Infrastructure Networks

Prior studies of the fragmentation of both virtually generated and real-world, coupled scale-free networks, have suggested that coupled scale-free networks, as a result of interdependecies, are less robust to random node removal strategies than are independent scale-free networks [62, 74]. The additional links representing additional opportunity for the initiation of cascading failures. Additional factors such as the correlation between the topological metrics of interconnected nodes have been shown to further increase the susceptibility of coupled scale-free networks to random node-removal, as depicted in Figure 3.3 ([74]).

Using networks modeled after the academic author, coauthor network, Lee et al showed that differences in the strategy of coupling nodes influenced the susceptibility of the coupled network to random node removal, comparing coupling strategies based on maximally positive (The combined degree of coupled nodes is as high as possible) and maximally negative (The combined degree of coupled nodes is as low as possible) correlations of node-degree, as well as uncorrelated random inter-connectivity and the actual inter-connectivity of the networks. The results finding size of the largest connected component of coupled networks following uncorrelated, real and maximally-positive inter-connection strategies to decrease in

a mostly linear fashion in response to random node-removal while the size of the largest connected component of networks coupled following maximally-negative connection strategies were relatively more vulnerable to random node removal [74].

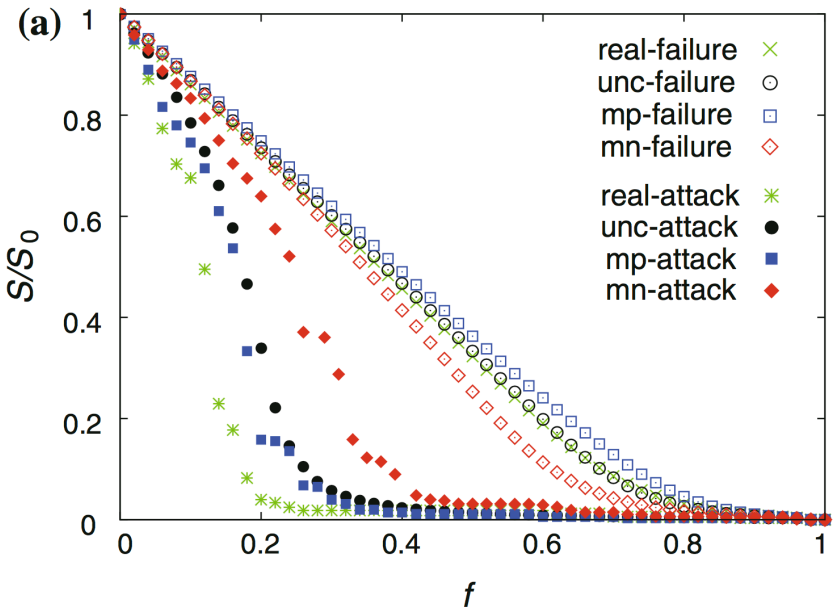

Fig. 3.4. Different correlations in the connection strategies of two interdependent networks is shown. A maximally negative correlation strategy is shown to be relatively more vulnerable to random node-removals than alternate connection strategies. This same connection strategy is however seen to be more robust against target failure as compared to the alternate strategies. In all cases targeted removal is show to result in the size of the largest connected component diminishing faster than random removal strategies. Figure taken from Lee et al. [74].

Empirical Evidence

Of the 52 cities examined by Klinkhamer et al network data for both UDN and Road and/or WDN and road networks were available for 32 [34] (See Appendix A). These networks were used to construct interdependent, coupled networks The coupling strategy of these networks was based on the spatial dependencies imposed by the co-location of infrastructure

networks. These dependencies were assumed to be directed, from the subterranean (dual-UDN or dual-WDN) network to the dual-road network, cascade initiating events, wherein the removal of UDN nodes would result in the removal of all geospatially co-located dual-road nodes. The effects of the removal of road network components as a result of cascading failures initiated by spatially coupled UDN and/or WDNs was analyzed by measuring the size of the largest connected component.

Each of the coupled networks examined by Klinkhamer et al were comprised of individual road, UDN, and WDNS containing different numbers of nodes, typically with road networks having far more nodes than their coupled, subterranean counterparts. In addition, because road and subterranean infrastructure networks, as was shown by Klinkhamer et al, Mair et al and Blumensaat et al, are not fully co-located, with each network containing some autonomous nodes that are spatially separated from other network type, the coupled networks thus do not have full inter-connectivity, limiting the extent of cascading failures [34,57,59,75] (See Appendices A and C). As a result not even 100% removal of interdependent links in the coupled infrastructure networks analyzed by Klinkhamer et al could result in complete fragmentation of any of the analyzed road network components, as is shown in Figure 3.4, Panel A [34] (See Appendix A).

While Lee et als analysis of the response of coupled networks following different connection strategies to random node-removal showed maximally negative connection strategies to be more vulnerable to random node removals, the results of the analysis by Klinkhamer et al showed the opposite [34, 74] (See Appendix A). Larger infrastructure networks of high-population cities though tending to have the majority of their connections between low degree road and WDN and/or UDN features, these networks exhibited decreased susceptibility to random node-removal as compared to the smaller infrastructure networks of less-populous cities following more positively correlated connection strategies as shown in Figure 3.4, Panels A and B and C [34] (See Appendix A).

Given that entire road segments are unlikely to fail as a result of small pipe failures, the node removal strategy chosen by Klinkhamer et al is very aggressive and not necessarily representative of real world scenarios. Despite this however, the road networks maintain con-

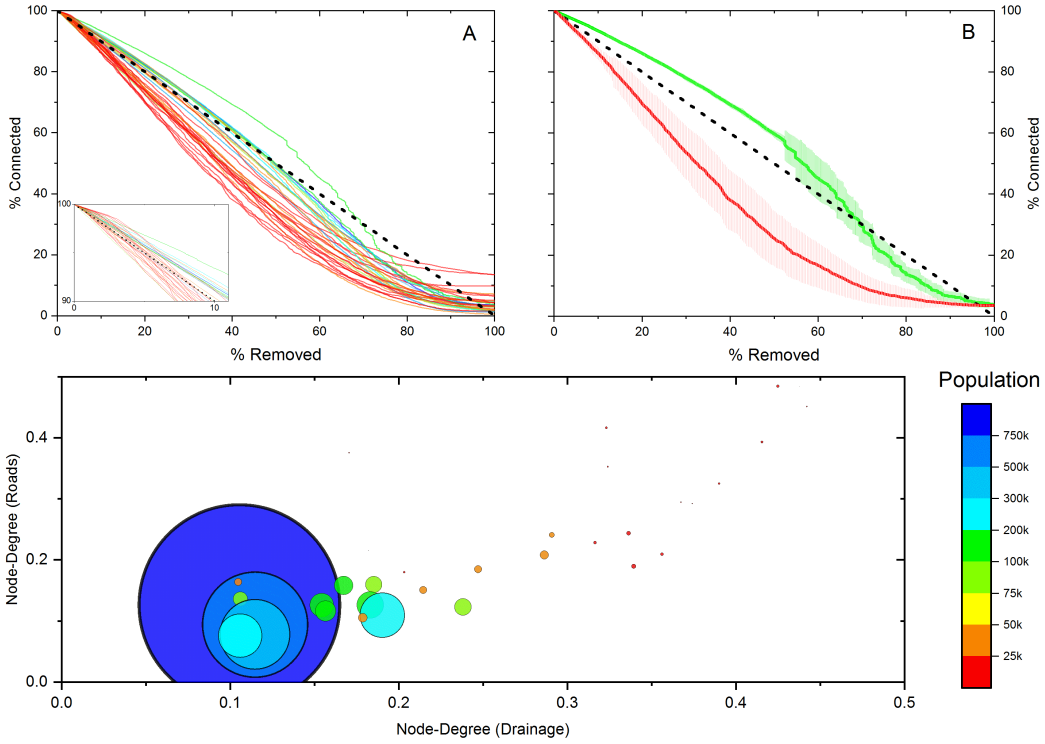

Fig. 3.5. (A) Size of the largest connected component (B) The most and least robust road networks are highlighted (C) Connection strategies between nodes in connected networks. Smaller networks tend maximally positive correlation while larger networks tend towards maximally negative correlation strategies. Size of circles and color correspond to urban area population in all panels.

nectivity remarkably well, with none of the studied road networks fully fragmenting. These findings suggest that strategies, such as separation of key components may lend robustness to random failure to the networks.

3.1.3 Structural Factors

Loops and Branches

Neither disruptions nor networks are unique to engineered systems, they exist throughout nature and are routinely subjected to external shocks. While in most studies optimal network design, in terms of efficiency, has been found to be a minimum spanning tree structure, multiple natural networks exhibit a looped structure [17,36]. These loops may be long lasting such as cyclic deposits of minerals, or highly transient, as is the case with blood capillaries that create loops only when certain stress thresholds, such as excess body heat [76], are exceeded. Despite what are likely large differences in the forces driving the formation of these loops, one commonality associated with the presence of loops in different types of networks is the existence of volatility and external shocks [76, 77].

Loops have proven to be an effective strategy for dealing with volatility in natural networks. One of the more prominent examples of looped networks in nature are leaves. Loops within leaves have evolved over time with early phyla possessing mainly branched structure, although even in these ancient designs loops still develop in response to attack [76]. Loops in the capillary structure of leaves allow vital nutrient transport and gas exchange processes to continue even when leaves are damaged by physical or herbivorous forces. Mycorrhizal networks meanwhile possess a hub and spoke structure with multiple interconnections between hubs forming loops at distance, a structure analogous to air transportation networks, that allows for the transport of nutrients and water throughout the network in times of stress [78].

One prominent example of a branched network in nature is that of rivers. Through self-organized processes river networks have developed a scale-free bifurcating-tree structure that efficiently drains the landscape [72]. Controlled by gravitational forces, rivers are more or less impervious to failure. A river spilled over its banks will still flow as fast as gravity

will allow and will wash away or reroute around obstacles. And yet even these networks will display branching in response to the right conditions. When volatility exists in the form of highly erodible banks or highly variable discharge or when the ratio of sediment to slope is below a threshold value, braided rivers may develop [79].

Parallels to these examples exist in engineered urban infrastructure networks. UDNs have been shown by Yang et al to evolve and drain the urban landscape in a manner similar to rivers [46,47]. Being primarily gravity driven and considered less prone to failure than WDNs and road networks, UDNs typically possess branching tree-like structures. Road networks on the other hand possess nearly fully looped structures allowing for travel from any point to any destination with minimal travel in incorrect direction and facilitating rerouting in the event of disruptions such as traffic jams or blocked roadways.

Valve Networks

WDNs exist as hybrids between branched and looped networks, having more loops than UDNs, but lacking the fully looped design of road networks. The reasons for this hybrid structure are multiple. Being pressure driven systems, repairing a leaking or burst pipe within the WDN requires the damaged portion of the network to be isolated by closing two or more valves. In a fully branched network, this isolation would cut off the supply of water to all downstream portions of the network potentially affecting large areas of the city. Valves and loops allow for isolation of damaged components with minimal loss of service by rerouting the flow. Due to cost considerations however the number of valves in a WDN is limited.

Zischg et al examined the effects of valve placement on WDN service loss induced by the necessity of isolating damaged WDN components, by analyzing valve based dual-representations of two WDNs. Their analysis revealed large differences in the topological metrics of the two WDNs reflecting the availability of financial resources. Despite being less than one tenth the size of the European case study network, 385 and 5,394 nodes respectively, the Asian case study network serves a population approximately thirty times larger

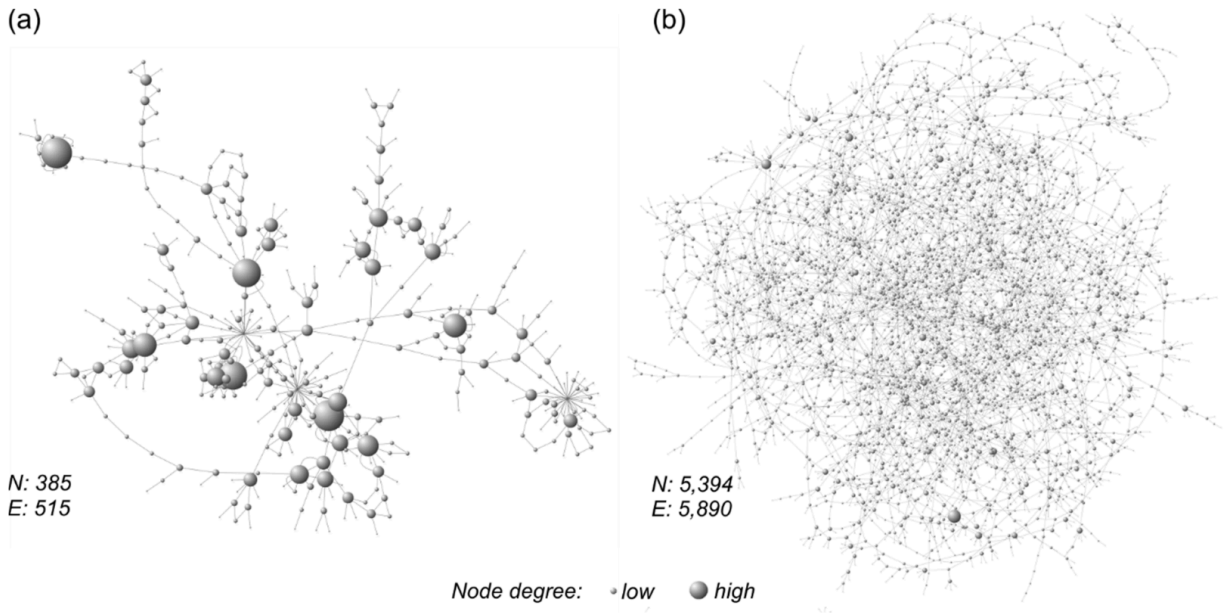

Fig. 3.6. Left: Topology of the dual graphs: (a) Asian case study and (b) European case study Source: Zischg et al

than the European counterpart (4,000,000 vs 132,000 respectively). These results reveal the inherent vulnerability of the Asian case study WDN, indicating that even a minor issue in the network requiring isolation is likely to disrupt service to a large portion of the city [80] (See Appendix G).

4. APPLICATIONS

4.1 Long-Term Network Design Strategies

Given that the spatial distribution of topological metrics and the physical layout of city structure are established early and are long-lasting, how can design decisions be made so as to increase the robustness of existing urban infrastructure to external shocks and cascading failures? In this section I highlight variance exiting within UDN, WDN, and road networks at local scales.

Although the scale-invariance of infrastructure networks would seem to imply that their topology and spatial distribution would remain stable at all hierarchical scales within and between cities, just as a head of broccoli when broken down into small enough pieces will eventually loose the backbone defining its structure, failing to resemble the head as a whole, so to do small cities and neighborhoods, display variance around the mean values describing the functional topology to which all infrastructure networks converge [34,53] (See Appendices A and C). This variance represents opportunities to prioritize retrofitting infrastructure networks and identify potential existing risks.

4.1.1 Variance Within Cities

Klinkhamer et al (See Appendix C) examined the local scale variance present in the topological characteristics of the UDN and road networks of one sample city by producing randomly distributed, nested subnets as shown in Figure 4. Subnets were created by selecting randomly distributed points within the study area, and buffers of 1.25, 2.5, 5, and 7.5 km radii applied. These buffered areas were then used to extract, via the clip process in ArcGIS, intersecting road and drainage features. For UDNs and road networks,functional topological metrics, derived from high-resolution data (70,000 nodes) revealed the convergence functional

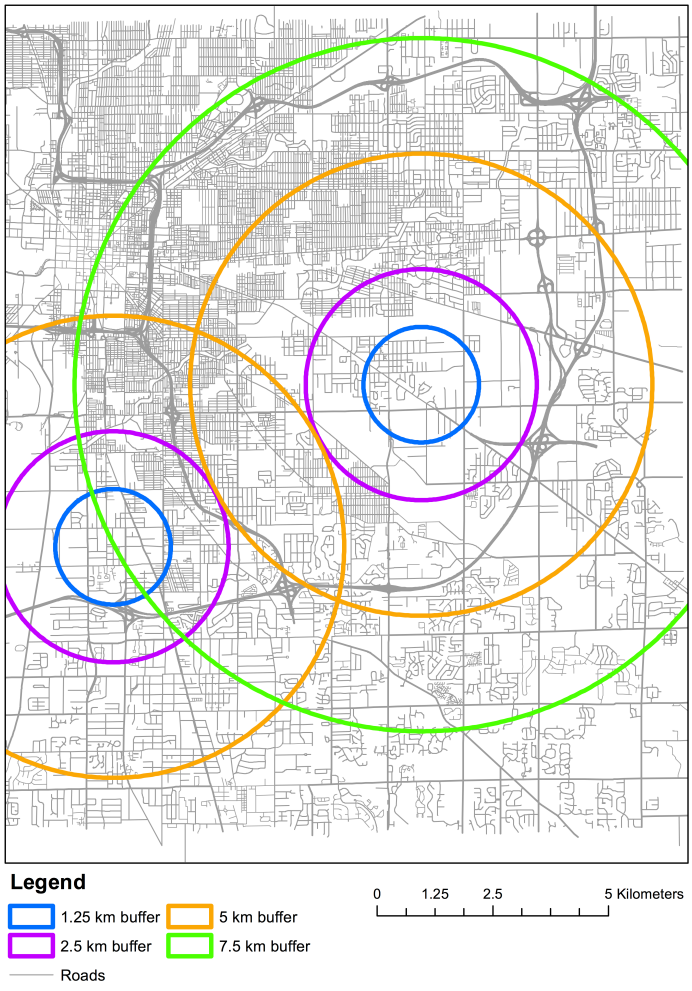

Fig. 4.1. Subnets of the UDN and Road networks of a large Midwest, USA were created by clipping features within 1.25, 2.5, 5, and 7.5km radii of 25 random points.

topology between subnets, in spite of differences in multiple local attributes. Variability of p(k) between individual networks was found to sharply decrease as network size increases, converging to values near the mean of $\gamma = 2.49$ [$MSE <= 4.85E-7$]. Subnets serving populations of less than approximately 20,000 were shown to display higher variance around the mean $\gamma = 2.49$ values than larger subnets [53].

In some of these smaller sub-nets γ was found to occasionally exceed $\gamma = 2.49$, a known threshold where network percolation transitions from a continuous 2nd order process, wherein network connectivity decreases gradually as nodes or links are removed with grater probability, to an instantaneous 1st order process, wherein complete fragmentation of the network can occur instantaneously even at very low probabilities of node or link removal. Such subnets, with γ values outside of the normal range of $2 < \gamma < 3$ may be more prone to sub-net-wide loss of service in response to disruptions, and represent opportunities for prioritize retrofitting of aging systems to decrease the incidence and duration of service losses.

In a similar analysis of variability within infrastructure networks, Krueger et al examined variability in the WDN structure of a large Asian case study city [48]. The city's WDN, due to the city's location in an arid region, is capable of providing only intermittent supply of non-potable water. The WDN is divided into over 50 distribution zones that distribute water local residents once or twice a week. Krueger et al analyzed the structure and functional topology of each of these zones revealing the functional topology of zones to converge to universal values as network size increased. Variance presence in the structure of three smaller distribution zones was notice to be far more branching, than typical WDNs and possessing fewer but larger than expected hubs. These zones were noted and when mentioned to the local water minister, identified as zones known to have a large number of pipe bursts. Zischg et al later analyzed the valves networks of these zones, finding them to have fewer valves per length of pipe than other zones with more valves, more looped structures, and less frequent pipe bursts [80] (See Appendix G).

Small networks may also have ($\gamma > 3$), as shown in Figure 4.3 [34] (See Appendix A). As with sub-nets within large infrastructure networks, these conditions represent additional opportunities for managers and city planners to address localized risks through planned maintenance or expansion by redesigning or relocating network features while maintaining city-wide performance and enhancing urban community resilience.

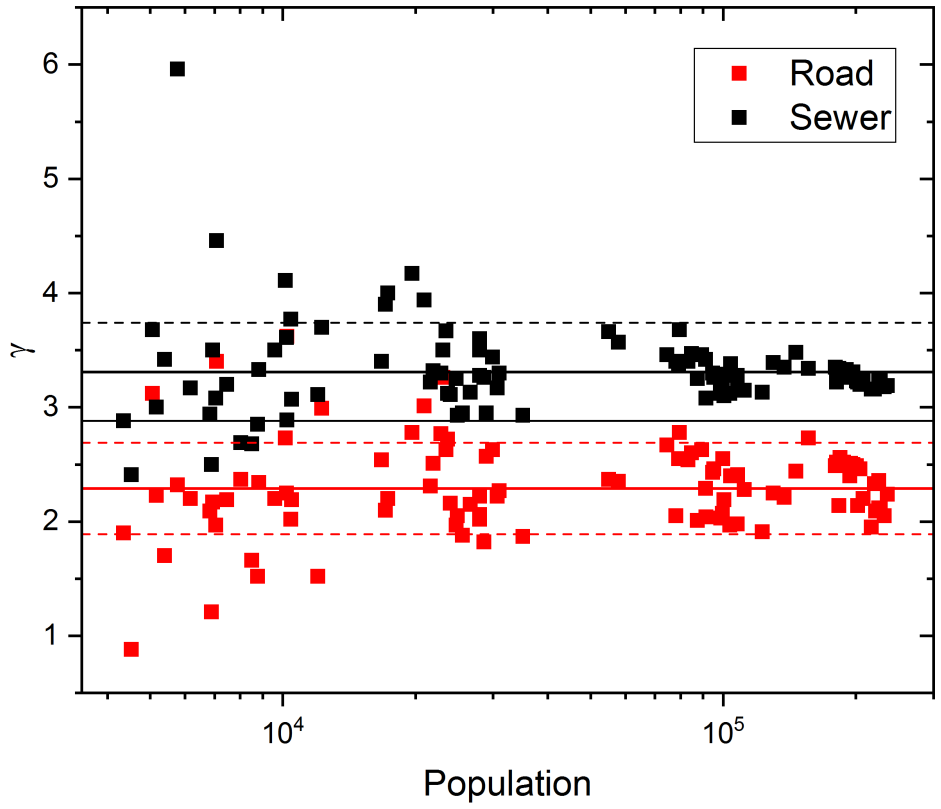

Fig. 4.2. Range of γ values for randomly distributed subnets. Variance between subnets as their size, and population served, increase. Modified from Klinkhamer et al [53] (See Appendix C)

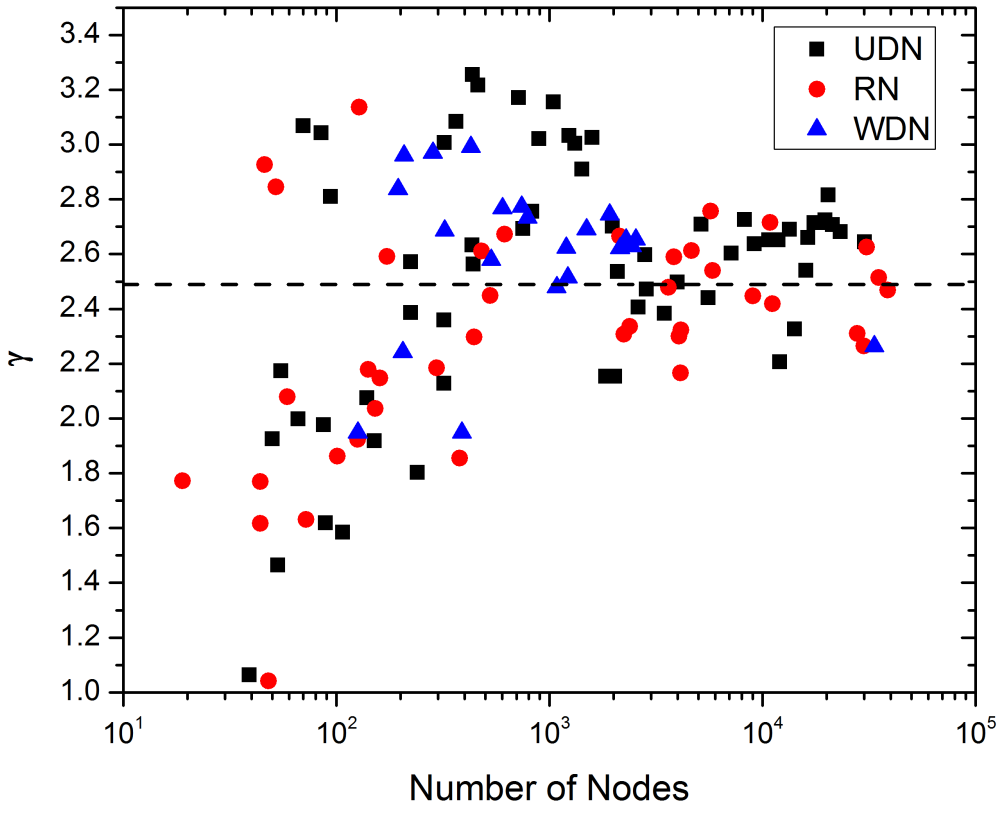

Fig. 4.3. γ values from 125 networks in 52 global cities. Variability in γ is shown to decrease and converge to the mean as network size increases. Taken from Klinkhamer et al [34] (See Appendix A)

4.1.2 Variance Between Cities

Variance in functional topology between cities may also be indicative of potential risks as a result of sub-optimal engineering design and infrastructure co-location strategies and. Smaller cities, may exhibit features such as near complete geospatial co-location of networks. As was seen in Chapter 3, co-location strategies such as the correlation of node-degree and introducing autonomy by keeping certain network isolated affect the rate of network fragmentation when disrupted. City planner can use analyses of node-degree correlations, as shown in figure 4.4 to target individual components that are at most risk of cascading failure for either isolation or relocation. Over long time horizons such locally-focused strategies can alter the global correlation between nod-degree of co-located infrastructure.

Due to the hysteric nature of engineering design decision early in the city's evolution, equally long-term planning and coordination of local-scale projects carried out with a focus on balancing local constraints and use cases with network wide design objectives is necessary to redistribute the spatial distribution of key topological metrics.

Policy decisions also play a critical role in increasing the robustness of interdependent infrastructure networks. Policy that encourages behavioral changes such as decreasing reliance on personal automobiles as a primary means of transport have been shown to increase the effective capacity of road ways and reduce urban sprawl [56]. Other management strategies such as controlling the interaction between multimodal transport systems has been shown to increase the efficiency of both networks. As was the case for the London tube and road networks, where Strano et al showed that decreasing the average speed of cars running in the tube would reduce congestion and overall travel times in both networks [12].

4.2 Preferential Transport Pathways

Multiple recent studies have identified sewer gas as a potential pathway for volatile organic compound (VOC) vapor intrusion [82–86]. VOCs are a common component of sewage and sewer gas. VOCs may enter the sanitary sewer network through multiple sources including direct discharge of industrial [87] and domestic [88] waste water flow. Household laundry

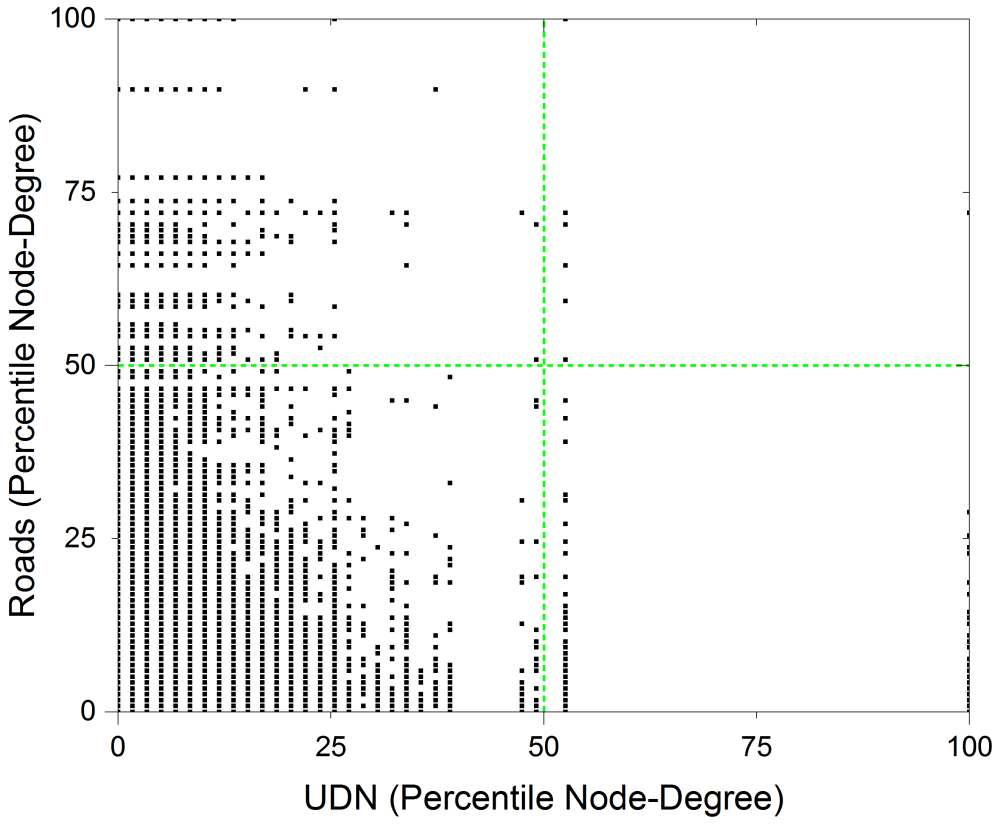

Fig. 4.4. Normalized node-Degree of UDN network component plotted against co-located road feature node-degree. Over long time-horizons, relocating or isolating features above the 50th percentile in either network can help shift the global correlation between node-degree.

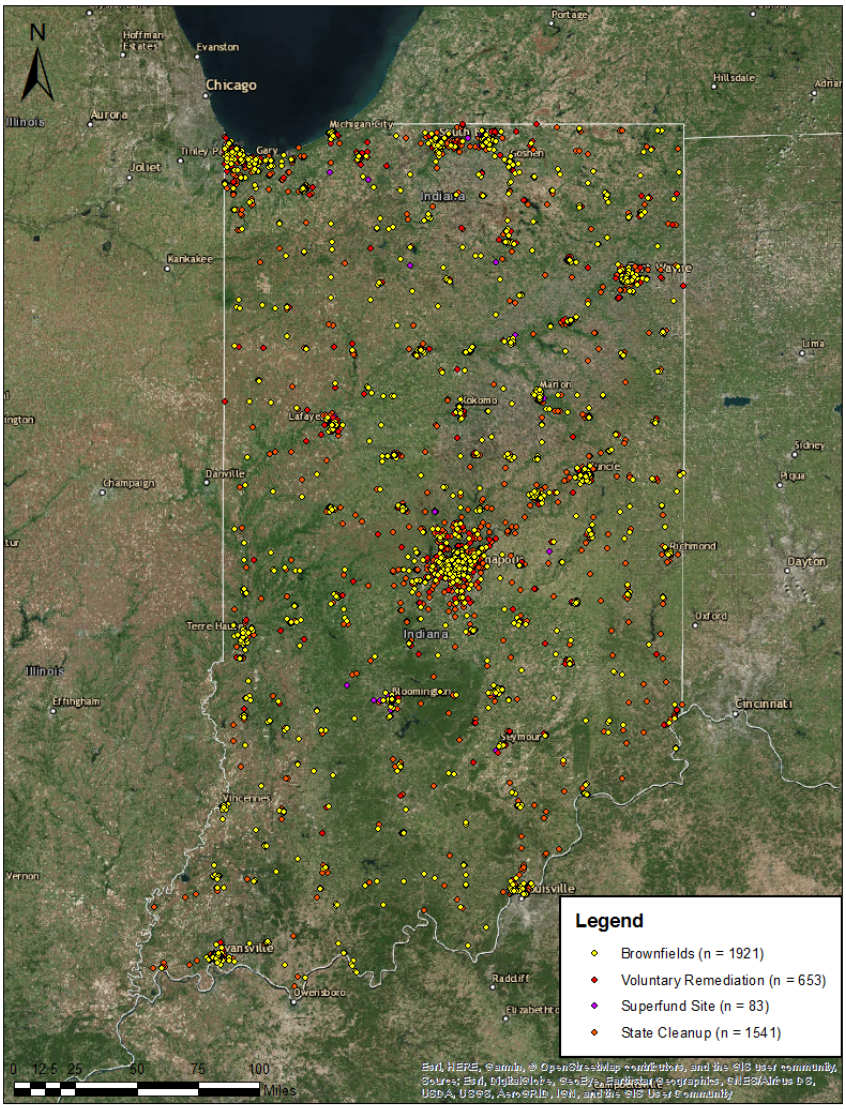

Fig. 4.5. Locations of land parcels in rolled in IDEM VRP (n = 663), State Cleanup (n = 1541), Brownfields (n = 1921), or Superfund site programs (n = 83). Data reported by IDEM 2019 [81]

and bleaching discharges have been shown to increase daytime chloroform concentrations in sewers [88] and dry-cleaning operations have long been known to be a major contributor of PCE [87] in the sewer system.

In addition to direct discharge, VOCs present in soil or groundwater of Brownfields, as a result of industrial operations or spills, may enter the UDN through cracks and other

openings. Izzo et al. [87] conducted one of the first studies confirming the role of sewers in VOC transport, and identified five major pathways that VOCs may infiltrate or ex-filtrate from a sewer, through defects in the pipe walls or joints, leaching through sewer walls, liquid VOC saturation of sewer walls that is then volatilized, or by direct penetration of gas through the sewer walls. Evidence for these pathways was given in the form of elevated soil gas VOC readings near sewer lines.

In the vadose zone, VOCs may be sorbed to soil particles or contained in soil moisture through immiscible-liquid dissolution and transported during saturated periods [89]. These VOCs may enter the sewer through cracks and other openings during wet weather events or by saturation of the sewer walls [87]. In fact, sewer design standards recognize sewer infiltration as an inevitability that must be accounted for [90].

VOC transport between contaminated groundwater and the vadose zone is bidirectional and is driven by multiple factors including soil type and temperature [89]. Once volatilized however, VOCs may be transported through the vadose zone in gaseous form [89, 91] and, driven by pressure or concentration gradients [33], enter the sewer system through cracks and other openings or by passing through pipe walls [87].

Regardless of the mode of entry, once VOCs are present in the sewer system they may be transported either in the sewage itself or in sewer gas and exit the system through cracks or defective joints far from the initial source of contamination [86]. Consideration of the current state of sewer infrastructure in the United States (D+ rating from ASCE [92]) and the voluminous number of contaminated land parcels, shown in Figure 4.1, in Indiana alone suggest that issues related to VOC transport and vapor intrusion from sewers may be widespread [81]. However, despite existing evidence for the role of UDNs as preferential flow pathways for contaminant transport, a recent review of the literature uncovered only six peer-reviewed studies investigating the role of sewers in VOC transport.

A recent study by Roghani et al investigating the potential for sewers to act as alternative VOC vapor intrusion pathways analyzed a portion of a UDN passing through a Brownfield, finding significant spatial and temporal variability of VOC concentrations in sewer gas [86]. Localized areas of turbulent flow, sewer liquid temperature, head space velocity, sewer slope,

sewer elevation, and other factors within the sewer were thought to lead to increased volatilizing of VOCs, driving spatial variance.

Roghani et al also found that significant temporal variability in VOC concentrations within the sewer exists on all scales from hours to months [86]. Short term temporal variability was thought likely to exist as a consequence of the typical diurnal flow regime observed in sewers, and from differences in the types of discharges made during day and nighttime hours. Longer scale variability was thought attributable to seasonal changes in temperature and rain patterns.

Modeling the flow of sewer gas is a complicated endeavor. Sewer gas within sewers is capable of bidirectional flow either with or against the flow of liquid sewage, driven by pressure gradients and the observed variability in sewer gas VOC concentrations further complicates modeling sewer gas VOC transport using existing, traditional models. As a result of these and other complexities, traditional methods of modeling sewer-gas transport have extensive data requirements akin to fully functional SWMM models [33, 93–96].

High-degree UDN components hold the greatest potential for the widespread transport of VOCs through sewers by virtue of their high connectivity. Prioritization of regulatory efforts by targeting the remediation of contaminated land and groundwater with the potential to infiltrate nearby high-degree, could community health by reducing the incidence of low-level chronic exposure to VOCs.

4.3 Conclusions

Novel applications of principles of graph theory and network science to the analysis of urban infrastructure networks developed in the course to research leading to this thesis, have produced valuable insights into the functional topology of UDN, WDN, and road infrastructure networks. These insights cut through the inherent complexity of the multiple, interconnected CI's from which cities are composed and depend upon.

Research conducted by Yang et al, Krueger et al, and Klinkhamer et al represent the first studies to analyze the scale-invariant properties of the functional topology of subterranean

Dual-UDNs and Dual-WDNs [47,48,53] (See Appendix C). Subsequent work by Klinkhamer et al further advanced the field by providing evidence for the existence of a "Spatially-Constrained Preferential Growth Mechanism" driving the the space filling properties and hierarchial structure of infrastructure networks, mechanisms known to produce scale-free and scale-free-like networks, possessing node-degree distributions characterized by high variance [34] (See Appendix A).

The importance of forward-thinking long-term design decisions when designing new infrastructure networks, as is the case rapidly developing countries, such as china, was illustrated by examining the difficulty of altering the backbone characteristics of infrastructure networks after the initial expansionary periods [17]. The effects of failing to address the spatial distribution of topological metrics and inherent spatial interdependencies of co-located infrastructure was shown to impact the ability of these networks to withstand disruptions [34] (See Appendix A). Klinkhamer et al also demonstrated the significance of these findings to the stability of the interdependent road networks of 32 global cities when subjected to cascading failures induced by geospatially co-located subterranean infrastructure networks [34] (See Appendix A).

These findings have led to ongoing research topics related to the real-world applicability of these findings to aid engineering design decisions, increase the robustness of existing individual and coupled infrastructure networks, and prioritize environmental remediation projects so as to minimize vapor intrusion concerns related to preferential transport pathways.

Finally, attention has been brought to variance between and within the functional topology of existing infrastructure networks at local scales as priority action areas for retrofitting projects designed to provide locally adapted engineering solutions as part of long-term network wide projects to redistribute topological metrics, increase the robustness of individual and coupled networks to disruptions, and increase community resilience.

REFERENCES

REFERENCES

[1] R. Louf and M. Barthélemy, "How congestion shapes cities: from mobility patterns to scaling," *Scientific Reports*, vol. 4, 2014.

[2] D. S. G. W. Luis bettencourt, Jose Lobo, "Urban scaling and its derivations: Revealing the structure of wealth, innovation, and crime across cities," *PLOS One*, vol. 5, no. 11, 2010.

[3] H. Xu and Y. Xie, "The causal effects of rural-to-urban migration on children's well-being in china," *European Sociological Review*, vol. 31, no. 4, 2015.

[4] D. Bell and A. De-Shalit, "The spirit of cities." Princeton Press, 2011.

[5] M. Batty and P. Longley, "Fractal cities: a geometry of form and function." Springer, 1994.

[6] M. Batty, "The size, scale, and shape of cities," *Science*, vol. 319, no. 5864, pp. 769–771, 2008.

[7] ——, "The new science of cities." MIT Press, 2002.

[8] U. nation Department of Economic and S. Affairs, "World urbanization prospects: The 2014 revision," *European Sociological Review*, vol. A, no. 366, 2014.

[9] T. McPherson, S. Pickett, N. Grimm, J. Niemela, M. Alberti, T. Elmqvist, C. Weber, D. Hasse, J. Breuste, and S. Qureshi, "Advancing urban ecology toward a science of cities," *BioSience*, vol. 66, no. 3, 2016.

[10] W. Kroger and C. Nan, "Addressing interdependencies of complex technical networks," in *Networks of Networks: The Last Frontier of Complexity*, 2014.

[11] G. DAgostino and A. Scala, "Networks of networks: The last frontier of complexity." Springer, 2014.

[12] E. Strano, S. Shai, S. Dobson, and M. Barthelemy, "Improving incomplete water distribution system data," *Journal of the Royal Society Interface*, vol. 12, no. 111, 2015.

[13] E. Izadi, "Massive sinkhole along florence river swallows dozens of cars," in *Washington Post*, 2016.

[14] Park, Seager, and Rao, "Lessons in risk versus resilience based design and management," *Integrated Environmental Assessment and Management*, vol. 7, no. 3, 2011.

[15] P. World, "Fukushima costs doublet," *Physics World*, vol. 30, no. 1, 2017.

[16] v Santiago-Fandino, S. Sato, N. Maki, and K. Iuchi, "The 2011 japan earthquake and tsunami: Reconstruction and restoration insights and assessment after 5 years," *Natural and Technological Hazards Research*, vol. 47, 2018.

[17] M. Barthelemy, "Morphogenesis of spatial networks," *Springer*, vol. 1, 2018.

[18] W. Harrop and A. Matteson, "Cyber resilience: A review of critical infrastructure networks and cyber security protection measures in the uk and usa," *Journal of Business continuity and Emergency Planning*, vol. 7, no. 2, 2013.

[19] K. Hemme, "Critical infrastructure protection: Maintenance is national security," *Journal of Strategic Security*, vol. 8, no. 5, 2015.

[20] M. Buzby, "Outdated infrastructure poses national security risk," *Defense Transportation Journal*, vol. 73, no. 1, 2017.

[21] M. Barthélemy, P. Bordin, H. Berestycki, and M. Gribaudi, "Self-organization versus top-down planning in the evolution of a city," *Scientific Reports*, vol. 3, 2013.

[22] E. Strano, V. Nicosia, V. Latora, S. Porta, and M. Barthélemy, "Elementary processes governing the evolution of road networks," *Scientific Reports*, vol. 2, 2012.

[23] E. Strano, A. Giometto, S. Shai, E. Bertuzzo, P. J. Mucha, and A. Rinaldo, "The scaling structure of the global road network," *Royal Society Open Science*, vol. 4, no. 10, 2017.

[24] V. Kalapala, V. Sanwalani, A. Clauset, and C. Moore, "Scale invariance in road networks," *Physical Review E Statistical Nonlinear Soft Matter Physics*, vol. 73, no. 2, 2006.

[25] L. bettencourt, J. Lobo, D. Helbing, C. Kuhnert, and G. West, "Grwoth, inovation, scaling, and the pace of life in cities," *PNAS*, vol. 104, no. 17, 2007.

[26] T. Vicsek, "Fractal growth phenomena." World Scientific, 1989.

[27] G. West, "Scale: The universal laws of growth, innovation, sustainability, and the pace of life in organisms, cities, economies, and companies." Penguin Press, 2017.

[28] B. Mandelbrot, "How long is the coast of britain? statistical self-similarity and fractional dimension," *Science*, vol. 156, no. 3775, 1967.

[29] ——, "The fractal geometry of nature." Freeman, 1983.

[30] D. Levinson and B. Yerra, "Self organization of surface transportation networks," *Transportation Science*, vol. 40, no. 2, pp. 179–188, 2006.

[31] X. Liu, H. E. Stanley, and J. Gao, "Breakdown of interdependent directed networks," *Proceeding of the National Academy of Science*, vol. 113, no. 5, 2016.

[32] A. P. Masucci, K. Stanilov, and M. Batty, "Limited urban growth: London's street network dynamics since the 18th century," *PLoS One*, vol. 8, no. 8, 2013.

[33] F. McMasters, "Air flow in sewers: Approach to design sewers for both air and water," *AECOM*, 2012.

[34] C. Klinkhamer, J. Zischg, E. Kruegera, S. Yang, F. Blumensaat, C. Urich, T. Kaeseberg, K. Paik, D. Borchardt, J. R. Silva, R. Sitzenfrei, W. Rauch, G. McGrath, P. Krebs, S. Ukkusuri, and P. Rao, "Topological convergence of urban infrastructure networks," *ArXiv*, 2019.

[35] Y. Lu and J. Tang, "Fractal dimension of a transportation network and its relationship with urban growth: A study of the dallas-fort worth area," *Environmental Planning B Planning and Design*, vol. 31, no. 6, pp. 895–911, 2004.

[36] M. Newman, "The structure and function of complex networks," *SIAM*, vol. 45, no. 2, pp. 167–256, 2003.

[37] ——, "Networks: An introduction." Oxford University Press, 2011.

[38] H. Xiao, T. Sun, B. Meng, and L. Cheng, "Complex network analysis for characterizing global value chains in equipment manufacturing," *PLoS One*, vol. 12, no. 1, 2017.

[39] F. Serinaldi and C. G. Kilsby, "When do evolutionary food web models generate complex networks?" *Physica A: Statistical Mechanics and its Applications*, vol. 450, pp. 585–600, 2016.

[40] C. Dal Maso, G. Pompa, M. Puliga, G. Riotta, and A. Chessa, "Voting behavior, coalitions and government strength through a complex network analysis," *PLoS One*, vol. 9, no. 12, 2014.

[41] K. T. Allhoff and B. Drossel, "When do evolutionary food web models generate complex networks?" *Journal of Theoretical Biology*, vol. 334, pp. 122–129, 2013.

[42] Watts and Strogatz, "Collective dynamics of 'small-worlds' networks," *Nature*, vol. 193, 1998.

[43] A. Barabasi and R. Albert, "Emergence of scaling in random networks," *Science*, vol. 286, no. 5439, pp. 509–512, 1999.

[44] A. Clauset, C. R. Shalizi, and M. Newman, "Power-law distributions in empirical data," *Physica A: Statistical Mechanics and its Applications*, vol. 51, no. 4, pp. 661–703, 2009.

[45] A. Corral and A. Deluca, "Fitting and goodness of fit test of non-truncated and truncated power-law distributions," *Acta Geophysica*, vol. 61, no. 6, pp. 1351–1394, 2013.

[46] S. Yang, K. Paik, G. McGrath, C. Urich, P. Kumar, and P. S. C. Rao, "Reducing cascading failure risk by increasing infrastructure network interdependence," *Water Resources Research*, vol. 53, pp. 8966–8979, 2017.

[47] T. Yang, X. Gao, and X. Li, "Simulating csalifornai reservoir operation using the classification and regression tree algorithm combined with a shuffled cross-validation scheme," *Water Resources Research*, pp. 1626–1651, 2016.

[48] E. Krueger, C. Klinkhamer, C. Ulrich, X. Zhan, and P. Rao, "Generic patterns in the evolution of urban water networks: Evidence from a large asian city," *Physical Review E*, vol. 95, no. 3, 2017.

[49] M. Barthélemy, "Spatial networks," *Physics Reports*, vol. 499, pp. 1–101, 2011.

[50] Morris and Barthelemy, "Spatial effects: Transport on interdependent networks," *Networks of Networks: The Last Frontier of Complexity*, 2016.

[51] Anez, Barra, and Perez, "Dual graph representation of transport networks," *Transportation Resources-B*, vol. 3, 1996.

[52] Hu, Jiang, Wang, and Wu, "Urban traffic simulated from the dual representation: Flow, crisis and congestion," *Physics Letters A*, vol. 373, no. 23-24, 2009.

[53] Klinkhamer, Krueger, Zhan, Ukkussuri, and Rao, "Functionaly fractal urban networks: Geospatial co-location and homogeneity of infrastrucutre," *Arxiv*, 2016.

[54] Klinkhamer and Segovia, "Unpublished research dual-representation of sparse brazillian state capital wdns," 2014.

[55] J. Zischg, C. Klinkhamer, X. Zhan, E. Krueger, S. Ukkusuri, P. Rao, W. Rauch, and R. Sitzenfrei, "Evolution of complex network topologies in urban water infrastructure," *World Environmental and Water Resources Congress 2017*, 2017.

[56] C. Barrington-Leigh and A. Millard-Ball, "A century of sprawl in the united states," *Proceedings of the National Academy of Science*, vol. 112, no. 27, pp. 8244–8249, 2015.

[57] M. Mair, J. Zischg, W. Rauch, and R. Sitzenfrei, "Where to find water pipes and sewers?on the correlation of infrastructure networks in the urban environment," *Water*, vol. 9, no. 2, 2017.

[58] M. Mair, W. Rauch, and R. Sitzenfrei, "Improving incomplete water distribution system data," *Procedia Engineering*, vol. 70, pp. 1055–1062, 2014.

[59] Blumensaat, Wolfram, and Krebs, "Sewer model development under minimum data requirements," *Environmental Earth Sciences*, vol. 65, no. 5, 2011.

[60] T. Carletti, F. Gargiulo, and R. Lambiotte, "Preferential attachment with partial information," *European Physical Journal B*, vol. 88, no. 18, 2015.

[61] X. Z. P. S. C. R. R. S. Jonatan Zischg, Christopher Klinkhamer, "A century of topological coevolution of complex infrastructure networks in an alpine city," *Complexity*, 2019.

[62] G. J. Baxter, S. N. Dorogivstev, A. V. Goltsev, and J. F. F. Mendes, "Avalanches in multiplex and interdependent networks," in *Networks of Networks: The Last Frontier of Complexity*, 2014.

[63] S. V. Buldyrev, R. Parshani, G. Paul, H. E. Stanley, and S. Havlin, "Catastrophic cascade of failures in interdependent networks," *Nature*, vol. 464, no. 7291, pp. 1025–1028, 2010.

[64] M. Korkali, J. G. Veneman, B. F. Tivnan, J. P. Bagrow, and P. D. Hines, "Reducing cascading failure risk by increasing infrastructure network interdependence," *Scientific Reports*, vol. 7, 2017.

[65] R. M. DSouza, C. D. Brummitt, and E. A. Leicht, "Modeling interdependent networks as random graphs: Connectivity and systemic risk," in *Networks of Networks: The Last Frontier of Complexity*, 2014.

[66] B. A. Carreras, D. E. Newman, I. Dobson, V. E. Lynch, and P. Gradney, "Thresholds and complex dynamics of interdependent cascading infrastructure systems," *Networks of Networks: The Last Frontier of Complexity*, 2016.

[67] E. Rome, P. Langeslag, and A. Usov, "Federated modelling and simulation for critical infrastructure protection," *Networks of Networks: The Last Frontier of Complexity*, 2016.

[68] K.-M. Lee, J. Y. Kim, W.-k. Cho, K. I. Goh, and I. M. Kim, "Correlated multiplexity and connectivity of multiplex random networks," *New Journal of Physics*, vol. 14, no. 1, 2012.

[69] K. D, G. J, X. Huang, S. Shao, I. Vodenska, S. Bulydrev, G. Paul, H. Stanley, and S. Havlin, "Network of interdependent networks: Overview of theory and applications," in *Networks of Networks: The Last Frontier of Complexity*, 2014.

[70] R. Albert, H. Jeong, and A. Barabasi, "Error and attack tolerance of complex networks," *Nature*, vol. 406, 2000.

[71] Barabasi, "Love is all you need," *https://www.barabasilab.com/post/love-is-all-you-need*, 2018.

[72] Rinaldo, Rigon, Banavar, Maritan, and Rodriguez-Iturbe, "Evolution and selection of river networks: statics, dynamics, and complexity," *PNAS*, vol. 111, no. 7, 2014.

[73] X. Zhan, S. V. Ukkusuri, and P. S. C. Rao, "Exploring the evolution of london's street network in the information space: a dual approach," *Physical Review E*, vol. 96, no. 5, 2017.

[74] K. Lee, Y. K., S. Lee, and K.-I. Goh, "Multiplex networks," in *Networks of Networks: The Last Frontier of Complexity*, 2014.

[75] M. Mair, R. Sitzenfrei, M. Moderl, and W. Rauch, "Identifying multi utility network similarities," *World Environmental and Water Resources Congress 2012: Crossing Boundaries*, pp. 3147–3153, 2012.

[76] H. Ronellenfitsch and E. Katifori, "Global optimization, local adaptation, and the role of growth in distribution networks," *Physical Review Letters*, vol. 104, 2010.

[77] Corson, "Fluctuations and redundancy in optimal transport networks," *Physical Review Letters*, vol. 104, 2010.

[78] D. L. Bryan and M. E. O'kelly, "Hubandspoke networks in air transportation: an analytical review," *Journal of regional science*, vol. 39, 1999.

[79] Rice, Roy, and . Rhoads, "River confluences, tributaries, and the fluvial network," *Wiley*, 2008.

[80] J. Zischg, J. D. Reyes-Silva, C. Klinkhamer, E. Krueger, P. Krebs, P. S. C. Rao, and R. Sitzenfrei, "Complex network analysis of water distribution systems in their dual representation using isolation valve information," *EWRI*, 2019.

[81] I. D. of Environmental Management, "Indiana map layer gallery," *IDEM*, 2019.

[82] K. G. Pennell, M. K. Scammell, M. Michael D, J. Ames, B. Weldon, L. Friguglletti, E. M. Suuberg, R. Shen, P. Indeglia, and W. J. Heiger-Bernays, "Sewer gas: An indoor air source of pce to consider durring vapor intrusion investigations," *Groundwater Monitoring and Remediation*, vol. 33, no. 3, pp. 119–126, 2013.

[83] T. McHugh, L. Beckley, T. Sullivan, C. Lutes, R. Truesdale, R. Uppencamp, B. Cosky, J. Zimmerman, and B. Schumacher, "Evidence of a sewer vapor transport pathway at the usepa vapor intrusion research duplex," *Science of the Total Environment*, vol. 598, pp. 772–779, 2017.

[84] R. Reichman, M. Roghani, E. J. Willett, E. Shirazi, and K. G. Pennell, "Air exchanges and alternative vapor entry pathways to inform vapor intrusion exposure risk assessments," *Review of Environmental Health*, vol. 32, no. 1-2, pp. 27–33, 2017.

[85] T. McHugh, P. Loll, and B. Eklund, "Advances in vapor intrusion site investigations," *Journal of Environmental Management*, vol. 204, pp. 783–792, 2017.

[86] M. Roghani, O. P. Jacobs, A. Miller, E. J. Willett, J. A. Jacobs, C. R. Viteri, E. Shirazi, and K. G. Pennell, "Occurrence of chlorinated volatile organic compounds (vocs) in a sanitary sewer system: Implications for assessing vapor intrusion alternative pathways," *Science of the Total Environment*, vol. 616, no. 617, pp. 1149–1162, 2018.

[87] V. Izzo, "Dry cleaners - a major source of pce in groundwater." *California Regional Quality Board*, 1992.

[88] J. Shepherd, R. Corsi, and J. Kemp, "Chloroform in indoor air and wastewater: the role of residential washing machines," *Air Waste Management Association*, vol. 46, pp. 631–642, 1996.

[89] M. Brusseau, K. Carroll, M. Truex, and D. Becker, "Characterization and remediation of chlorinated volatile organic cntaminants in the vadose zone: An overview of issues and approaches," *Vadose Zone Journal*, 2013.

[90] M. Eddy, "Wastewater engineering-treatment/disposal/reuse," *McGraw-Hill*, vol. 2, 1979.

[91] M. Costanza-Robinson and T. C. Brusseau, "Vapor-phase transport of trichloroethane in an intermediate-scale vadose-zone system: Retention processes and tracer-based prediction," *Journal of Contaminant Hydrology*, vol. 145, 2013.

[92] ASCE, "Infrastructure report card: A comprehensive assessment of america's infrastructure," *ASCE*, 2017.

[93] J. Witherspoon, D. Apgar, M. Ward, W. Parker, R. Corsi, C. Quigley, and C. Easter, "Collection system ventilation research report," *CH2M Hill*, 2009.

[94] H. Madsen, T. Hvitved-Jacobsen, and J. Vollertsen, "Gas phase transport in gravity sewers: A methodology for determination if horizontal gas transport and ventilation," *Water Environment Research*, vol. 78, no. 11, 2006.

[95] S. Edwini-Bonsu, ASCE, P. Steffler, and ASCE, "Modelling ventilation in sanitary sewer systems: A system theoretic approach," *Journal of Hydraulic Engineering*, 2006.

[96] M. Ward, R. Corsi, R. Morton, T. Knapp, D. Apgar, C. Quigley, C. Easter, J. Witherspoon, A. Pramanik, and W. Parker, "Characterization of natural ventilation in wastewater collection systems," *Water Environment Research*, vol. 83, no. 3, 2011.

APPENDIX

A. PUBLICATIONS

Topological Convergence of Urban Infrastructure Networks

Christopher Klinkhamer[a,1], Jonathan Zischg[b], Elisabeth Krueger[a,c], Soohyun Yang[a], Frank Blumensaat[d,e], Christian Urich[f], Thomas Kaeseberg[g], Kyungrock Paik[h], Dietrich Borchardt[i], Julian Reyes Silva[g], Robert Sitzenfrei[b], Wolfgang Rauch[b], Gavan McGrath[j], Peter Krebs[g], Satish Ukkusuri[a], and P.S.C. Rao[a,k]

[a]Lyles School of Civil Engineering, Purdue University, West Lafayette, IN, USA; [b]Keramida Inc., Indianapolis, IN, USA; [c]Unit of Environmental Engineering, Department for Infrastructure, University of Innsbruck, Innsbruck, Austria; [d]Helmholtz Centre for Environmental Research, UFZ, Leipzig, Germany; [e]Eawag, Swiss Federal Institute of Aquatic Science and Technology, Dübendorf, Switzerland; [f]ETH Zürich, Institute of Environmental Engineering, Zürich, Switzerland; [g]Monash Infrastructure Research Institute, Department of Civil Engineering, Monash University, VIC, Australia; [h]Institute of Urban Water Management, Technische Universität Dresden, Dresden, Germany; [i]School of Civil, Environmental, and Architectural Engineering, Korea University, Seoul, Korea; [j]Helmholtz Centre for Environmental Research – UFZ, Department of Aquatic Ecosystems Analysis and Management, Magdeburg, Germany; [k]UWA School of Agriculture and Environment, The University of Western Australia, Perth, Australia; [l]Agronomy Department, Purdue University, West Lafayette, IN, USA

This manuscript was compiled on February 5, 2019

Urban infrastructure networks play a major role in providing reliable flows of multitude critical services demanded by citizens in modern cities. We analyzed here a database of 125 infrastructure networks [roads (RN); urban drainage networks (UDN); water distribution networks (WDN)] in 52 global cities, serving populations ranging from 1,000 to 9,000,000. For all infrastructure networks, the node-degree distributions, $p(k)$, derived using undirected, dual-mapped graphs, fit Pareto distributions, $p(k) = \alpha k^{-\gamma}$, $k > 2$, with a mean of $\gamma = 2.49$ and mean $\alpha = 2.41$ [$MSE = 4.85E-7$]. Variance around mean γ reduces substantially as network size increases. Convergence of functional topology of these urban infrastructure networks suggests that their co-evolution results from similar generative mechanisms. Analysis of growing UDNs over non-concurrent 40 year periods in three cities suggests the likely generative process to be partial preferential attachment under geospatial constraints. This finding is supported by high-variance node-degree distributions as compared to that expected for a Poisson random graph. Directed cascading failures, from UDNs to RNs, are investigated. Correlation of node-degrees between spatially co-located networks are shown to be a major factor influencing network fragmentation by node removal. Our results hold major implications for the network design and maintenance, and for resilience of urban communities relying on multiplex infrastructure networks for mobility within the city, water supply, and wastewater collection and treatment.

Network Analysis | Critical Infrastructure | Resilience | Universality

Differences in multiple factors result in cities with stark contrasts in topography, climate, regulations and financial constraints that drive their designs (structure). In addition, readily apparent disparities exist in the functions of urban infrastructure networks (e.g., mobility, water supply, urban drainage, wastewater collection). Beyond structural and functional differences, infrastructure networks evolve at different rates and in diverse patterns in cities (1–4). These networks are comprised of components of mixed ages (because of growth and replacement) and design standards that vary substantially based on local factors (topography, climate, population, density) and management decisions (engineering design, cost, maintenance, regulations) (4–6).

Despite these dissimilarities, infrastructure networks of various types are known to follow certain universal patterns. For example, total length of road or pipes infrastructure scale sub-linearly with urban population, consistent with economies of scale (7). Further, land-use patterns within cities as well as their physical forms are known to follow fractal geometries influenced by essential functions carried out within the city (1, 5).

Recent work shows that because of competition for space within urban areas WDN and UDNs are geospatially co-located with RNs with as much as 80% of the length of subterranean pipe networks in European cities expected to be geospatially co-located with the RN (8). Such high degrees of geospatial co-location suggest that multiple infrastructure networks are likely to co-evolve and exhibit similar topological features, even though these networks have different layouts, and are vastly different in terms of their structure (acyclic and cyclic graphs), functions (type and directionality of flow), and tolerance for failure (frequency and consequences). Major similarities and differences in several attributes of surface (RN) and subterranean (WDN; UDN) networks are summarized in Table 1.

Recent topological analyses, based on dual representations of the water distribution (WDN) and urban drainage networks (UDN) in a large Asian city, revealed that heavy-tailed (Pareto) node-degree distributions $p(k)$ characterize these networks (9), consistent with findings for the topology of RNs at city, national and continental scales (7, 10). Motivated by these findings, we assembled a database of 125 infrastructure networks of different types and sizes (RN, WDN, UDN) for 52 global cities.

Four key questions motivating our study are: (1) how does the functional topology of infrastructure networks vary among and within cities given their diversity?; (2) is there commonality between node-degree distributions, independent of specific functional form?; (3) does a generic generative mechanism underlie the growth of these networks?; and (4) How do failures cascade across geospatially co-located infrastructure networks?

Despite multiple structural, functional, and historical differences, as we show here, we find striking convergence in the functional topologies of RN, WDN, and UDNs across our case study cities. The effects of these findings to network fragmentation are analyzed by investigating cascading failures (directed from UDNs to RNs). These results hold significant implications to network performance, stability and resilience of urban communities relying on multiple critical services.

Table 1. General Comparison of Surface (Road) and Subterranean Infrastructure Networks (Urban Drainage and Water Distribution)

Attribute	Road	Water Distribution	Urban Drainage
Data Availability	Global Availability	Restricted or Confidential	Limited Availability
Structure	Highly looped; all origins to all destinations; cyclic graphs	Less looped; flows directed from one or more sources to all points; sources may be dynamic (emergency flow strategies); cyclic graphs	Typically Branching; flows directed from all points to a single outlet; acyclic graphs
Evolution	Primary Driver traffic demands; mobility	Constrained by road and building placement; multi-objective optimization of costs for maximum flow efficiency, but also for conflicting interests (resilience); ultimate design chosen from pareto fronts as a tradeoff of competing objectives	
Optimal Design	Full, bidirectional connectivity to all origins and destinations, full irregular grids	Loops for redundancy; valves for reliability	Similar to rivers, but less space-filling Branching/gravity driven
Function	Multi origin multi destination transport	Single (or few) origin multi destination	Multi origin single (or few) destinations
Management / Maintenance	Disrupts flow of traffic	Requires closing valves or diversions, disrupting water or wastewater transport; may also result in traffic disruptions on roads due to co-location	
Reliability	Highly reliable, locally vulnerable to failures	Highly reliable, vulnerable to failures, impacted population may be higher than roads	Reliable, high-tolerance to failures (urban flooding); largely externalized to other networks (roads, rivers)
Direction of Failure Cascades	Heavy traffic reduces lifetime of subterranean infrastructure	Bursts affect roads, leaking pipes leads to pressure losses and service disruptions	Roadways flooding; potholes, road segments collapse

Topology of Infrastructure Networks

The structure of a network is often less important from a management standpoint, than the functions of the network. Traditional network analysis, the primal representation, of infrastructure networks, with intersections as nodes and segments as edges, reveals the structure of the network, but fails to identify key functional aspects related to the use of the networks (11). If instead we consider the dual representation of infrastructure networks (3, 11), where in an entire length of a road or pipe is considered a node and each intersection a link we can explore the information space of the network where functional aspects are revealed by giving importance to key attributes of network segments that influence how they are utilized (e.g., speed limit; pipe size; angle of incidence) (3, 9, 11). Such analyses reveal universal similarities in network graphs following heavy-tailed, Pareto node-degree distributions [p(k)] (7, 9, 10, 12).

We begin by examining p(k) using dual representation for 125 infrastructure networks consisting of RN, UDN and WDNs in 52 global cities [see SI for details of dual representation]. We find striking consistency in their probability density functions, p(k), for all studied infrastructure networks (Figure 1) exhibit striking consistency across all three infrastructure-network types in all cities, despite distinct differences in sizes (proportional to populations served), resolution of data available, and their physical layouts. For each of the three network types, we find the mean slope (γ) of p(k) to be in a narrow range of 2.35 to 2.6. Variability of p(k) between individual networks (Figure 2) was found to sharply decrease as network size increases, converging to values near the mean of $\gamma = 2.49$ [$MSE <= 4.85E-7$].

High Node-Degree Variance in Urban Infrastructure Topology

Fitting Pareto distributions to empirical node-degree distributions is fraught with methodological challenges and controversies in interpretations regarding scale-invariance within a finite range (i.e., due to the finite size of physical networks) (13, 14). However, our goal here is not to definitively assign scale-free (or any other) distributions to these data, but instead to show that sufficient variance exists within p(k) to approximate the properties of scale-free random graphs. Multiple previous studies have shown that scale-free and other networks with highly variable node-degree distributions, identified by comparing variance

Please provide details of author contributions here.

The authors declare no conflict of interest.

[1]To whom correspondence should be addressed. E-mail: cklinkhapurdue.edu

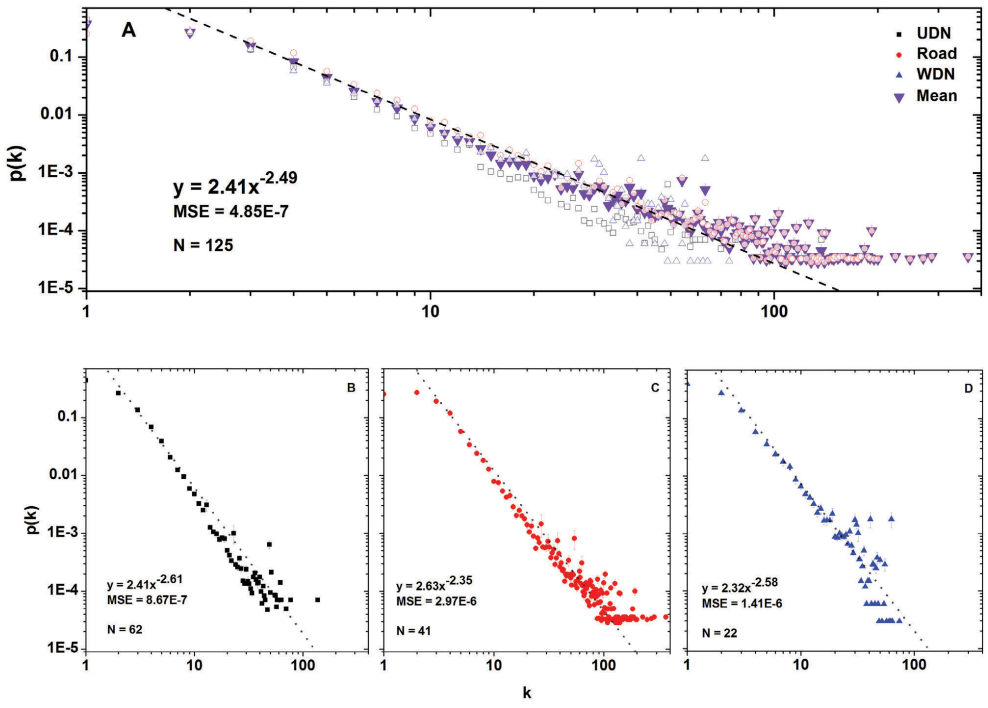

Fig. 1. (A) Mean p(k) (purple triangle; n = 125) of node-degree distributions (dual representation; n = 62) for all UDN (black square; n = 41) RN (red circle; n = 22), and WDNs (blue triangle (B) Mean p(k) of UDNs ; (C) Mean p(k) of RNs; (D) Mean p(k) of WDNs. Regression lines are shown for fits to Pareto probability density functions, $p(k) = \alpha k^{-\gamma}$, $k > 2$, with (A): $\alpha = 2.41$; $\gamma = 2.49$; $MSE = 4.85E-7$ (B): $\alpha = 2.41$; $\gamma = 2.61$; $MSE = 8.67E-7$ (C): $\alpha = 2.63$; $\gamma = 2.35$; $MSE = 2.97E-6$ (D): $\alpha = 2.32$; $\gamma = 2.58$; $MSE = 1.41E-6$

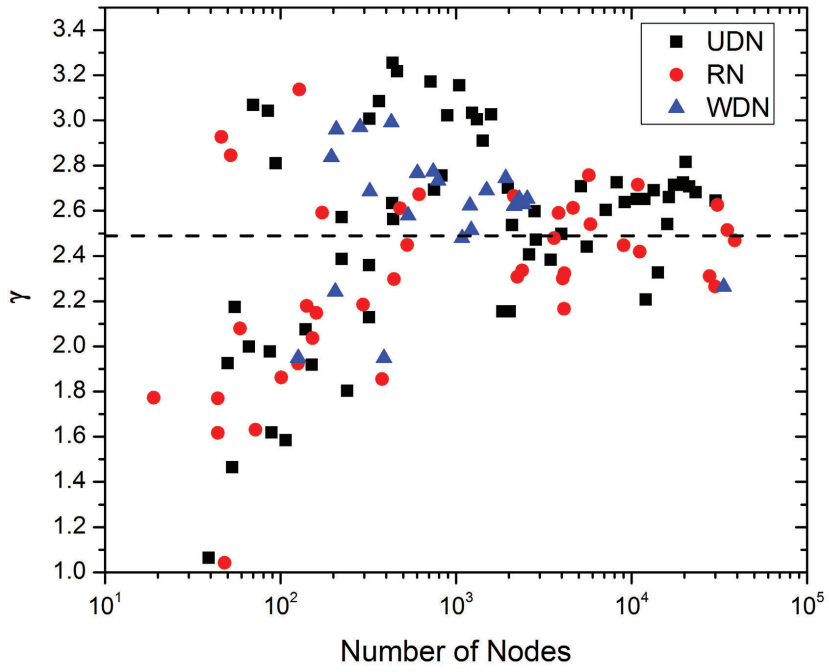

Fig. 2. gamma values for all UDN (black square; n = 62), RN (red circle; n = 41) and WDNs (blue triangle; n = 22). Dashed line represents mean gamma value of all networks; $\gamma = 2.49$. (γ) values are shown to rapidly approach the mean and decrease in variance network size increases. A reduction in variance is observed beyond a threshold network size of 2,000 nodes.

to that expected of a similar random graph, are highly robust against random failure of nodes but are susceptible to the loss of high-degree nodes (15–18).

Figure 3 compares the variance in node-degree of the networks studied here to that of a Poisson random graph of equal average node degree, <k>. In all cases, the variability of the real-world infrastructure networks exceeds that of a random graph, indicating that these networks are likely to resemble "scale-free" graphs in terms of their functional topological properties, and similar failure dynamics (i.e., robustness to random failure, vulnerability to targeted attack), the latter having significant implications for urban community resilience (19–27).

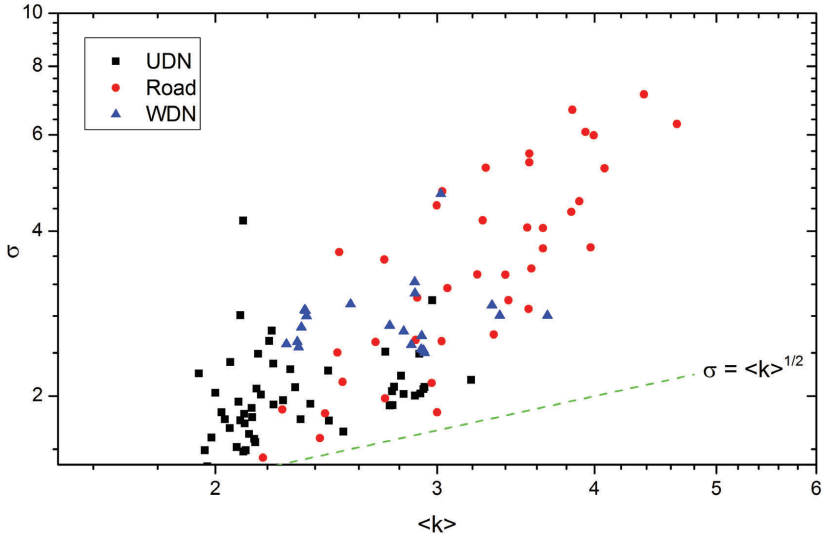

Fig. 3. <k> vs variance for all infrastructure networks (RN: red circle, UDN: black square, and WDN: blue triangle. The variance within the node-degree for each infrastructure network is shown to be greater than that expected of a random graph (dashed green line; $\sigma =< k >^{1/2}$), suggesting that these networks would likely exhibit failure dynamics typical of scale-free random graphs.

Spatially Constrained Preferential Attachment

The convergence of functional topology of three types of urban infrastructure networks in 52 diverse cities suggests similar generative mechanisms with constraints for engineering design-optimization (cost; efficiency). Recent studies further highlight this trend toward topological convergence, having shown that evolving networks and subnetwork components rapidly develop heavy-tailed distributions, and converge to the slope of the larger, "mature" networks (9) (28).

In network science preferential attachment is a well-known generative mechanism, involving a preference for new links added to the network to attach to existing high node-degree hubs, resulting in scale-free random graphs (29). This model requires that each new node entering the existing network posses complete knowledge of network connectivity in order to preferentially select an existing, high-degree hub to attach itself to. This is often not the case in real networks and the addition of new nodes confronts various constraints including, partial knowledge of connectivity, and in the case of spatial networks, topography and associated costs (30, 31).Variations of the preferential attachment generative mechanism are characterized by different degrees and types of tempering(30).

Here, we analyzed UDN growth in three different cities each over non-concurrent 40-year time lines, offering direct evidence for a variation of preferential attachment as the generative mechanism. We refer to this process as spatially constrained preferential attachment, the constraint likely being imposed by engineering and costs concerns related to the long and convoluted pipe routing that would be necessary to achieve perfect preferential attachment.

At all time-steps during the growth of these UDNs, new additions to the network are shown to be much less likely to attach to existing nodes in the 1st (lowest) quintile of node-degrees and with a preference to attach to nodes in the 2-5th quintiles (Figure 4A and B). At all time-steps, new additions to the network are most likely to attach to existing nodes in the 2nd

quintile of node-degree. This pattern of UDN growth likely results from spatial and cost constraints in the placement of new infrastructure, influencing engineers to attach new components to the nearest existing feature of sufficient capacity, resulting in a geospatially constrained preferential attachment growth mechanism.

Infrastructure Network Disruptions

For the networks reported here we observe a mean co-location of over 60% of the total length of the UDNs with RNs across the studied cities at a buffer distance of 15m from the road centerline (See SI). Thus, we infer that these spatially coupled infrastructure multiplex networks may be vulnerable to fragmentation due to the loss of relatively few components, particularly at smaller scales (e.g. small cities and neighborhoods). Some smaller infrastructure networks are also shown to have $\gamma > 3$, a known threshold at which point percolation (i.e., fragmentation) transitions occur from a second-order to a first-order process (32). As a result failures causing total fragmentation of the networks via the removal of only a small percentage of nodes are more likely in smaller networks or neighborhoods as a result of spatial variability, within subnets of a given infrastructure network. It is unlikely however that failures of this type would cascade through the extent of a large city due to neighborhood level variability. (See SI for analysis of spatial variability within infrastructure networks).

In isolation, networks with heavy-tailed p(k) (i.e. with high variance node-degree distributions) exhibit known failure dynamics wherein the underlying network is robust against fragmentation caused by random removal, but vulnerable to the targeted removal of important nodes (e.g., high node-degree; or centrality hubs) (15). However, research on coupled or multiplex networks has shown that coupling two randomly generated scale free graphs alter the normal failure dynamics of scale-free random graphs, resulting in vulnerability to failures of all types (random or targeted) (19–21, 24–27, 33). The severity of this behavior is influenced by the orientation and connection strategies between coupled networks. However, many of these theoretical studies have been conducted on randomly generated networks that differ significantly from the empirical networks studied here. Typical assumptions include full interconnectivity, networks of equal size, and with the potential for cascades to occur in either direction between networks. All of these are assumptions that are not true of the city-scale empirical networks presented here (34, 35).

Here we investigate directed cascading failures (from UDNs to RNs) for 32 cities for which data were available. Random removal of RN segments spatially co-located with UDN segments is shown to result in fragmentation of the networks (See figure 5). The speed with which the networks fragment however is variable with some networks showing greater than expected robustness (those above the dashed line and others displaying less than expected robustness (Those below the dashed line). This variance is explained by correlations between the node-degree of spatially co-located UDN and RN features, Figure 5C. A tendency for lower node-degree features to co-locate is observed, as population increases while in lower population cities, high node-degree features are more commonly located with each other leading to rapid fragmentation of the coupled networks. These results highlight the significance of separating high node-degree features when planning the city layout.

Conclusions and Implications

Complex networks are ubiquitous in natural, engineered and social systems, with important examples including river networks (36), regional and global trade networks (37), social networks (38), as well as communication, mobility, and water infrastructure networks (31, 39, 40). Together, these interdependent, multiplex networks compose the urban fabric and provide diverse critical services in cities at multiple spatial and temporal scales. Furthermore, due to their interdependence and co-location, disruptions in one network may be able propagate to another (19). Therefore, characterizing the structure (topology), functions (flows), and interdependence of urban infrastructure networks has become a major topic of research in a broad range of disciplines with wide ranging applications (1, 19, 31, 41–43).

Road networks (RN) are known to evolve sometimes in a decentralized growth pattern from simple grid-patterns to more complex layouts, while in other cases in the opposite direction, to increasingly more gridded patterns under centralized design and expansion (44). Quantifying the similarities in structure of globally distributed RNs has been a major focus of complex infrastructure network analysis, revealing graphs $[R(N, E)]$ that are remarkably similar despite differences in the geographical constrains, history, and design philosophies influencing the evolution of RNs over time (5, 10, 44, 45). Data for subterranean infrastructure networks, such as urban drainage networks (UDN) and water distribution networks (WDN), are not readily available due to security and confidentiality concerns. As such, these networks have received considerably less attention from a complex network analysis standpoint (41, 46–49).

Our findings suggest that a universal scaling exists for functional topology [e.g., Pareto node-degree distribution; $p(k) = \alpha k^{-\gamma}$, $k > 2$ for three urban infrastructure networks [RN; UDN; WDN] in 52 diverse global cities. Cities exhibit fractal geometries in terms of space-filling attributes of aboveground physical assets (1, 6, 7, 44, 47). Roads and subterranean infrastructure networks (UDN, WDN) in cities occupy the spaces between physical assets, such as buildings (8). Thus, geospatially co-located infrastructure networks exhibit comparable self-similar patterns.

Growth of three UDNs are shown to exhibit properties of spatially constrained partial preferential attachment. Our findings also reveal these networks to highly variable node-degree distributions with heavy tailed p(k). These properties suggest that these real-world networks while robust against random failures may be vulnerable to the loss of high node-degree hubs (15, 29). Furthermore, the observed geospatial co-location of infrastructure networks within cities introduces the possibility for cascading failures affecting multiple infrastructure networks. In an urban infrastructure context these cascading failures are likely to be predominantly directed from subterranean UDNs or WDNs to the overlying RN (23, 47, 50). Examples of these types

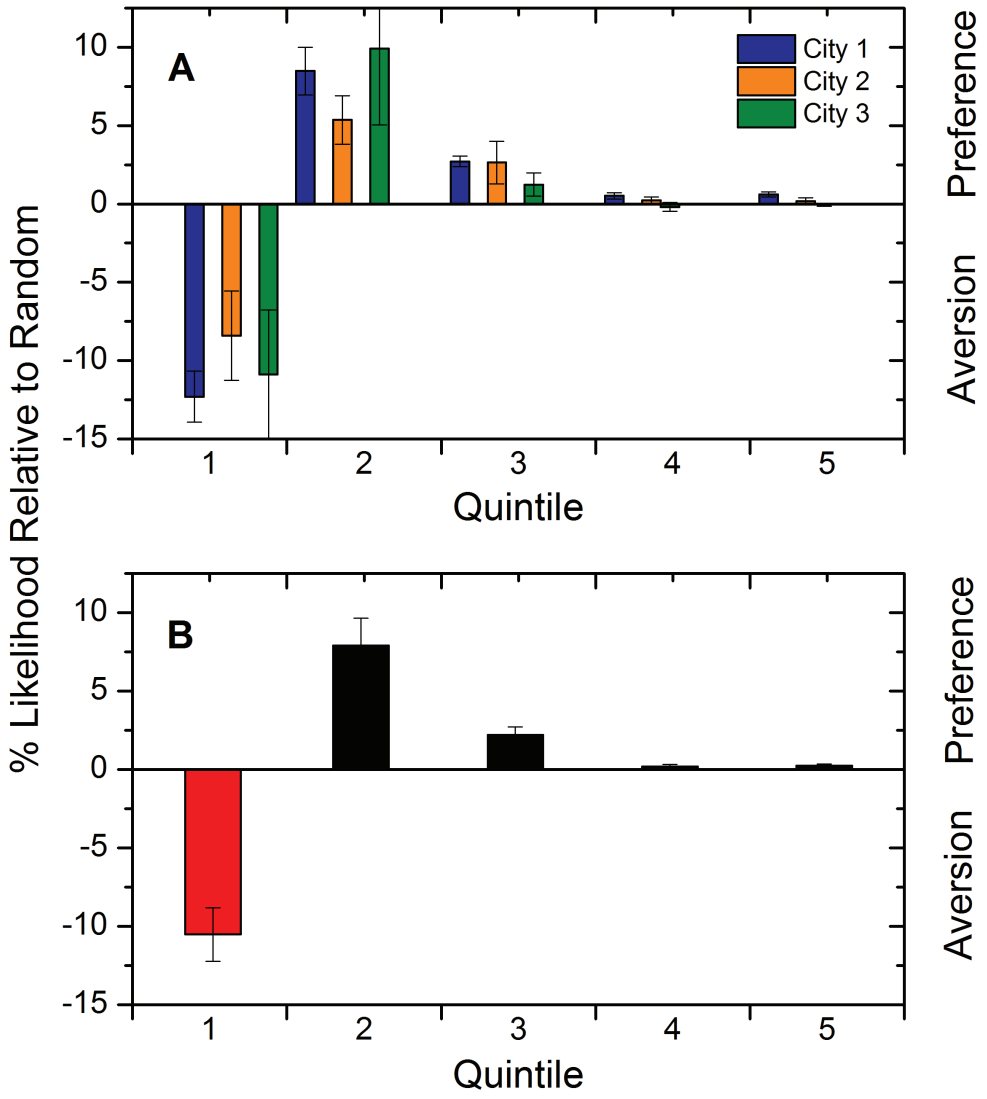

Fig. 4. Average attachment of of new network components for individual cities (A) and for all cities (B). In all cases there is an observed aversion for new network components to attach to existing components in the first quintile (lowest 20%) of node-degree and a preference for attachment to second quintile (21st - 40th%) and third quintile (41st -

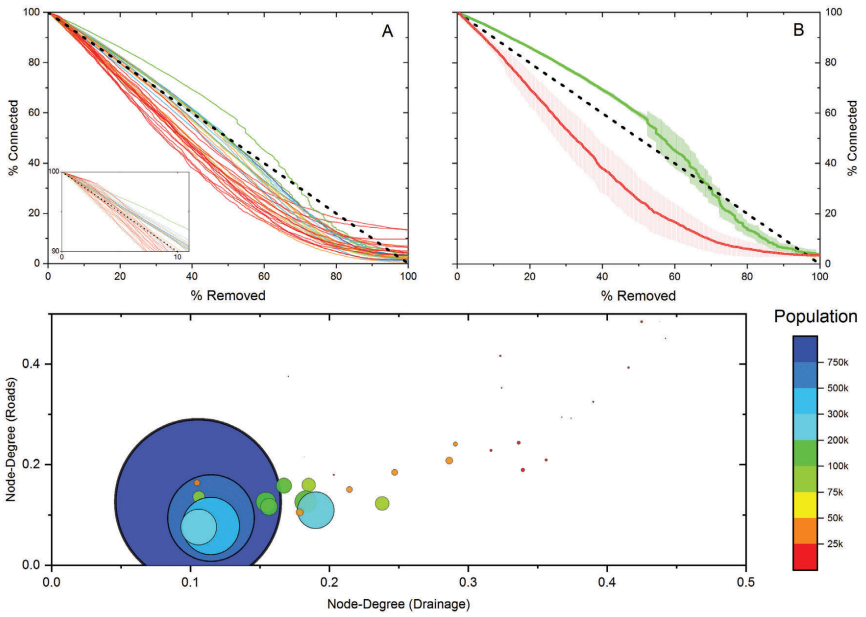

Fig. 5. (A) Percent connectivity of the largest connected component of all studied road networks vs percent of interconnected nodes removed. dashed-line indicates indicates 1:1 line of connectivity vs removal. networks above this line indicate greater robustness to failure than networks below the 1:1 line. Inset shows first 20% of removal in greater detail. (B) The least (red) and most (blue) robust networks are highlighted. Shaded areas indicate standard deviation of 100 repetitions of random node removal. The more robust network retains connectivity far longer than the smaller, less robust network. (C) Correlations in node-degree between co-located drainage and road networks are shown. Smaller networks tend to have a higher ratio of co-location between high node-degree features leading to a decrease in robustness as nodes are randomly removed. Size of circles and color correspond to urban area population.

of cascades may include leaking pipes leading to soil subsidence in turn causing the collapse of road segments, or bursts of pressurized water pipes, storm events overwhelming the UDN resulting in surface flooding rendering the RN impassable (51). Similarly, wash out of roads during large storms can also damage WDN and UDN.

Fragmentation of RNs resulting from cascading failures were shown to differ significantly from theoretical models. All cities displayed robustness to random removal of co-located features with larger cities, and those with separation of high-node-degree feature displaying increased robustness to removal.Smaller cities or subnets, may exhibit features such as near complete geospatial co-location of networks and have topological properties such as very steep NDDs ($\gamma > 3$) that alter the nature of failure cascades across networks by shifting the percolation from a continuous, second-order transition to a discontinuous first-order transition (32). These subnets represent opportunities for managers and city planners to address localized risks through planned maintenance or expansion by redesigning or relocating network features while maintaining city-wide performance and enhance urban community resilience.

Materials and Methods

Network data were obtained in the form of GIS shapefiles from a variety of sources including local governments, private companies, research institutions, and OpenStreetMap. These data were first cleaned using ESRI ArcGIS 10.1.1 to ensure network continuity. Raw shape files were cleaned and analyzed following a five-step process:

1. Using ArcGIS Create a geometric network from OpenStreetMap data (Snap at 0.001m, Enable complex edges)
2. Using the snapped file create a Network Dataset (Enable all vertex connectivity)
3. Export the newly created road and junction features as shapefiles
4. Run the Split Line at Points tool to split the exported road shapefile (Search radius at 0.001m)
5. Extract the graph from the split shapefile via the NetworkX Python package

Output of this process is in the form of edge and node lists that were then analyzed in Matlab R2016b.

We estimated topological metrics for each infrastructure network by considering the dual representation, as described by Massucci et al (11). For RNs, this process consisted of two rules that must be met for two edges (road segments) to be joined into a dual node: 1.) the angle between the two road segments must not deviate from a straight line by more than 45°, and 2.) all road segments to be joined into a dual edge must be of the same speed limit. In drainage networks, the vast majority of junctions occur at either 45 or 90°. As such the rules for joining to pipe segments into a dual node were relaxed with the only necessary criteria being that each segment to be joined be of the same diameter. All analyses in this study are based on the dual representation.

Node-degree distributions were fitted as Pareto distributions based on Maximum Likliehood Estimation, following the methods proposed by Clauset et al, and Corral and DeLuca (13, 14). We further assess the appropriateness of Pareto fits to the p(k) of the node-degree distributions using two well-accepted approaches for detecting "scale-free" properties of complex networks. First, we directly examine the variance of the node-degree distribution of the empirical pdfs and compare to that of a random network (i.e., a Poisson random graph) of identical average node-degree (<k>). Second, we identify the generative mechanism (preferential attachment) necessary to generate scale-free graphs through the analysis of the evolution of three UDNs over non-concurrent 40 year intervals at 5 year time steps

Fragmentation of the largest connected RN component was analyzed by simulating directed cascading failures (from UDNs to RNs). RN features co-located with UDN features were removed from the network one-by-one and the largest connected component was measured. Simulations were repeated 100 times to account for variability resulting from the order of node removal. All analyses were conducted using Matlab R2015B.

ACKNOWLEDGMENTS. This research was supported by NSF Award Number 1441188 (Collaborative Research– RIPS Type 2: Resilience Simulation for Water, Power and Road Networks). CK was funded by the NSF grant, while EK was supported by the Helmholtz Center for Environmental Research, Leipzig, Germany, and by a Graduate Fellowship from the Purdue Climate Change Research Center. Additional financial support for the last author (PSCR) was provided by the Lee A. Reith Endowment in the Lyles School of Civil Engineering, Purdue University, and partially by the NSF grant. RS and JZ: This research is partly funded by the Austrian Research Promotion Agency (FFG) within research project ORONET (project number: 858557).

1. Batty M, Longley P (1994) Fractal cities: a geometry of form and function. (Springer).
2. Lu Y, Tang J (2004) Fractal dimension of a transportation network and its relationship with urban growth: A study of the dallas-fort worth area. *Environmental Planning B Planning and Design* 31(6):895–911.
3. Masucci AP, Stanilov K, Batty M (2013) Limited urban growth: London's street network dynamics since the 18th century. *PLoS One* 8(8).
4. Barrington-Leigh C, Millard-Ball A (2015) A century of sprawl in the united states. *Proceedings of the National Academy of Science* 112(27):8244–8249.
5. Batty M (2008) The size, scale, and shape of cities. *Science* 319(5864):769–771.
6. Batty M (2002) The new science of cities. (MIT Press).
7. Strano E, et al. (2017) The scaling structure of the global road network. *Royal Society Open Science* 4(10).
8. Mair M, Zischg J, Rauch W, Sitzenfrei R (2017) Where to find water pipes and sewers?—on the correlation of infrastructure networks in the urban environment. *Water* 9(2).
9. Krueger E, Klinkhamer C, Ulrich C, Zhan X, Rao P (2017) Generic patterns in the evolution of urban water networks: Evidence from a large asian city. *Physical Review E* 95(3).
10. Kalapala V, Sanwalani V, Clauset A, Moore C (2006) Scale invariance in road networks. *Physical Review E Statistical Nonlinear Soft Matter Physics* 73(2).
11. Masucci AP, Stanilov K, Batty M (2014) Exploring the evolution of london's street network in the information space: a dual approach. *Physical Review E* 89(1).
12. Zhan X, Ukkusuri SV, Rao PSC (2017) Exploring the evolution of london's street network in the information space: a dual approach. *Physical Review E* 96(5).
13. Clauset A, Shalizi CR, Newman M (2009) Power-law distributions in empirical data. *Physica A: Statistical Mechanics and its Applications* 51(4):661–703.
14. Corral A, Deluca A (2013) Fitting and goodness of fit test of non-truncated and truncated power-law distributions. *Acta Geophysica* 61(6):1351–1394.
15. Albert R, Jeong H, Barabasi A (2000) Error and attack tolerance of complex networks. *Nature* 406.
16. Bao ZJ, Cao YJ, Ding LJ, Wang GZ (2009) Comparison of cascading failures in small-world and scale-free networks subject to vertex and edge attacks. *Physica A: Statistical Mechanics and its Applications* 388(20):4491–4498.
17. Song C, Havlin S, Makse H (2005) Self-similarity of complex networks. *Nature* 433.
18. Wang J, Rong L, Zhang L, Zhang Z (2008) Attack vulnerability of scale-free networks due to cascading failures. *Physica A: Statistical Mechanics and its Applications* 387(26):6671–6678.
19. DAgostino G, Scala A (2014) Networks of networks: The last frontier of complexity. (Springer).
20. Baxter GJ, Dorogivstev SN, Goltsev AV, Mendes JFF (2014) Avalanches in multiplex and interdependent networks in *Networks of Networks: The Last Frontier of Complexity*.

21. Lee K, K. Y, Lee S, Goh KI (2014) Multiplex networks in *Networks of Networks: The Last Frontier of Complexity*.
22. Baroud H, Barker K, Ramirez-Marquez J, Rocco C (2014) Inherent costs and interdependent impacts of infrastrucure network resilience. *Risk Analysis* 35(4).
23. Chan C, Duenas-Osorio L (2014) Spatial-temporal quantification of interdependencies across infrastrucure networks in *Networks of Networks: The Last Frontier of Complexity*.
24. Dal Maso C, Pompa G, Puliga M, Riotta G, Chessa A (2014) Voting behavior, coalitions and government strength through a complex network analysis. *PLoS One* 9(12).
25. DSouza RM, Brummitt CD, Leicht EA (2014) Modeling interdependent networks as random graphs: Connectivity and systemic risk in *Networks of Networks: The Last Frontier of Complexity*.
26. Lee KM, Kim JY, Cho Wk, Goh KI, Kim IM (2012) Correlated multiplexity and connectivity of multiplex random networks. *New Journal of Physics* 14(1).
27. Liu X, Stanley HE, Gao J (2016) Breakdown of interdependent directed networks. *Proceeding of the National Academy of Science* 113(5).
28. Yang S, et al. (2017) Reducing cascading failure risk by increasing infrastructure network interdependence. *Water Resources Research* 53:8966–8979.
29. Barabasi A, Albert R (1999) Emergence of scaling in random networks. *Science* 286(5439):509–512.
30. Carletti T, Gargiulo F, Lambiotte R (2015) Preferential attachment with partial information. *European Physical Journal B* 88(18).
31. Barthélemy M (2011) Spatial networks. *Physics Reports* 499:1–101.
32. Bastas N, Giazitzidis P, Maragakis M, Kosmidis K (2014) Explosive percolation: Unusual transitions of a simple model. *Physica A: Statistical Mechanics and its Applications* 407:54–65.
33. Buldyrev SV, Parshani R, Paul G, Stanley HE, Havlin S (2010) Catastrophic cascade of failures in interdependent networks. *Nature* 464(7291):1025–1028.
34. Radicchi F (2014) Driving interconnected networks to supercriticality. *Physical Review X* 4.
35. Radicchi F (2015) Percolation in real interdependent networks. *Nature Physics* 11.
36. Serinaldi F, Kilsby CG (2016) When do evolutionary food web models generate complex networks? *Physica A: Statistical Mechanics and its Applications* 450:585–600.
37. Xiao H, Sun T, Meng B, Cheng L (2017) Complex network analysis for characterizing global value chains in equipment manufacturing. *PLoS One* 12(1).
38. Jackson M (2007) Social and economic networks.
39. Newman M (2003) The structure and function of complex networks. *SIAM* 45(2):167–256.
40. Newman M (2011) Networks: An introduction. (Oxford University Press).
41. Mair M, Sitzenfrei R, Moderl M, Rauch W (2012) Identifying multi utility network similarities. *World Environmental and Water Resources Congress 2012: Crossing Boundaries* pp. 3147–3153.
42. Rosvall M, Trusina A, Minnhagen P, Sneppen K (2005) Networks and cities: an information perspective. *Physical Review Letters* 94(2).
43. Guo Y, Walters G, Savic D (2008) Optimal design of storm sewer networks: Past, present and future. *11th International Conference on Urban Drainage*.
44. Strano E, Nicosia V, Latora V, Porta S, Barthélemy M (2012) Elementary processes governing the evolution of road networks. *Scientific Reports* 2.
45. Levinson D, Yerra B (2006) Self organization of surface transportation networks. *Transportation Science* 40(2):179–188.
46. Mair M, Rauch W, Sitzenfrei R (2014) Improving incomplete water distribution system data. *Procedia Engineering* 70:1055–1062.
47. Strano E, Shai S, Dobson S, Barthelemy M (2015) Improving incomplete water distribution system data. *Journal of the Royal Society Interface* 12(111).
48. Yazdani A, Jeffrey P (2011) Complex network analysis of water distribution systems. *Chaos* 21(1).
49. Yazdani A, Jeffrey P (2012) Water distribution system vulnerability analysis using weighted and directed network models. *Water Resources Research* 48(6).
50. Kroger W, Nan C (2014) Addressing interdependencies of complex technical networks in *Networks of Networks: The Last Frontier of Complexity*.
51. Izadi E (2016) Massive sinkhole along florence river swallows dozens of cars in *Washington Post*.

Hindawi
Complexity
Volume 2019, Article ID 2096749, 16 pages
https://doi.org/10.1155/2019/2096749

WILEY | Hindawi

Research Article

A Century of Topological Coevolution of Complex Infrastructure Networks in an Alpine City

Jonatan Zischg,[1] **Christopher Klinkhamer**,[2] **Xianyuan Zhan**,[3] **P. Suresh C. Rao**,[2] **and Robert Sitzenfrei**[1]

[1] *Unit of Environmental Engineering, Department of Infrastructure, University of Innsbruck, Technikerstrasse 13, 6020 Innsbruck, Austria*
[2] *Lyles School of Civil Engineering, Purdue University, 550 Stadium Mall Drive, West Lafayette, IN 47907, USA*
[3] *Urban Computing Business Unit, JD Finance No. 18 Kechuang 11 Street, Beijing, China*

Correspondence should be addressed to Jonatan Zischg; jonatan.zischg@uibk.ac.at

Academic Editor: Albert Diaz-Guilera

In this paper, we used complex network analysis approaches to investigate topological coevolution over a century for three different urban infrastructure networks. We applied network analyses to a unique time-stamped network data set of an Alpine case study, representing the historical development of the town and its infrastructure over the past 108 years. The analyzed infrastructure includes the water distribution network (WDN), the urban drainage network (UDN), and the road network (RN). We use the dual representation of the network by using the Hierarchical Intersection Continuity Negotiation (HICN) approach, with pipes or roads as nodes and their intersections as edges. The functional topologies of the networks are analyzed based on the dual graphs, providing insights beyond a conventional graph (primal mapping) analysis. We observe that the RN, WDN, and UDN all exhibit heavy tailed node degree distributions [$P(k)$] with high dispersion around the mean. In 50 percent of the investigated networks, $P(k)$ can be approximated with truncated [Pareto] power-law functions, as they are known for scale-free networks. Structural differences between the three evolving network types resulting from different functionalities and system states are reflected in the $P(k)$ and other complex network metrics. Small-world tendencies are identified by comparing the networks with their random and regular lattice network equivalents. Furthermore, we show the remapping of the dual network characteristics to the spatial map and the identification of criticalities among different network types through co-location analysis and discuss possibilities for further applications.

1. Introduction

Many complex systems can be described as networks [1], and with recent increases in computing power it is now feasible to investigate the topologies of entire networks consisting of high-resolution data [2]. Examples of these types of investigations range from molecular interaction networks (e.g., protein interactions of cells) and social networks (e.g., communication between humans) to global transportation systems and individual human mobility [3–6].

Despite the differences in various types and representations of these networks, important commonalities exist. The analysis of complex networks gives insight to structural morphologies, similarities, recurring patterns, and scaling laws [7, 8]. The applications are multifaceted: identification of central nodes; prediction of future developments and network growth; information transfer; identification of vulnerabilities to enhance security [9]; and improvement of network resilience [10, 11]. Complex network analyses of critical infrastructure, such as water distribution networks (WDNs) and urban drainage networks (UDNs), provide valuable insights beyond the traditional engineering approaches, to design and operate systems in a more reliable way and to help build-up structural resiliency [12, 13].

In the past, most structural features in complex networks were investigated based on a conventional graph representation (so-called "primal space"), where pipes or conduits are the edges and their intersections the vertices

of a mathematical graph [14, 15]. Conversely, different approaches, based for example on common attribute classification (i.e., road name or pipe size) or intersection continuity (i.e., maximum angle of deflection), consider the network structure in its "dual space", i.e., functional components (e.g., pipes with same diameter) which belong together, represent the vertices and their intersection the edges of the graph [16, 17]. Further explanations are provided in the next section. Unlike the conventional primal representation, dual mapping approaches may also consider the continuity of links (pipes or conduits) over a variety of edges and hierarchy (e.g., pipe diameter; isolation valves; maximum designed flow; speed limits; road class) for further graph analysis.

There exist different ways of creating the dual graph of a network, taking into account physical (e.g., geometric) and/or behavioral (e.g., symbolic) considerations. The street name (SN) approach, for example, uses the historical naming conventions to create the dual graph, but neglects the geometrical properties of the network. Hybrid approaches, like the Hierarchical Intersection Continuity Negotiation (HICN) [16], combine geometric (e.g., maximum angle of deflection of connected roads) and hierarchical (e.g., road class) attributes, to better capture the structural network topology resulting from top-down (centralized designs) and bottom-up local-planning actions (self-organization).

Previous studies using the dual mapping approach were mainly performed on road networks (RNs) [16–18], but some also on water distribution and urban drainage networks [19–21]. In principle, an extension to each network type is possible. Masucci et al. [16] investigated the road network growth for the city of London and found stable statistical properties to describe the topological network dynamics. Krueger et al. [20] applied the HICN principle for the first time to the evolving sewer networks in a large Asian city with 4 million people. The authors found that sewer network types quickly evolve to become scale-free in space and time. In Jun and Loganathan [19] a dual mapping approach was used to describe the connectivity of isolation zones in water distribution networks.

Klinkhamer et al. [21] examined the co-location of existing road and sewer networks in a large Midwestern US city and homoscedasticity of subnets across the city but did not examine temporal evolution of these networks. In Mair et al. [22] the geospatial co-location of roads, pipes, and sewers was investigated using data set for three Alpine case studies, finding strong similarities between these networks. Studies on the coevolution of water infrastructure networks (water distribution and urban drainage) and road network are crucial when investigating functional interdependencies and cascading vulnerabilities across multiplex network layers. Examples are the flood-induced change in road traffic or the collapse of entire road segments causing flow disruptions in all networks to different extents.

In this paper, we present for the first time a topological analysis of three infrastructure networks coevolving over a century. The results of the dual mapping for a unique dataset of 11 time-stamped water distribution and urban drainage network states and 8 time-stamped road networks of the medium-size Alpine case study city, as the town and its infrastructure, evolved during the past 108 years, and the population tripled from about 40,000 to about 130,000. First results of this case study are presented in Zischg [23]. We investigated network topological metrics using the HICN dual mapping approach [16]. We observe that some infrastructure networks show node degree distributions that behave like truncated power-laws under the dual representation. However, this "scale-free" network characteristics depend on the network type and change over time. With the presented methodology, differences and similarities of patterns (e.g., vertex connectivity) and trends for the infrastructure development are obtained. This study includes an investigation of the sensitivity of the dual mapping approach, using different criteria to build the new graph. The reflected structural features, such as the backbone of the networks, were uncovered for each network type and remapped to the spatial map. A further analysis shows the pairwise co-location of high node degree components ("network hubs") across different infrastructure network types, which builds the basis for analyzing disturbances and structural resilience.

2. Data Analyses

2.1. Network Connectivity. Node degree distribution $P(k)$ is a significant topological property of complex networks. The degree (k) of a node i in an undirected network describes the number intersecting links and is calculated through the network's adjacency matrix A, where the degree of node i is defined by the sum of the i-th row of A. For example, the node degree in social networks represents the number of contacts. Scale-free networks show node degree distributions that follow a Pareto power-law distribution [20, 21], with $P(k) \sim k^{-\gamma}$ for $k \geqslant k_{min}$, whereas random networks have Poisson distributed node degrees. We use the method proposed by Clauset et al. [24] to test the power-law hypothesis and determine scaling parameters of the node degree distributions for the various network states. By calculating the p value, an indicator for the goodness-of-fit is determined. In case the p value is greater than 0.1, the power-law is a plausible hypothesis for the data within given ranges. However, the definitive recipe to fit power-law distributions does not yet exist [25]. The mean node degree for undirected networks is defined as $\langle k \rangle = (2 \times e)/n$, where e is the total number of edges and n is the total number of vertices. In the limits a mean node degree of 2 indicates a tree-like network structure, and grid patterns or cyclic structures have mean node degrees around 4 [26]. Higher statistical moments of $P(k)$ are also important, including the variance $\langle k^2 \rangle$ that reflects the dispersion around the mean [27].

Along with the node degree distribution, the characteristic path length $\langle l \rangle$ (or average path length) is an important and robust measure of network topology. It quantifies the level of integration/segregation throughout the network. In water infrastructure and power grid networks energy losses are dependent on the characteristic path length. It is calculated by the average shortest path distance between all couples of nodes as follows:

$$\langle l \rangle = \frac{1}{n \times (n-1)} \times \sum_{i \neq j} d\left(v_i, v_j\right), \quad (1)$$

where n is the number of vertices and $d(v_i, v_j)$ denotes the shortest path between vertex v_i and v_j [3]. The probability density function of the shortest path lengths (between all couples of nodes for RNs; between all terminal nodes and the source or sink node, for WDNs and UDNs, respectively), $P(l)$ can, for example, be considered as the approximation of the travel-time distribution with a nearly consistent distribution of flow velocities.

The local clustering coefficient C_i of node i describes the connectivity (number of edges m) among its k neighbors. A perfect cluster/clique ($C_i = 1$) indicates a full connection of all nodes/individuals. If an isolation of one node in the cluster occurs, the other nodes remain connected. Conversely, a $C_i = 0$ indicates that node i holds together all its neighboring nodes. Regarding infrastructures, a higher clustering coefficient indicates the existence of local and alternative flow paths in the network. In undirected graphs, C_i for an individual node is defined as follows:

$$C_i = \frac{2 \times m}{k_i \times (k_i - 1)}. \quad (2)$$

The overall (average) clustering coefficient C can be determined by averaging the local clustering across all nodes. When the network reveals a high C, which is typical for regular lattice networks (high local efficiency), and has a small $\langle l \rangle$, as found in random networks (high global efficiency), then the network can be characterized as small-world network [30]. Telesford et al. [31] developed methodology to test the "small worldness" by comparing the network with its equivalent random and regular lattice networks, which have the same node degree distribution, as follows:

$$\omega = \frac{\langle l_R \rangle}{\langle l \rangle} - \frac{C}{C_L}, \quad (3)$$

where $\langle l_R \rangle$ is the characteristic path length of the randomized network equivalent and C_L is the clustering coefficient of the regularized network equivalent. A ω-value of 0 indicates a network that is in perfect balance between normalized values of high clustering and low characteristic path length. Negative values indicate a graph with more regular characteristics, whereas positive values indicate more random graph characteristics [31]. Small-world networks are significantly more clustered (segregated) than random networks and have the same characteristic path length as random (integrated) networks, making them locally and globally efficient, for example, for optimal information transfer [30].

2.2. HICN Principle for Dual Mapping. The HICN approach emphasizes the functional topology of the network by aggregating components (e.g., pipes, conduits, and roads) with identical attributes (e.g., pipe diameter, pipe segments, and road type), while also maintaining a certain level of straightness (e.g., road sections) [16]. After reducing the network complexity with this "generalization model," the aggregated edges are converted into vertices and the intersections are converted into edges. The resulting graph is the so-called "dual" (mapped) representation of the "primal" graph (see Figure 1). In addition to the edge class, the angular threshold Θ_{max} is a second criterion used for the generalization model. It defines the maximum exterior convex angle of connected edges being merged [17].

The HICN allows for reducing the network complexity of the primal map and considers the hierarchy of network elements (e.g., different level of detail of the pipe representation). Identical cohorts of edges are considered as a single component, the dual node. However, the dual mapped network circumvents this issue through generalization and still preserves the connectivity information of the original network. Another advantage is the detachment from the geographical embedding, allowing the network to be nonplanar. With this methodology, the underlying hierarchy (e.g., highly connected components) of the network can be uncovered.

3. Alpine Case Study

To investigate the coevolving topology of three urban infrastructure networks with the HICN dual mapping methodology, we utilize available, high-resolution network data for a medium-size Alpine city. The temporal evolution of the urban infrastructure networks is defined through time-stamped system states at 10-year intervals, starting with the year 1910 for water distribution and urban drainage networks. The road network data starts with the year 1940, since historical orthophotos to reconstruct the network were only available from that time. The city has grown from approximately 40,000 inhabitants in 1910 to 130,894 in 2016. The historical data set describes the expansion of the networks and includes pipe rehabilitation, changing source (e.g., reservoirs), and sink nodes (e.g., sewer outfalls), altering population densities and variations of water consumption patterns of the water distribution and urban drainage systems. The detailed description of the network reconstruction for this case study can be found in the works of Sitzenfrei et al. [32] and Glöckner [33].

Figure 2 shows the time-stamped networks at selected stages in the primal map. For the UDN a greater thickness and a darker color of the edges indicate a larger conduit size, which connect to one large (biological) waste water treatment plant (WWTP) in the eastern part of the city after the 1970s. Before the wastewater was discharged to the river after mechanical treatment (sedimentation, rack), outside the urban areas at the eastern parts of the city. When actually building the WWTP, there were no major changes in the combined drainage network necessary (combined transportation of sewage and storm water) and the old outlets were transferred to combined sewer overflows (CSOs). For security reasons the pipe diameter for the WDN cannot be shown. The color shading at the road network in 2010 indicates the different road types, ranging from residential (light grey), tertiary, secondary, and primary roads to motorways (black). Furthermore, the water demand which directly influences the flows of the WDN and the UDN during dry weather periods is illustrated. Clearly noticeable is the general

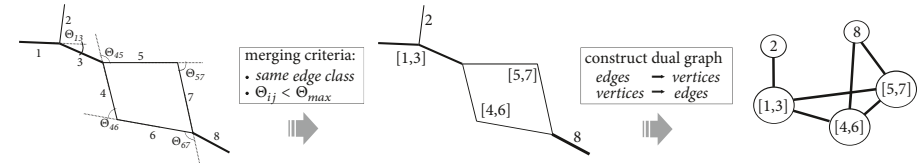

Figure 1: HICN method to construct the dual graph from the primal map. Resulting dual graphs are dependent on the generalization model (adapted from Zischg et al. [28] with permission from ASCE).

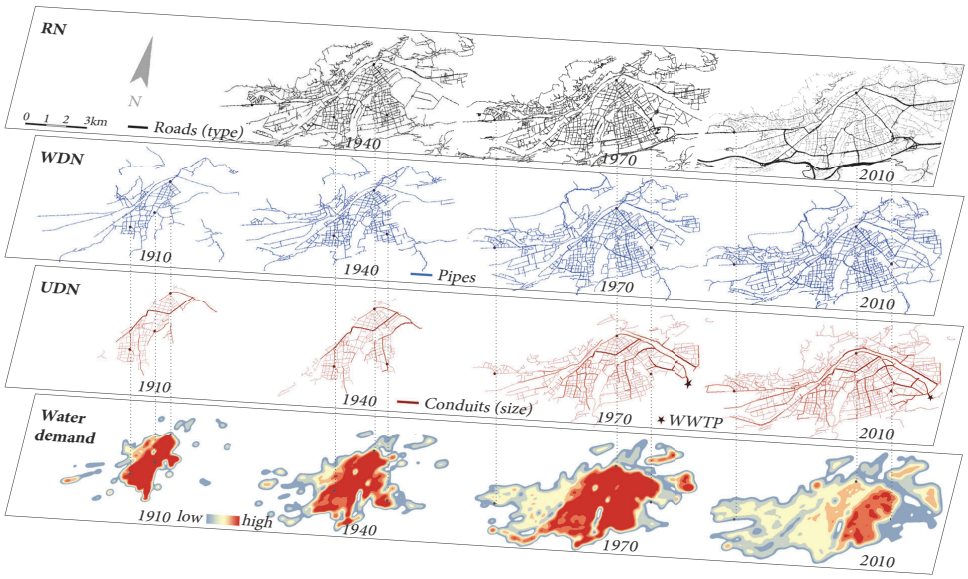

Figure 2: Time-stamped coevolution of the water distribution network (WDN), the urban drainage network (UDN), and the road network (RN) of an Alpine city.

reduction of the average water demand after the 1970s mainly due to water saving measures.

Table 1 gives a short narrative introduction on the history of the infrastructure networks of the investigated case study during the last century.

4. Results and Discussion

In this section, we present the results of the historical coevolution in the dual representation of the three infrastructure networks (WDN, UDN, and RN). In a sensitivity analysis of the HICN method, we determine the effects on $P(k)$ based on the variations of the angular threshold, the edge class, and the network partition (entire network vs. largest connected component (LCC)), before we present the development of the network characteristics over time. Finally, we also show the remapping of dual network characteristics to the primal map, investigate correlations between dual node degree and edge class (e.g., road type), and identify pairwise spatial co-locations of dual nodes among the three network types.

4.1. Dual Mapping. The application of the HICN dual mapping to the historical infrastructure networks for the first (year 1910 for WDN and UDN, and 1940 for RN) and last stages (year 2010) is illustrated in Figure 3. The dual graphs show the node degree (darker and larger nodes represent central network "hubs" with high node degree). For the application of the HICN method to the water infrastructure networks, we used identical pipe diameters (for WDN) and conduit sizes (for UDN) for the edge class criterion, in combination with an angular threshold Θ_{max} of 180 degrees; i.e., we ignore the curvature of pipe/conduit segments. On the

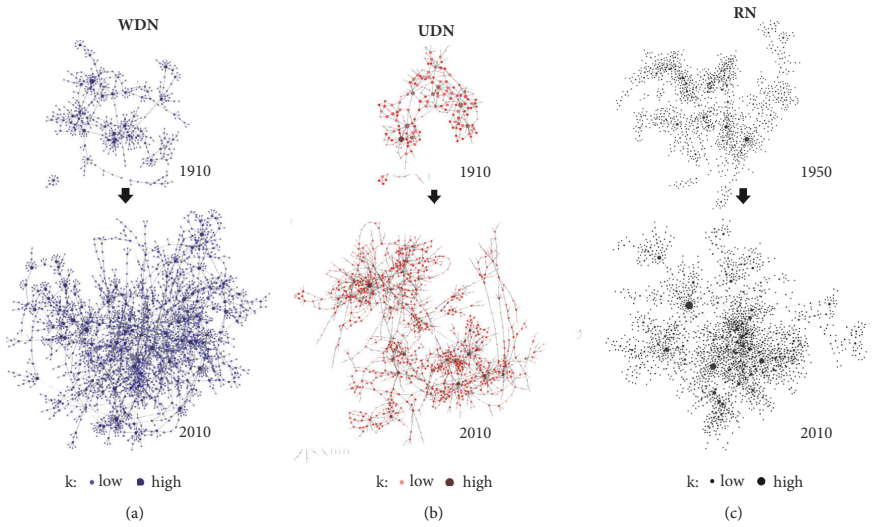

Figure 3: Dual mapped evolution of the infrastructure networks: (a) WDN, (b) UDN, and (c) RN. The color shading and size of the node indicates its degree. The network visualization was done using the program Cytoscape [29].

Table 1: Narrative changes of the infrastructure networks [32–34].

Years	Narrative
Before 1910	WDN for about 23,000 inhabitants; total population 49,727 in 1900; design demand 150 liters per capita and day, transporting a significant amount of water in the city; also the massive amount of waste water had to be transported out of the city by a newly build combined sewer system; a mandatory connection of the consumers to both networks was enforced by law
1910-1929	1st world war; maximum recorded water consumption of 500 liters per capita and day in 1927 due to unaccustomed consumer behavior (still used to the central supply of running wells); 30% of the current WDN structure (year 2017) existed already in 1910; opening of the airport at the eastern part of the city in 1925
1930-1949	2nd world war; massive influx of refugees, infrastructure mainly unaffected; opening of a new airport at the western part of the city in 1948; supply deficits; reduction of water consumption below 300 liters per capita and day through information campaigns
1950-1969	Strong population growth, city and road network expansion; construction of the WWTP (mechanical treatment) in 1966; strong UDN expansion in western and eastern direction; biggest growth rates for the WDN between 1960 and 1970.
1970-1989	380 liters per capita and day; construction of the motorway and connection with the city (1970s); construction of the biological treatment at the WWTP in 1974; connection of neighboring villages to the WWTP; maximum loads of 330,000 people equivalents (PE) in 1987; production industries with high water demand and waste water accumulation leave the city
1990-2009	Further connection of neighboring villages; expansion of the WWTP to 400,000 PE; minor network expansions, increased pipe and sewer rehabilitation
2009-present	Steady population growth, urban expansion is limited by the topographic boundary conditions; densification of city districts (from detached houses to apartment blocks); approximately 250 liters per capita and day (domestic water demand is app. half of it); actually connected people equivalent to the WWTP: 270,000 PE (2011); roads: 476 km; WDN: 320 km; UDN 244 km.

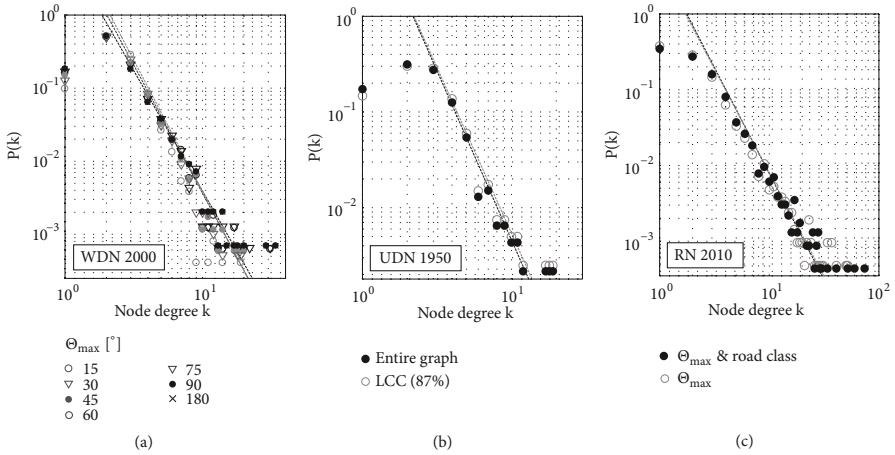

Θ_{max} [°]:	15	30	45	60	75	90	180
n	3,050	2,393	2,102	1,972	1,887	1,764	1,764
γ	5.00	4.09	3.80	3.70	3.61	3.39	3.39
k_{min}	4	3	3	3	3	3	3
p-value	0.000	0.000	0.015	**0.146**	**0.441**	**0.269**	**0.257**

(d)

	Entire graph	LCC
n	462	401
γ	3.57	3.50
k_{min}	3	3
p-value	**0.348**	**0.222**

(e)

	Θ_{max} & road class	Θ_{max}
n	2,295	2,094
γ	2.72	2.66
k_{min}	3	3
p-value	**0.694**	**0.309**

(f)

Figure 4: Parameter sensitivity of the HICN approach on the node degree distribution of the WDN 2000; the UDN 1950 and the RN 2010 (n: number of dual nodes, γ: power-law exponent, k_{min}: lower bound to the power-law behavior, p value: *goodness-of-fit* for the power-law hypothesis).

other hand, for the dual mapping of the road networks, we used the Θ_{max} of 45 degrees [35] and the road type (residential road to motorway) as criteria for the generalization model. We discuss the application of different parameter values in the next section.

4.2. Sensitivity of the Dual Mapping. For the HICN approach different angular thresholds and edge attributes can be considered to construct the dual graph. In Figure 4 we show the results of the sensitivity analysis on the node degree distribution for three parameters used for the HICN approach. First, we identify the sensitivity of the angular threshold Θ_{max} using the WDN of 2000 as reference. Second, we choose the UDN 1950 with 10 subnetworks and investigate the graph characteristics for the entire network and the largest connected component (LCC) only. Finally, we show the effect of neglecting the edge class criterion (road type) for the RN in 2010 as reference.

With increasing angular threshold Θ_{max} (see Figure 1) and the associated less strict criterion for aggregation of edges, we observe that more pipes (of the same class) are merged together and therefore the size of the dual graph is reduced (see Figure 4(a)). For example, the reference network has 7,827 edges in the primal space, which are generalized to 3,050 and 1,764 dual nodes for angular thresholds of 15 and 180 degrees, respectively. Figure 4(d) shows the outcome of 7 variations of the angular threshold Θ_{max} from 15 to 180 degrees. All resulting node degree distributions are heavy tailed and by visual inspection relatively similar. However, when applying the method to test the power-law hypothesis as proposed by Clauset et al. [24], only for $\Theta_{max} > 45$ degrees Pareto distributions $P(k) \sim k^{-\gamma}$, $k \geq k_{min}$ are plausible data fits (p value ≥ 0.1). At this point it should be mentioned that power-law fitting is still a controversial issue and a definitive recipe to fit power-law distributions and to distinguish between power-law and power-law-like distributions does not yet exist [25]. A minimum node degree k_{min} of 3 for curve fitting was determined to be the most likely one, for all three network types. For higher threshold angles slightly decreasing slopes γ are observed. The results using angular thresholds of 90 and 180 degrees are identical, meaning that no sharp inner angles between connected pipes of the same class are found in the graph. Unlike for road networks, where Θ_{max} also is a criterion for visibility and navigation, we suggest that restricting Θ_{max} in WDNs and UDNs is less important to find and aggregate pipe segments with unique identity because of their underground locations. We conclude that for investigating the node degree distribution of the historical networks, the angular threshold Θ_{max} is of minor importance, but must be consistently applied between the types and the states of the networks.

Figure 4(b) shows the results when investigating the entire graph (all subnetworks) and the largest connected component (LCC), which contains 87% of the total nodes.

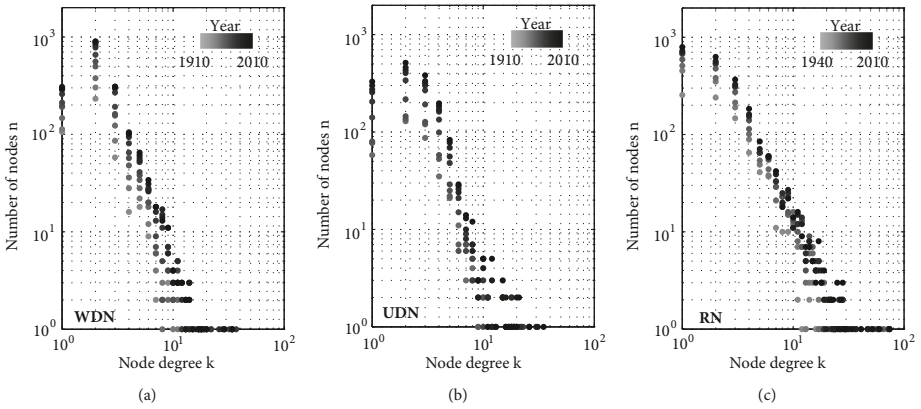

Figure 5: Heavy tailed dual degree distribution overtime of (a) the WDN, (b) the UDN, and (c) the RN. The color shading from light grey to black indicates the evolution of the network. Detailed results of the statistical curve fitting can be found in Appendix A.

For the reference network UDN 1950, no significant changes in the Pareto exponent are seen (see Figure 4(e)). Finally, the neglect of the road class as additional criterion for the HICN method slightly decreases the size of the network but has a low effect on the probability density function $P(k)$ (see Figures 4(c) and 4(f)). This can be interpreted with the low incidence of changing road types across straight road segments.

In this study, we used the pipe diameter to identify functionally identical pipe segments. Other examples could be the age or the material of the pipe, but also classified (design) flows or (measured or modeled) head losses might be used to construct the dual graph. The advantage of using the pipe diameter is that it is a surrogate measure of the flow and is independent of a hydraulic simulation. The black dots in Figure 4 represent the network configuration as presented in the subsequent section.

4.3. Characteristics of the Dual Graph. Resulting node degree distributions, $P(k)$, for the WDN, UDN, and RN in the dual representation are presented in Figure 5, plotted for all network types on log-log axes for the time-stamped states. A darker node color indicates a younger and more mature network state. We observe heavy-tailed node degree distributions for 30 network states with dispersion indices D ($\langle k^2\rangle/\langle k\rangle$) > 1, indicating high variance around the mean. Detailed analyses showed that 50% of the time-stamped networks follow truncated power-law [Pareto] distributions across all network types. This does not necessarily mean, however, that alternative (e.g., log-normal, exponential) distributions are more plausible. The scaling parameters γ fall in the range between 3.23 and 3.50 for WDN (k_{min} = 2 or 3), 3.25 and 3.76 for UDN (k_{min} = 3 or 5), and 2.67 and 2.78 for RN (k_{min} = 3). For the WDN (mean: 3.35 ± 0.09) and UDN (mean: 3.49 ± 0.12) larger slopes γ and a stronger decrease of the number of leaf nodes (k = 1) are found compared with the RN (mean: 2.70 ± 0.04). A possible explanation of the truncation could be the missing house (low degree) connections for both water infrastructure networks. For the detailed parameters and the statistical tests, we refer to Appendix A.

The truncated power-law [Pareto] distribution also indicates that the probability of finding nodes with many connecting links ("hubs") is much lower than of nodes with few connections (terminal dual nodes). According to the literature this behavior is typical for scale-free networks, which are dominant in most natural networks. The extent to which these distributions fit a power-law can be a useful marker of network resilience [36].

The "scale-free" similar characteristics, within the observed range [$k_{min} \leqslant k \leqslant k_{max}$], are also indicated with the significant higher maximum degrees k_{max} (representing a "network hub") compared to the mean degree $\langle k\rangle$ (see Appendix B). Although the mean degree $\langle k\rangle$ of the UDN is larger than that for the WDN, the maximum degree k_{max} of both water infrastructure networks is similar. One reason for that is fewer changes in the conduit diameters, resulting in the aggregation of more conduits and thus having higher connectivity. The highest connectivity and dispersion index D is found for the road network, indicated by high k_{max} and high $\langle k^2\rangle/\langle k\rangle$ (see Appendix B and Figure 6(c)).

The growth of the networks in terms of total number of dual nodes n over time is illustrated in Figure 6(a). Highest growth rates of the networks are seen in the 1960s and 1970s, which can be partly related to the economy boom and the implementation of the waste water treatment plant [32]. Figure 6(b) presents the scaling parameter γ of the node degree distributions $P(k)$ over time. A change in the lower bound k_{min} is indicated in round brackets. Although the power-law hypothesis could only be clearly proven in 50% of the time-stamped networks (see Appendix A), we show the scaling parameter for all network states for comparison purposes. The statistical analysis shows that the RN tends towards a clear scale-free behavior during evolution, whereas the opposite is observed for the UDN. No clear trends were

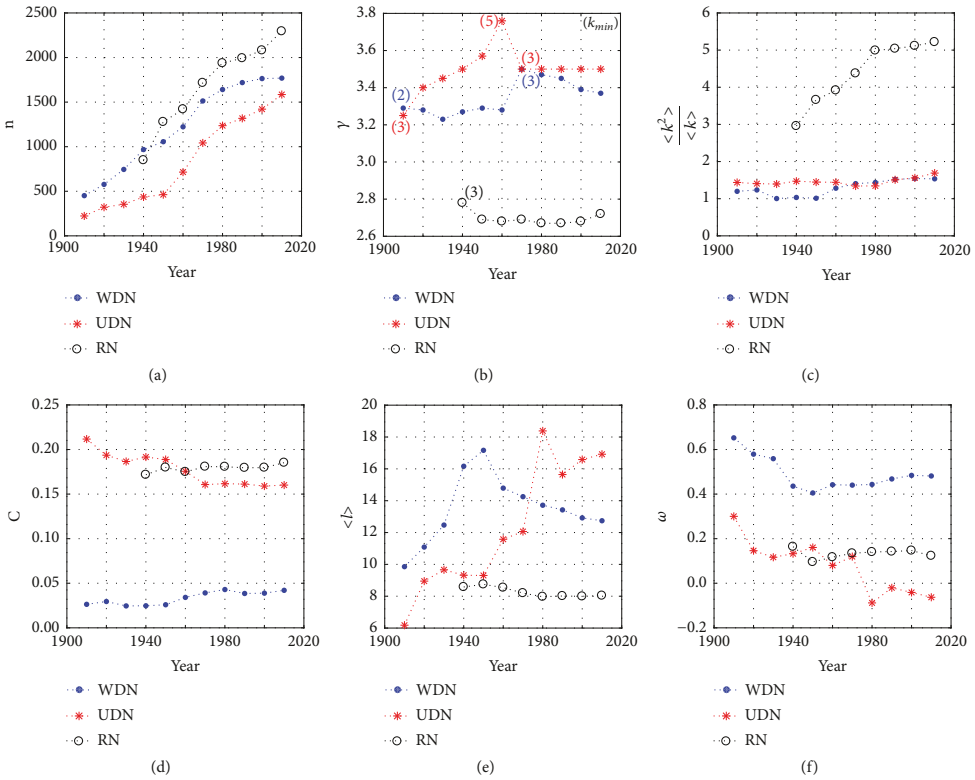

FIGURE 6: Topological properties of coevolving WDN, UDN, and RN: (a) number of vertices n; (b) power-law exponent γ; (c) dispersion index; (d) clustering coefficient C; (e) characteristic path length $\langle l \rangle$; and (f) small worldness ω.

identified for the WDN (see p values ≥ 0.1 in Appendix A). According to Achard et al. [36] the extent to which these distributions fit a power-law can be a useful indicator of network resilience. Furthermore, when comparing γ with previous studies in the literature, similar ranges between 2 and 4 are reported [17, 20, 21].

In this study, the lowest exponents γ are reported for the RN compared to those for the WDN and UDN. Peaks of γ for the WDN and UDN can be explained with the tree-like expansion of the network to new parts of the city and without a strong network densification at those times (see description in Table 1). During the last part of the 20th century the γ for the WDN tends to decrease, whereas the UDN and RN evolution is characterized by a network growth with a nearly constant power-law exponent γ. This could indicate that the networks are now topologically "mature"; i.e., a similar behavior is expected when the network grows further. The ratios of variance $\langle k^2 \rangle$ and the mean $\langle k \rangle$ of the node degrees are illustrated in Figure 6(c). For WDN and UDN it is nearly constant during their evolution [$1 \leq D \leq 2$]. An increasing bilinear trend of dispersion is observed for the RN, indicating the preferential attachment tendencies of new nodes to already well connected nodes. All networks show dispersion indices greater than 1 and thus exceed the value of expected random graphs following a Poisson distribution ($D = 1$).

As a measure of functional segregation (local efficiency), high average clustering coefficients describe the presents of cliques, where neighboring nodes are well connected among each other. During the last half of the century, C remained nearly constant for all infrastructure networks, with highest values for the RN, followed by UDN and WDN at year 2010.

The characteristic path length $\langle l \rangle$ of the network states in dual representation is shown in Figure 6(e). In the dual representation, the path length defines the number of changing edge attributes (e.g., diameter changes) between two dual vertices. Small $\langle l \rangle$ indicate a global efficiency meaning that every vertex is connected to every other through a short distance. In general, $\langle l \rangle$ increases with expanding geographical boundaries of the network (Figure 2). During the 1980s there is a significant increase of $\langle l \rangle$ for the UDN, possibly because of the tree-like connections of peripheral zones and neighboring villages to the central wastewater treatment plant. In contrast, $\langle l \rangle$ for the WDN decreases

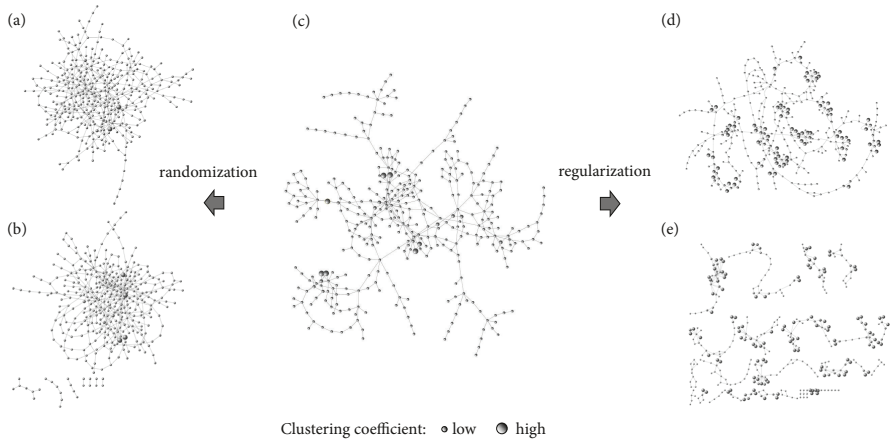

Figure 7: Creation of the equivalent random and regular lattice networks (same node degree distribution) by edge rewiring to test the small worldness. (a)-(b) Randomized networks with and without maintaining connectivity; (c) LLC of the dual mapped WDN 1910; (d)-(e) the lattice equivalents with and without maintaining connectivity.

during the past few years, as a result of the WDN densification and the construction of alternative flow paths for redundancy purposes. Furthermore, it is remarkable that $\langle l \rangle$ for the UDNs at the early stages of the 20th century is lower compared to that for WDNs. One reason for that is that the UDN at the historical center of the Alpine city had fewer alterations of conduit diameters (see Figure 2, middle left), resulting from the coarse design concepts and material limitations at that time. As the road network grows over time, we observe the lowest values for $\langle l \rangle$ are nearly constant trend over time, indicating a high network integrity.

Figure 6(f) provides a quantitative measure of the small-world properties ω over a spectrum of network topologies. Telesford et al. [31] describe ω in proximity to zero as small-world network; however, no sharp boundary of the small-world region exists. Positive ω indicate a graph with more random characteristics, as we observe for all infrastructure during the first half of the 20th century. However, over time, the networks tend to become less random and closer to small worldness. While ω is always larger than 0.40 for the WDN, UDN and RN have $|\omega|$- values less than 0.16 after the first network state. Therefore, we claim the small-world property of UDN and RN, while the former in recent decades can be considered as the closest to the small-world optimum.

Figure 7 shows an example of the random and regular lattice equivalents for the WDN 1910, needed to determine the small worldness. By preserving the same node degree distribution, edges of the initial network (see Figure 7(c)) are rewired in a stochastic process [37, 38]. Differences between the networks in Figures 7(a) and 7(b), as well as in Figures 7(d) and 7(e), are the preservation of the network connectivity. The effective number of rewiring per edge for creating the network equivalents is around 10 (for the regularization approximately 100 times more iterations needed), determined though parameter convergence (see Appendix C).

Previous studies have shown that understanding the network structure gives insights to vulnerabilities and structural resilience of the systems (i.e., scale-free networks are found to be highly resilient against random failure but vulnerable to targeted attacks) [9, 39]. Implications to the infrastructure management could, for example, relate to system operation to emphasize special protection or increased maintenance of critical network components ("hubs"). While this is relatively obvious at key points (such as water or wastewater treatment plants), in most cases less attention has been paid to individual pipe sections due to their complexity. A first step towards more resilient networks is already proposed by Mair et al. [40] and Zischg et al. [41], to use a "less-critical" subset of the colocated road network with strong similarities to generate possible WDNs. Second, when considering all infrastructure networks as an entire system ("multiplex network"), severe failure cascades through the network layers should be prevented through avoiding certain interlayer links (e.g., co-location of "hubs") [42]. Resulting resilient infrastructure systems should be capable of minimizing the failure impacts and a fast recovery to a stable system state [11]. While the former factor certainly depends on the (multiplex) network topology and on the type of network disruption (see e.g., [43, 44]), for the latter one several influencing factors exist, which in most cases are more difficult to quantify (e.g., resources availability, societal needs, preparedness actions, economy adjustments, etc.) [6]. However, the assessment of infrastructure system resilience goes beyond the scope of this study.

4.4. Remapping from Dual to Primal Space. Remapping the dual graph characteristics to the primal graph representation allows for georeferenced visualization and further spatial

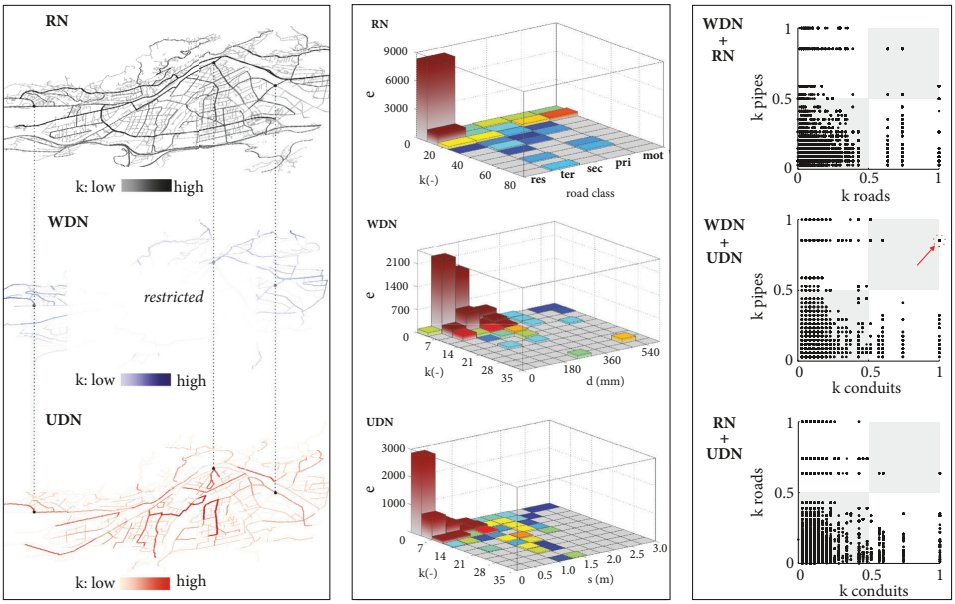

(a) (b) (c)

Figure 8: Remapping of the dual (node) degree to the primal space for WDN, UDN, and RN. (a) Remapped dual degree; (b) correlation analysis between dual degree and functional edge class describing flow capacity: e is the number of primal edges and the road classes represent residential (**res**), tertiary (**ter**), secondary (**sec**), and primary (**pri**) roads and motorways (**mot**); and (c) co-location of dual degree among different network types.

analyses among the different network types. Figure 8(a) shows the example of remapping the dual (node) degree to the original physical embedded infrastructure networks at year 2010. The highlighted bold edges represent the dual network "hubs", i.e., the elements with the most interconnections. In case those elements fail, the network gets easily fragmented, making for example the emergency supply very difficult through the central WDN. A comparison of the dual degree and the edge class (pipe diameter, conduit size, and road type) shows that they do not necessarily correlate. This implies that edges with the highest capacity (large diameter in WDN, large conduits sizes in UDN, and motorways (mot) in the RN) do not have the most intersections.

For the RN the "high degree hubs" are identified to be tertiary and primary roads. The reason for this finding for the WDN and UDN is that the source and sink nodes (water sources and WWTP) are located outside the city, requiring "high capacity transmission edges" to the inner parts of the network, which usually have fewer connections. However, low degree "terminal dual nodes" are mostly found in the edge classes with the lowest capacity (see bivariate histograms in Figure 8(b)).

4.5. Geospatial Co-location. We present the results of the geospatial co-location analysis to identify the spatial relationships of dual node degrees among the three network types. Mair et al. [22] found that approximately 90% of the WDN and UDN are located below the RN for this case study, however without considering their topological characteristics. Here we pairwise compare the normalized dual (node) degrees of the colocated infrastructure networks (see Figure 8(c)). Nodes in the upper right corner of the scatter plots indicate that high node degree components of both networks are colocated. For example, one conduit segment (UDN) with the highest k is colocated with one pipe segment (WDN) with the second highest k (indicated with the arrow and a red circular marker). This could be an indicator for an increased cascading vulnerability when failures occur across multiple networks.

These findings provide a first step towards the assessment of structural resilience and network interdependencies. Besides the identification of the "connectors" (high connectivity nodes), the "carriers" (high capacity node) should be further addressed. One future direction of this work could be the analysis of cascading failure across multiple network layers (e.g., a pipe break occurs which affects the water supply but also influences the colocated road and urban drainage network parts due to traffic rerouting and additional inflow to sewers). These analyses could provide helpful insights in the resilient (re)design of networks, providing an integrated view across the usually separated systems.

Table 2: Statistical tests of the small world (C: average clustering coefficient; $\langle l \rangle$: characteristic path length; and ω: ratio indicating the small-world property) and power-law hypotheses (γ: scaling parameter; k_{min}: lower bound for curve fitting; p value: goodness-of-fit for power-law hypothesis) over time for the WDN, UDN, and RN according to Telesford et al. [31] and Clauset et al. [24].

Year	C			$\langle l \rangle$			ω			$\gamma(k_{min})$			p value	
	WDN	UDN	RN	WDN	UDN	RN	WDN	UDN	RN	WDN	UDN	RN	WDN	UDN	RN
1910	0.026	0.212	-	9.86	6.18	-	0.652	0.300	-	3.29 (2)	3.25 (3)	-	**0.158**	**0.169**	-
1920	0.030	0.194	-	11.09	8.95	-	0.579	0.146	-	3.28 (2)	3.40 (3)	-	**0.565**	**0.365**	-
1930	0.025	0.187	-	12.47	9.66	-	0.559	0.117	-	3.23 (2)	3.45 (3)	-	0.016	**0.518**	-
1940	0.025	0.192	0.172	16.16	9.32	8.58	0.436	0.133	0.164	3.27 (2)	3.50 (3)[3]	2.78 (3)	0.015	**0.754**	0.021
1950	0.026	0.189	0.180	17.16	9.30	8.75	0.405	0.161	0.095	3.29 (2)	3.57 (3)	2.69 (3)[2]	**0.102**	**0.348**	0.008
1960	0.034	0.176	0.175	14.79	11.58	8.54	0.442	0.080	0.117	3.28 (2)	3.76 (5)	2.68 (3)	0.084	**0.111**	0.038
1970	0.039	0.161	0.181	14.25	12.06	8.20	0.440	0.120	0.134	3.50 (3)	3.50 (3)[3]	2.69(3)	**0.187**	0.003	0.005
1980	0.043	0.162	0.181	13.71	18.38	7.97	0.443	-0.088	0.140	3.47 (3)	3.50 (3)[3]	2.67 (3)	**0.238**	0.004	0.010
1990	0.039	0.161	0.180	13.42	15.64	8.01	0.468	-0.020	0.142	3.45 (3)	3.50 (3)[3]	2.67 (3)	**0.791**	0.002	0.047
2000	0.039	0.159	0.180	12.92	16.59	7.99	0.484	-0.041	0.147	3.39 (3)	3.50 (3)[3]	2.68 (3)	**0.257**	0.001	**0.110**
2010	0.042	0.160	0.185	12.74	16.92	8.04	0.481	-0.063	0.123	3.37 (3)[1]	3.50 (3)[3]	2.72 (3)	0.051	0.002	**0.694**

[1,2,3] recalculated k_{min} to maximize p *value* from/to: = (5)/(3); (9)/(3); (4)/(3); p values ≥ 0.1 proving the power-law hypothesis are shown in **bold** (50% of the networks).

Table 3: Topological dual mapped properties (n: number of nodes; e: number of edges; $\langle k \rangle$: mean node degree; k_{max}: maximum node degree; and $\langle k^2 \rangle$: node degree variance) over time for the WDN, UDN, and RN.

Year	n			e			$\langle k \rangle$			k_{max}			$\langle k^2 \rangle$		
	WDN	UDN	RN	WDN	UDN	RN	WDN	UDN	RN	WDN	UDN	RN	WDN	UDN	RN
1910	451	223	-	535	356	-	2.37	3.19	-	15	16	-	2.84	4.59	-
1920	577	321	-	703	467	-	2.44	2.91	-	22	19	-	3.01	4.09	-
1930	745	354	-	907	510	-	2.43	2.88	-	14	19	-	2.45	4.02	-
1940	968	436	849	1,171	639	1,288	2.42	2.93	3.03	17	19	32	2.50	4.31	8.97
1950	1,056	462	1,278	1,284	676	1,868	2.43	2.93	2.92	17	19	52	2.46	4.24	10.70
1960	1,223	715	1,420	1,512	1,009	2,093	2.47	2.82	2.95	32	23	54	3.17	4.07	11.55
1970	1,513	1,042	1,716	1,913	1,441	2,575	2.53	2.77	3.00	37	22	65	3.55	3.71	13.13
1980	1,641	1,236	1,937	2,097	1,700	2,955	2.56	2.75	3.05	34	22	71	3.67	3.70	15.23
1990	1,719	1,318	1,993	2,203	1,821	3,040	2.56	2.76	3.05	34	30	74	3.90	4.17	15.37
2000	1,764	1,431	2,081	2,272	1,970	3,172	2.58	2.77	3.05	34	31	74	3.97	4.33	15.59
2010	1,769	1,585	2,295	2,293	2,226	3,479	2.59	2.81	3.03	34	35	74	3.98	4.75	15.82

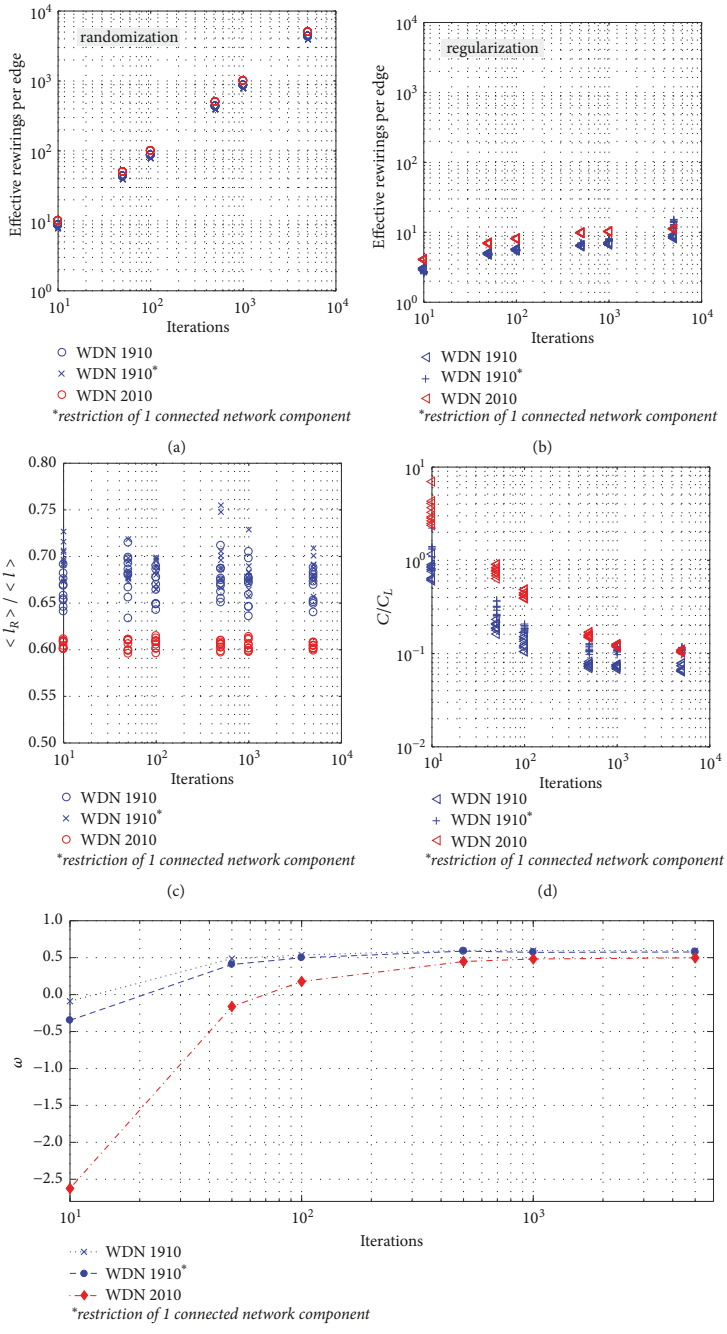

Figure 9: Convergence plots when creating the random and regular network equivalents (10 stochastic networks per iteration step) for the WDN 1910 and the WDN 2010. Effective edge rewiring in (a) the randomization process and (b) the regularization process; (c) ratio of the characteristic path length of the randomized and the original networks; (d) ratio of the clustering coefficient of the original and the regularized networks; and (e) the convergence of the small-world property ω. For further analysis the number of iterations was set to 10^1 and 10^3 for the randomization and regularization process, respectively.

5. Conclusions

The historical data set of water distribution, urban drainage, and road networks of an Alpine city was investigated using a dual mapping approach (Hierarchical Intersection Continuity Negotiation method) and complex network analysis metrics were estimated. From a sensitivity analysis for the angular threshold Θ_{max} using the HICN approach it is concluded that, unlike for road networks, where Θ_{max} also is a criterion for visibility, we suggest that restricting Θ_{max} in WDNs and UDNs is less important than finding and aggregating pipe segments with unique identity because of their underground locations.

The node degree distributions are heavy tailed with greater variance than expected for random networks. Across all three network types and for 50% of the time-stamped networks truncated [Pareto] power-law functions $P(k) \sim k^{-\gamma}$, $k \geq k_{min}$ (γ between 2.67 and 3.76; k_{min} mostly ranging between 2 and 3) were proven and were in the range of previous studies on urban infrastructure networks. While the RN tends towards a clear scale-free behavior during evolution, the opposite is observed for the UDN. No clear trends were identified for the WDN. All networks tend to fall in the small-world region characterized by high global and local efficiencies, during their spatiotemporal evolution. We conclude that similar to other "self-organized" networks, infrastructure networks in their dual representation can also exhibit scale-free properties and thus exhibit the failure dynamics typical of scale-free networks.

Previous studies showed that networks with highly variable node degree distributions, such as scale-free networks, are highly resilient to random failures but have high vulnerabilities to targeted attacks. Furthermore, the extent to which these distributions fit a power-law can be a useful indicator of network resilience. With the presented dual mapping methodology, patterns (e.g., vertex connectivity) and trends for the future infrastructure development were obtained. Furthermore, the reflected structural features, such as the "highly connected" components of the networks, were identified and remapped to the primal map. It was shown that the "highly connected" components do not necessarily correlate with "high capacity" components. Through the pairwise comparison of the dual degree of different network types, we identified the location where "high degree" components are colocated. These findings could be a measure of assessing the interdependencies and cascading vulnerabilities across multilayer networks.

Appendix

A.

See Table 2.

B.

See Table 3.

C.

See Figure 9.

Data Availability

(1) The current and historical georeferenced data of the water distribution and urban drainage networks, used to support the findings of this study, have not been made available because they are protected for security reasons. (2) The road network data which was used to support the findings of this study was taken from open street maps. (3) The dual mapped representation of the water distribution, urban drainage, and road networks, used to support the findings of this study, is available from the corresponding author upon request.

Conflicts of Interest

The authors declare that there are no conflicts of interest regarding the publication of this paper.

Acknowledgments

This work was initiated at the international synthesis workshop "Dynamics of Structure and Functions of Complex Networks", held at Korea University, Seoul, South Korea, during summer 2015. The authors gratefully acknowledge Sybille Glöckner, who provided the historical water distribution network, reconstructed during her master thesis. This research was partially funded by the Austrian Research Promotion Agency (FFG) within the research project ORONET [Project number: 858557], the Austrian Science Fund (FWF) [Project number: P 31104-N29], the Austrian Marshall Plan Foundation, and the NSF Collaborative Research RIPS Type 2: Resilient Simulation for Water, Power, and Road Networks [Project number: 1441188].

References

[1] P. Blanchard and D. Volchenkov, *Mathematical Analysis of Urban Spatial Networks*, Understanding Complex Systems, 1, Springer, Berlin, Germany, 2009.

[2] S. H. Strogatz, "Exploring complex networks," *Nature*, vol. 410, no. 6825, pp. 268–276, 2001.

[3] Y. Assenov, F. Ramírez, S.-E. Schelhorn, T. Lengauer, and M. Albrecht, "Computing topological parameters of biological networks," *Bioinformatics*, vol. 24, no. 2, pp. 282–284, 2008.

[4] M. C. González, C. A. Hidalgo, and A.-L. Barabási, "Understanding individual human mobility patterns," *Nature*, vol. 453, no. 7196, pp. 779–782, 2008.

[5] S. Uhlmann, H. Mannsperger, J. D. Zhang et al., "Global microRNA level regulation of EGFR-driven cell-cycle protein network in breast cancer," *Molecular Systems Biology*, vol. 8, article 570, 2012.

[6] D. A. Eisenberg, J. Park, and T. P. Seager, "Sociotechnical Network Analysis for Power Grid Resilience in South Korea," *Complexity*, vol. 2017, 14 pages, 2017.

[7] A. Barabasi and R. Albert, "Emergence of scaling in random networks," *Science*, vol. 286, no. 5439, pp. 509–512, 1999.

[8] A. P. Riascos, "Universal scaling of the distribution of land in urban areas," *Physical Review E: Statistical, Nonlinear, and Soft Matter Physics*, vol. 96, no. 3, Article ID 032302, 2017.

[9] K. A. Zweig and K. Zimmermann, "Wanderer between the worlds - Self-organized network stability in attack and random failure scenarios," in *Proceedings of the 2nd IEEE International Conference on Self-Adaptive and Self-Organizing Systems, SASO 2008*, pp. 309–318, Italy, October 2008.

[10] J. P. G. Sterbenz, E. K. Çetinkaya, M. A. Hameed, A. Jabbar, S. Qian, and J. P. Rohrer, "Evaluation of network resilience, survivability, and disruption tolerance: analysis, topology generation, simulation, and experimentation: Invited paper," *Telecommunication Systems*, vol. 52, no. 2, pp. 705–736, 2013.

[11] H. Klammler, P. S. C. Rao, and K. Hatfield, "Modeling dynamic resilience in coupled technological-social systems subjected to stochastic disturbance regimes," *Environment Systems and Decisions*, vol. 38, no. 1, pp. 140–159, 2018.

[12] A. Yazdani, R. A. Otoo, and P. Jeffrey, "Resilience enhancing expansion strategies for water distribution systems: a network theory approach," *Environmental Modelling & Software*, vol. 26, no. 12, pp. 1574–1582, 2011.

[13] A. Yazdani and P. Jeffrey, "Applying network theory to quantify the redundancy and structural robustness of water distribution systems," *Journal of Water Resources Planning and Management*, vol. 138, no. 2, pp. 153–161, 2012.

[14] F. Zeng, X. Li, and K. Li, "Modeling complexity in engineered infrastructure system: Water distribution network as an example," *Chaos: An Interdisciplinary Journal of Nonlinear Science*, vol. 27, no. 2, Article ID 023105, 2017.

[15] S. Porta, P. Crucitti, and V. Latora, "The network analysis of urban streets: a primal approach," *Environment and Planning B: Planning and Design*, vol. 33, no. 5, pp. 705–725, 2006.

[16] A. P. Masucci, K. Stanilov, and M. Batty, "Exploring the evolution of London's street network in the information space: A dual approach," *Physical Review E: Statistical, Nonlinear, and Soft Matter Physics*, vol. 89, no. 1, Article ID 012805, 2014.

[17] S. Porta, P. Crucitti, and V. Latora, "The network analysis of urban streets: A dual approach," *Physica A: Statistical Mechanics and its Applications*, vol. 369, no. 2, pp. 853–866, 2006.

[18] M. Hu, R. Jiang, R. Wang, and Q. Wu, "Urban traffic simulated from the dual representation: Flow, crisis and congestion," *Physics Letters A*, vol. 373, no. 23-24, pp. 2007–2011, 2009.

[19] H. Jun and G. V. Loganathan, "Valve-controlled segments in water distribution systems," *Journal of Water Resources Planning and Management*, vol. 133, no. 2, pp. 145–155, 2007.

[20] E. Krueger, C. Klinkhamer, C. Urich, X. Zhan, and P. S. C. Rao, "Generic patterns in the evolution of urban water networks: Evidence from a large Asian city," *Physical Review E: Statistical, Nonlinear, and Soft Matter Physics*, vol. 95, no. 3, Article ID 032312, 2017.

[21] C. Klinkhamer, E. Krueger, X. Zhan, F. Blumensaat, S. V. Ukkusuri, and P. S. C. Rao, Functionally Fractal Urban Networks: Geospatial Co-location and Homogeneity of Infrastructure, 2017, https://export.arxiv.org/abs/1712.03883v1.

[22] M. Mair, J. Zischg, W. Rauch, and R. Sitzenfrei, "Where to find water pipes and sewers?-On the correlation of infrastructure networks in the urban environment," *Water (Switzerland)*, vol. 9, no. 2, p. 146, 2017.

[23] J. Zischg, *Understanding patterns, dependencies and resilience in complex urban water infrastructure networks*, 2018, https://static1.squarespace.com/static/559921a3e4b02c1d7480f8f4/t/5af00302758d4670efbdc46d/1525678950226/Zischg+Jonatan_782.pdf.

[24] A. Clauset, C. R. Shalizi, and M. E. Newman, "Power-law distributions in empirical data," *SIAM Review*, vol. 51, no. 4, pp. 661–703, 2009.

[25] Á. Corral and Á. González, Power-law distributions in geoscience revisited, https://arxiv.or/pdf/1810.07868.pdf, 2018.

[26] M. Barthélemy, "Spatial networks," *Physics Reports*, vol. 499, no. 1–3, pp. 1–101, 2011.

[27] E. Weisstein, "Pareto distribution," in *mathworld–a wolfram web resource*, 2018, http://mathworld.wolfram.com/ParetoDistribution.html.

[28] J. Zischg, C. Klinkhamer, X. Zhan et al., "Evolution of Complex Network Topologies in Urban Water Infrastructure," in *Proceedings of the 17th World Environmental and Water Resources Congress 2017*, pp. 648–659, USA, May 2017.

[29] P. Shannon, A. Markiel, O. Ozier et al., "Cytoscape: a software Environment for integrated models of biomolecular interaction networks," *Genome Research*, vol. 13, no. 11, pp. 2498–2504, 2003.

[30] D. J. Watts and S. H. Strogatz, "Collective dynamics of "small-world" networks," *Nature*, vol. 393, no. 6684, pp. 440–442, 1998.

[31] Q. K. Telesford, K. E. Joyce, S. Hayasaka, J. H. Burdette, and P. J. Laurienti, "The Ubiquity of Small-World Networks," *Brain Connectivity*, vol. 1, no. 5, pp. 367–375, 2011.

[32] R. Sitzenfrei, M. Mair, F. Tscheikner-Gratl, B. Hupfauf, and W. Rauch, "What can we learn from historical water network transition?" in *Proceedings of the World Environmental and Water Resources Congress 2015: Floods, Droughts, and Ecosystems*, pp. 907–916, USA, May 2015.

[33] S. Gloeckner, *Die Historie der Hochdruckwasserversorgungsanlage in Innsbruck - Hydraulische Modellierung und Ausblick (in German) [Master Thesis]*, University of Innsbruck, Innsbruck, Austria, 2017.

[34] M. Schulze, *Historische entwicklung der kanalisation innsbrucks und die entwicklung der technischen regelwerke (in German)*, University of Innsbruck, Innsbruck, Austria, 2012.

[35] X. Zhan, S. V. Ukkusuri, and P. S. Rao, "Dynamics of functional failures and recovery in complex road networks," *Physical Review E: Statistical, Nonlinear, and Soft Matter Physics*, vol. 96, no. 5, 2017.

[36] S. Achard, R. Salvador, B. Whitcher, J. Suckling, and E. Bullmore, "A resilient, low-frequency, small-world human brain functional network with highly connected association cortical hubs," *The Journal of Neuroscience*, vol. 26, no. 1, pp. 63–72, 2006.

[37] M. Rubinov and O. Sporns, "Complex network measures of brain connectivity: Uses and interpretations," *NeuroImage*, vol. 52, no. 3, pp. 1059–1069, 2010.

[38] S. Maslov and K. Sneppen, "Specificity and stability in topology of protein networks," *Science*, vol. 296, no. 5569, pp. 910–913, 2002.

[39] Z. J. Bao, Y. J. Cao, L. J. Ding, and G. Z. Wang, "Comparison of cascading failures in small-world and scale-free networks subject to vertex and edge attacks," *Physica A: Statistical Mechanics and its Applications*, vol. 388, no. 20, pp. 4491–4498, 2009.

[40] M. Mair, W. Rauch, and R. Sitzenfrei, "Spanning Tree-Based Algorithm for Generating Water Distribution Network Sets by Using Street Network Data Sets," in *Proceedings of the World Environmental and Water Resources Congress 2014: Water Without Borders*, pp. 465–474, USA, June 2014.

[41] J. Zischg, W. Rauch, and R. Sitzenfrei, "Morphogenesis of Urban Water Distribution Networks: A Spatiotemporal Planning Approach for Cost-Efficient and Reliable Supply," *Entropy*, vol. 20, no. 9, p. 708, 2018.

[42] S. V. Buldyrev, R. Parshani, G. Paul, H. E. Stanley, and S. Havlin, "Catastrophic cascade of failures in interdependent networks," *Nature*, vol. 464, no. 7291, pp. 1025–1028, 2010.

[43] C. D. Brummitt, R. M. D'Souza, and E. A. Leicht, "Suppressing cascades of load in interdependent networks," *Proceedings of the National Acadamy of Sciences of the United States of America*, vol. 109, no. 12, pp. E680–E689, 2012.

[44] A. Vespignani, "Complex networks: The fragility of interdependency," *Nature*, vol. 464, no. 7291, pp. 984-985, 2010.

Functionally Fractal Urban Networks:

Geospatial Co-location and Homogeneity of Infrastructure

Christopher Klinkhamer[1, *], Elisabeth Krueger[1,2], Xianyuan Zhan[1],

Frank Blumensaat[3], Satish Ukkusuri[1], and P. Suresh C. Rao[1,4]

1/ Lyles School of Civil Engineering, Purdue University, West Lafayette, IN 47907, USA

2/ Helmholtz Centre for Environmental Research - UFZ, Leipzig, Germany

3/ Institute of Environmental Engineering, ETH, Zurich, Switzerland

4/ Agronomy Department, Purdue University, West Lafayette, IN 47907, USA

Abstract

Just as natural river networks are known to be globally self-similar, recent research has shown that human-built urban networks, such as road networks, are also functionally self-similar, and have fractal topology with power-law node-degree distributions ($p(k) = a\,k^{-\gamma}$). Here we show, for the first time, that other urban infrastructure networks (sanitary and storm-water sewers), which sustain flows of critical services for urban citizens, also show scale-free functional topologies. For roads and drainage networks, we compared functional topological metrics, derived from high-resolution data (70,000 nodes) for a large US city providing services to about 900,000 citizens over an area of about 1,000 km^2. For the whole city and for different sized subnets, we also examined these networks in terms of geospatial co-location (roads and sewers). Our analyses reveal functional topological homogeneity among all the subnets within the city, in spite of differences in several urban attributes. The functional topologies of all subnets of both infrastructure types resemble power-law distributions, with tails becoming increasingly power-law as the subnet area increases. Our findings hold implications for assessing the vulnerability of these critical infrastructure networks to cascading shocks based on spatial interdependency, and for improved design and maintenance of urban infrastructure networks.

Introduction

Cities are important case studies of human-dominated ecosystems, where dynamics of flows of resources such energy, food, and water support human communities, and are examples of coupled relationships between humans and nature [1]. Feedbacks between humans and technical systems within the city have cascading impacts over much larger spatiotemporal scales beyond the urban boundaries [2, 3]. It is known that physical assets in cities are fractal, and so too are road networks that constrain the geometry of the urban fabric [4-6]. We posit that several infrastructure networks that support critical urban services are also located in close physical proximity to one another, and as such might also share functional topological features.

Studying urban infrastructure networks that support flows of critical services to communities distributed over large expanses is important for understanding urban dynamics, and for examining impacts on ecosystems beyond cities. Urban networks can be studied from either a structural perspective (e.g., evolution of road networks [4, 7] over time) or from a functional perspective (e.g., dynamics of flows on a network [6, 8]). Here, we conceive urban infrastructure as complex networks, and apply graph theory concepts and network analyses to examine similarities and differences in topologies of above- and below-ground infrastructure networks, and compare them to our recent analyses [9] of urban sewer networks and their natural analogs, river networks; both networks serving the same function: efficient drainage of landscapes.

We begin by providing an analysis of two urban infrastructure networks, roads and sewers, in a large US city (~900,000 residents within the study area of nearly 1,000 km^2) [10], based on high-resolution spatial data (~70,000 nodes), to reveal for the first time, the similarities in functional topology of these networks, and the spatial topological homogeneity of different

sizes of infrastructure subnets within the city with evident differences in urban structure (city center vs. suburbs) and other attributes.

Prior studies [11] of small water distribution networks have found them to be sparse and uninformative without accounting for the heterogeneity in importance of certain key features (reservoirs, tanks, pumps, etc.) within the networks, and suggest that functional properties are of major consequence in the analysis of water distribution networks and may be accounted for in the form of weighted networks [12]. Rather than analyzing weighted networks, functional aspects, related to flows, of the network can be implemented by considering the dual representation, where segments, defined by some attribute (such as street name or curvature; or pipe size), are instead considered as nodes and each intersection or junction an edge. We utilize a dual-mapping method, known as Hierarchical Intersection Continuity Negotiation (HICN) [13] to examine road and sewer networks. Previous studies have successfully utilized this and similar methods to produce dual representations to show the universality of functional topological attributes in road networks [5, 8, 13-16].

For reasons of practicality, reliability, and eminent domain, the geospatial location of many infrastructure networks, including road networks and other underground water networks (urban drainage; sanitary sewers; potable water distribution) are expected to be well correlated. Practical considerations, such as intense competition for space within urban areas, the ability to easily locate, access, and maintain existing infrastructure, and governmental control of land through eminent domain, further reinforce that urban infrastructure networks be spatially co-located [17-19].

Here, we first examine the functional topologies of road and drainage networks in the study area focusing on their node-degree probability density distributions (pdfs). In the next

section, we explore the spatial variability of the functional topology of multiple sizes of subnets within the city. Finally, the geospatial co-location of roads and below-ground drainage networks and their topological properties are evaluated. We close with implications of our findings to the design and maintenance of urban infrastructure and community resilience.

Results

A) Study Area and Infrastructure Network Topology

The topography of the studied urban area is flat, with moderate slopes and rolling hills, experiencing mid-continental climate with four distinct seasons. Peak rain occurs from May-July (mean annual rainfall: 16-19 mm/day) [10]. Urban drainage infrastructure for the case study city is a mix of public and privately owned utilities, consisting of both combined and separated sanitary and storm water sewers. High-resolution urban drainage and road network records are maintained by the city municipal GIS office, and were provided for our analyses presented here.

Dual representations of both road and sewer networks for the study area were generated, following the HICN method described by Masucci et al. [13] (details are given in Methods section). Fitting dual-mapped (HICN) node-degree probability density distributions (*pdf*s) for urban infrastructure network data is confounded by several constraints related to availability of sparse data over a limited data range, especially when these distributions are to be approximated as power-law distributions, in particular the “finite-size” effects (see details in methods). For these reasons, our analyses recognize these challenges by estimating power-law distributions with both frontal (to account for minimum node-degree and network resolution) and distal truncation (to acknowledge the finite-size effect) over the limited data range. Thus, double-truncation (Double Power-law) was examined similar to the method used by Massucci et al [13]

and following the power-law fitting guidelines proposed by Clauset et al. [20], and further refined by Corral and Deluca [21].

For both randomly generated subnets, and for the city as a whole, the node-degree *pdf*s of all dual-mapped road networks larger than 5 km^2, and dual-mapped sewer networks larger than 100 km^2, reveal two distributions. These node-degree *pdf*s were approximated as double power-law with greater than 90 % of tests (2,500 repetitions per subnet) failing to reject the null-hypothesis of a power-law distribution. The slopes of the entirety of the road and sewer networks were found to be approximately $\gamma_{r1} = 2.5$ and $\gamma_{r2} = 3.1$ for roads, and $\gamma_{s1} = = 2.9$ and $\gamma_{s2} = = 4.1$ for sewers. The results for the upper distributions (γ_{x1}) are in accordance with numerous other complex network studies indicating a narrow range of γ-values of about -2 to -3 [22-24] and are consistent among subnets of different sizes and location with minimal variability, especially when a subnet area greater than 20 km^2 is considered. The results for the tails of the *pdf*s (γ_{x2}) are both more variable and steeper than the upper trunk segments, and are influenced by the finite-size effect, and seem to gradually approach the slope of the upper segment as the subnet size is increased.

Confirming this convergence and comparing the slopes (γ) for different types and sizes of networks, along with the degree of truncation, should be a topic of future research and would allow for drawing inferences about likely differences in network topology. In addition, the emergence of power-law *pdf*s with increasing network size in road and water networks in diverse cities would also be useful in uncovering consistent patterns in urban infrastructure network topology, and thus provide an indication of the underlying generating mechanisms for the infrastructure networks.

B) Spatial Homogeneity of Functional Network Topology

Here, self-similar and scaling properties of these infrastructure networks were investigated by means of producing randomly distributed, nested subnets of 1.25, 2.5, 5, and 7.5 km radius, and analyzing four common topological metrics: node-degree distribution, average node-degree, clustering coefficient, and network density. In addition to the spatial co-location of roads and drainage pipes, a better understanding of the scaling and self-similar properties exhibited by these infrastructure networks would be a valuable resource for city planners and decision makers seeking to predict the location of water pipes in a city. If the water and drainage networks can be shown to be *functionally self-similar* at various scales, only a small area of sufficient size may be used to represent the city as a whole with reasonable certainty, rather than having to consider the entire city (a process requiring a great deal of data and computer processing time for large cities).

Beyond a threshold population of ~5% (~50,000 persons; 20 km^2 area) of the total, the average node-degree of both roads and pipes was found to be highly homoscedastic, with little variability throughout the city (Figure 3-A). This suggests that, spatially or with population variability, there is an overall homogeneity in terms of how these sewer and road networks are connected, i.e., the ratio of edges to nodes remained more or less constant among the subnets. The values of the average node-degree also provide insight to the physical structure of these networks. In the limits, a large average node-degree (near four), such as those found for roads, indicates a network with a highly looped structure, whereas a small average node-degree (near two), such as those found for pipes, indicates a more tree-like structure with fewer loops. These differences in structure provide important insights into the design principles based on functions (e.g., flow directionality) and performance reliability/redundancy demands of these networks.

Roads and sewers serve inherently different purposes. Sewers are primarily concerned with collection of inputs from multiple, spatially distributed sources, aggregation into larger pipes before reaching a single (the wastewater treatment plant) or few (combined sewage outfalls) destination points. For such a network, with converging flows towards an outlet, a tree-like structure is often the most efficient mode of transport, as is well known to be the case for natural river networks [25, 26]. Roads, on the other hand, must take multiple inputs (origins, drivers) and allow them to reach *any* possible destination within the city. While the optimal solution for a single origin or driver would likely be a spanning-tree network reaching all destinations, in order to accommodate multiple origins and multiple drivers needing to reach multiple destinations, overlapping trees must be created and the resulting irregular lattice-like road structure is familiar to most modern cities.

In addition to structural considerations, the average node-degree and corresponding tree-like or looped structure hints towards the perceived importance of the two types of infrastructures. Access to reliable transportation is well correlated with increased economic output, and an improved standard of living [27]. As such, it is critical that the transportation system does not fail. The grid-like structure of urban road networks allows for redundancy and alternate routes in the event of failure (congestion) at a given node. Flows in sewer networks are primarily gravity-driven, and failures are relatively infrequent (flooding during large return-period storm events, clogging, pipe collapses) or moderate (minor roadway flooding or subsidence) as long as major components (large node-degree) are segregated from other critical infrastructure or services (major roads, electric components, hospitals, etc.) [28]. In addition, cost efficiency dictates that loops should occur infrequently given that sewer pipes should be installed

along the shortest path possible at a minimum depth, and minimum capacity to meet service demands.

Based on the clustering coefficients, both road and sewer networks in the study area were found to be spatially homogenous in functional topology, again with a homoscedastic distribution after a threshold population of approximately 50,000 persons (see Figure 3-B), reinforcing the idea that these networks are similarly connected at all scales, i.e., self-similar topology. The small values of the clustering coefficients indicate that neighbors in these networks are not well connected and the network does not exhibit small world characteristics [29].

Overall, the clustering coefficient for the sewer networks was nearly double that of the road networks, indicating a greater tendency for roads to cluster together in cliques as compared to sewer networks in the same study area. This finding is in accordance with standard principles of sewer design. Being predominantly gravity-driven and converging-flow networks, sewer networks are often, though not always, organized to follow natural watersheds with only minimal connections between neighboring watersheds and a priority towards efficiently removing water from a given area. Roads and drivers on the other hand are less constrained by topography and may freely move between watersheds at multiple locations with a priority towards ease of mobility.

The average node-degree and clustering coefficients together show that road and sewer infrastructure networks in *this city* tend to be highly spatially homogenous, and reveal these networks to be self-similar at multiple scales throughout the city. At each spatial scale, the node-degree distribution, average node-degree, and clustering coefficient **all** fall within narrow ranges with minimal variability, indicating that the ways in which these networks connect remain

constant across spatial scale. Given this self-similarity, one would expect network density to decrease as the total number of possible edges increases approaching the limit at zero as city (i.e., entire network) size is increased towards infinity. In the smallest subnet these networks contain an average of ~1,000 nodes and edges while the city as a whole contains upwards of 70,000 nodes and edges. Indeed, we observed the network density of both types of infrastructure networks to scale with population following a truncated power-law slope, providing further affirmation of the self-similar, scale-free nature of these networks (Figure 3-C). Analyses of infrastructure network data from several cities is needed to examine if the spatial homogeneity pattern is a common feature.

The hierarchical nature of each infrastructure network was compared by plotting the average node-degree vs. the corresponding clustering coefficient (Figure 3-D). In a perfectly hierarchical network, wherein identical subcomponents are connected to each other perfectly and repeatedly, the slope of such a plot should result in a power-law distribution with negative slope and $\gamma = 1$ [30, 31]. Here, our results indicate that the plot of average node-degree vs clustering coefficient for the study area road network results in a power-law distribution, with $\gamma = 0.9$, indicating a highly regular and hierarchical network. Such a plot for sewers, in contrast, has a positive slope, owing to the gravity driven nature of these systems and a tendency to connect to any larger pipe capable of accommodating the designed maximum discharge. These connections are often irregular and produce a non-hierarchical, loop-less network structure with various sized and shaped components optimally connecting wherever is most convenient and cost-effective.

C) Geospatial Co-location of Infrastructure Networks

These topological analyses however do not take into account spatial information, such as where important, high node-degree pipes or roads are located. Thus, the spatial orientation of

roads and sanitary sewers were analyzed for the study area. Starting with a roadway centerline shapefile (provided by the municipal GIS office), buffers of 1 m increments (1 to 15 m range) were applied to the centerline and intersecting sanitary sewer lines were clipped out. In the United States the design standard for lane width is 3.6 m [32], meaning that the maximum buffering distance in this study is equivalent to the width of a two-lane road plus an equivalent area of right-of-way (land obtained through eminent domain) surrounding the road. The mean width of the actual right-of-way was found to be equivalent to an 11 m buffer on both sides of the centerline.

For the studied urban area, the total length of sewers located under the buffered area increased from ~18 % of the total length of the sewer system at a 1 m buffering distance, to ~74 % at the 15 m buffer (Figure 4-A) ~66 % of the total length of the sewer system was found to fall within the boundaries of the mean right-of-way distance. At a 15 m buffer distance, ~49 % of the length of the road network can be expected to have a sewer pipe beneath, and ~66 % of all roads can be expected to have a sanitary pipe beneath at least some portion of its length. Indeed, much of the length of the sewer network for this city can be expected to be found in close physical proximity to roads. These findings are in accordance with those for the city of Innsbruck, Austria [33, 34], and support the assumption that pipes are under roads [33-35].

In addition to co-location, correlation between the *size* of a pipe or *class* of a road and the underlying sewer pipes is essential for assessing the vulnerability of co-located infrastructure networks to cascading failures. Analysis of the size distribution of sewer pipes co-located with roads shows no correlation either positive or negative, for the co-location of large diameter pipes with roads (Figure 4-B). In fact, contrary to what might be expected, large diameter pipes (>250 cm diameter) are found to be almost entirely located under roads, while small (<75 cm diameter)

and medium (75-250 cm diameter) pipes exhibit a lesser degree of co-location with roads. Over time, leaking sewer pipes can lead to soil subsidence undermining the integrity of overlying road segments and eventually cause disruptions ranging from small potholes to complete collapse of a road segment. In addition, high traffic and heavy loads on major roadways may increase the deterioration rate of subsurface pipes. For these reasons, among others, city planners would be wise to avoid spatial co-location of major pipes and roads.

When network metrics are considered (i.e., betweenness centrality or node degree as proxy measures for the importance of each pipe or road segment in a network) of co-located segments are considered, a clear pattern emerges (Figure-5: A and B). A clustering of points in the bottom left corner of Figure 5-A indicates a preference for the co-location of low node-degree roads and pipes. While the upper left and bottom right hand quadrants indicate a preference for high node-degree pipes to be located under low node-degree roads, and for high node-degree roads to be located above low node-degree pipes respectively. An absence of points in the upper right hand corner suggests an aversion to the co-location of high node-degree pipes with high node-degree roads. In Figure 5-B the same pattern emerges when the colocation of sewers and roads based on betweenness centrality is considered. Again, an absence of points in the upper right quadrant suggests an aversion to the co-location of high centrality roads and sewers. Tendencies to separate the location of high node-degree and high centrality roads and sewer pipes are also visually evident (Figure 6). Both high-node-degree as well as high-centrality roads and sewers (magnitude represented by line thickness) are seen to be largely separate from each other with only minimal overlap.

Implications

Previous topological analyses of natural and human-built networks [4-7, 16, 23-26, 36] offer important guidance to our analyses of urban infrastructure networks presented here. While engineering analyses of the design and functions of urban infrastructure are well understood [32, 37], exploration of urban water network topologies, from a graph theory perspective, has received limited attention to date. Records detailing the location and attributes of above-ground infrastructure networks, such as roads, are often readily available and reliable**,** allowing for monitoring and modeling of features such as traffic flow [28, 33-35, 38-41]. However, risk and resilience analyses of critical urban infrastructure, those considering the performance, and mitigation of consequences resulting from system failures, require detailed data regarding the specific layout of above-ground and underground networks, as well as additional information on various physical attributes (e.g., traffic volume for roads; pipe size, flows, and connectivity for sewer networks; etc.), which are frequently not available. Thus, comparing topological similarities of roads and rivers with sewer networks will help in developing a general understanding of urban networks.

The similarities in functional topologies of two infrastructure networks (roads and drainage), and that of river networks, hold meaningful implications for their overall reliability under stress. Previous studies [22, 42-44] have shown that scale-free networks (those with power-law node-degree *pdf*s) are highly resilient to random failures but vulnerable to failures of high-degree nodes, which can quickly lead to network-wide discontinuity and system failure. The spatial co-location of urban infrastructure networks, while practical, also introduces the possibility of undesirable consequences. For instance, a leaky pipe can result in soil subsidence and potholes in the road above or a burst water main might cause collapse of road segments, local flooding, and bring traffic to a halt even though the road itself might not have suffered any

physical harm or degradation. Co-location of high node-degree or high centrality road and sewer features could exacerbate the issues of interdependence in the event of failure of hubs in one or both networks leading to the potential for cascading failures across networks. Such considerations should be accounted for and minimized during the design process, and included as a component when assessing interdependence of infrastructure networks is evaluated.

The spatial and network analyses performed for one large US metropolitan area in this study indicate that while the co-location of high node-degree and high centrality roads and sewers is generally avoided, in the case of the study city, outliers do exist. These co-located large node-degree features may be thought of as potential points of failure (loss of service; erosion of resilience), and can be used as a criterion for allocating resources for maintenance and service loss prevention.

Beyond the potential for cascading failures, the principles of self-similarity present in the underground sewer lines should allow modelers to develop more realistic hydraulic models given limited data, or setting rules for generating semi-virtual networks [33-35]. By setting rules for the clustering of sewer networks, degree of co-location, avoidance of co-located large node-degree roads and pipes, and overall tree-like structure, modelers can eliminate unrealistic designs that do not conform to known structural and functional features. A highly looped sewer network for instance would likely be unrealistic and cost-ineffective. While such a design would be preferable for high-value, critical, or variably loaded infrastructure networks such as roads.

Acknowledgements

The authors wish to acknowledge the city municipal GIS office for their assistance accessing and interpreting the data used in this study. This research was supported by NSF Award Number 1441188 (Collaborative Research-- RIPS Type 2: Resilience Simulation for

Water, Power and Road Networks). Two authors (CK, XZ) were funded by the NSF grant, while EK was supported by the Helmholtz Center for Environmental Research, Leipzig, Germany, and by a Graduate Fellowship from the Purdue Climate Change Research Center. Additional financial support for the last author (PSCR) was provided by the Lee A. Rieth Endowment in the Lyles School of Civil Engineering, Purdue University.

Competing Financial Interests

The authors report no competing financial interests.

Author Contributions

CK, EK, and PSCR planned the research, and wrote the main text. XZ, SU, and FB provided conceptual support, while EK and XZ provided data analysis. All authors reviewed and contributed to the paper.

Methods

A) Data Acquisition and Preparation:

Infrastructure data were obtained from the municipal GIS office and consisted of ESRI shapefiles indicating the spatial location of roads, sanitary sewer lines, and associated attributes (such as speed limit, street name, and road class for roads and pipe diameter, and construction material for the sanitary sewer lines). Starting with the existing shapefiles, z-measures were removed so that the networks could be approximated as planar graphs and existing segments were snapped to the nearest closest feature at a threshold of .25m in order to ensure network connectivity.

We analyze the spatial variability and scaling properties of the water and road networks in the study area. For this study, different size subnets were created. Randomly distributed and nested subnets were extracted from each network layer. Subnet creation consisted of selecting 25 random points throughout the city based on the location of manholes, and then running a clip process to extract circular selections surrounding each random point at buffered radii of 1.25, 2.5, 5, and 7.5 km. The population for each subnet was determined using data from the 2010 US census [10].

B) Network Extraction and Dual Mapping

For these analyses, the dual representation of the networks was utilized following the method of Hierarchical Intersection Continuity Negotiation (HICN) described by Masucci et al [13]. Generally urban infrastructure networks are analyzed using the primal representation where intersections or junctions are considered as nodes and the connecting segments as edges [23, 24]. This process has been utilized in several studies of urban infrastructure networks [11, 12, 36], and can be useful for determining geometric properties of the network, but by treating network as

homogenous (all nodes and links are of equal value and identical function) these types of analyses often obscures functional properties.

C) Network Topological Metrics

Here, we investigate four measures of network topology:

1. **Node-degree Distribution [*p(k)*]:** The node-degree *pdf* describes the overall connectivity of the network, i.e. the relative distribution of highly connected nodes to poorly connected nodes. In real-world networks, the node degree distribution will often resemble a power-law distribution, frequently with either frontal or distal truncation or both. Constraints to generating statistically robust estimation of power-law parameters using observational data include: (1) the "finite-size effect" (urban agglomerations are $\leq 10^3$ km^2; (2) total number of primal and dual-mapped nodes $\leq 10^4$; and (3) dual-mapped node-degrees $\leq 10^2$). Thus, the available network data, even at high resolution, as in this study, do not cover the multiple orders of magnitude needed to test for "pure" power-law *pdf*s. These challenges become more apparent when data for different sized sub-nets are analyzed for comparison or when network growth over time is examined.

   Here, we have fitted double power-law distributions to the data for roads and sewers, follow methods adapted from Clauset et al [32] and Corral and Deluca [20, 21]. The k_{min} used for determining the break point between the two distributions and the fit of the lower distribution (γ_{x2}) were found using the method and R code provided by Clauset et al [20], while the fit for the upper "trunk" distribution (γ_{x2}) was estimated by MLE and the comparison of CDFs by the Kolmogorov-Smirnoff test (both implemented using Matlab R2016b) as suggested by Corral and Deluca for fitting discrete power-law distributions [21]. In all cases the upper distribution was calculated as a power-law distribution from k=3 to the

break point determined by the Clauset et al method. If for a given subnet there was no significant power-law tail, as determined by the Clauset et al. method, a single power law distribution was estimated from k = 3 to the highest node-degree for the subnet.

2. **Average Node-degree**: A measure of the average connectivity of each node in a network and calculated as <k> = 2E/N. The average node-degree of a network serves as an indicator of the types of connections that are present in a network and can help distinguish between a network characterized by a tree-like structure (<k> = 2) or a more grid like or cyclic structure (<k> = 4) [23, 24] .

3. **Average Clustering Coefficient**: a measure based on the number of triplets within a network indicating the overall connectivity of neighboring nodes, and calculated as the number of closed triplets divided by the number of connected triplets of nodes. The clustering coefficient provides insight to the modularity or small world properties of a network. A high clustering coefficient would indicate that sections of the network (modules) are well connected within, but have only a few connections between different modules [29].

4. **Network Density**: A measure of the ratio of the number edges to the maximum possible number of edges, and calculated as the binomial coefficient (N/2). This measure has been used to assess the variability in network connectivity at various distances from the city center [45] and serves as indicator of connectivity at different spatial scales.

References

1. Marzluff, J.M.S., Eric; Endlicher, Wilifried; Alberti, Marina; Bradley, Gordon; Ryan, Clare; Simon, Ute; ZumBrunnen, Craig *Urban Ecology: An International Perspective on the Interaction Between Humans and Nature*. 2008, New Your, NY: Springer-Science+Business Media, LLC.
2. Seto, K.C.G., B.; Hutyra, L. R., *Global forecasts of urban expansion to 2030 and direct impacts on biodiversity and carbon pools.* PNAS, 2012. **109**(40): p. 16083-16088.
3. Seto, K.C.R., A.; Boone, C. G.; Fragkias, M.; Haase, D.; Langanke, T.; Marcotullio, P.; Munroe, D. K.; Olah, B.; Simon, Davis, *Urban land teleconnection and sustainability.* PNAS, 2012. **109**(20): p. 7687-7692.
4. Barrington-Leigh, C. and A. Millard-Ball, *A century of sprawl in the United States.* Proc Natl Acad Sci U S A, 2015. **112**(27): p. 8244-9.
5. Kalapala, V., et al., *Scale invariance in road networks.* Phys Rev E Stat Nonlin Soft Matter Phys, 2006. **73**(2 Pt 2): p. 026130.
6. Louf, R. and M. Barthelemy, *How congestion shapes cities: from mobility patterns to scaling.* Sci Rep, 2014. **4**: p. 5561.
7. Barthelemy, M., et al., *Self-organization versus top-down planning in the evolution of a city.* Sci Rep, 2013. **3**: p. 2153.
8. Hu, M.-B., et al., *Urban traffic simulated from the dual representation: Flow, crisis and congestion.* Physics Letters A, 2009. **373**(23-24): p. 2007-2011.
9. Yang, S.P., Kyungrock; Mcgrath, Gavan; Urich, Christian; Krueger, Elisabeth; Rao, P. Suresh C., *Self-similarity emerges in growing drainage networks.* PNAS, 2016. **Submitted, In Review**.
10. Bureau, U.C., *2010 US Census*. 2010, US Census Bureau.
11. Yazdani, A. and P. Jeffrey, *Complex network analysis of water distribution systems.* Chaos, 2011. **21**(1): p. 016111.
12. Yazdani, A. and P. Jeffrey, *Water distribution system vulnerability analysis using weighted and directed network models.* Water Resources Research, 2012. **48**(6).
13. Masucci, A.P., K. Stanilov, and M. Batty, *Exploring the evolution of London's street network in the information space: a dual approach.* Phys Rev E Stat Nonlin Soft Matter Phys, 2014. **89**(1): p. 012805.
14. Jiang, B., *A topological pattern of urban street networks: Universality and peculiarity.* Physica A: Statistical Mechanics and its Applications, 2007. **384**(2): p. 647-655.
15. Masucci, A.P., K. Stanilov, and M. Batty, *Limited urban growth: London's street network dynamics since the 18th century.* PLoS One, 2013. **8**(8): p. e69469.
16. Porta, S., P. Crucitti, and V. Latora, *The network analysis of urban streets: A dual approach.* Physica A: Statistical Mechanics and its Applications, 2006. **369**(2): p. 853-866.
17. Batty, M., *The Size, Scale, and Shape of Cities.* Science, 2008. **319**(5864): p. 769-771.
18. Batty, M., *The New Science of Cities*. 1 ed, ed. M. Press. 2013: The MIT Press. 520.
19. Strano, E., et al., *Elementary processes governing the evolution of road networks.* Sci Rep, 2012. **2**: p. 296.
20. Clauset, A., C.R. Shalizi, and M. Newman, *Power-law Distributions in Empirical Data.* SIAM Review, 2009. **51**(4): p. 661-703.

21. Corral, A. and A. Deluca, *Fitting and goodness of fit test of non-truncated and truncated power-law distributions.* Acta Geophysica, 2013. **61**(6): p. 1351-1394.
22. Barabasi, A.A., R., *Emergence of Scaling in Random Networks.* Science, 1999. **286**(5439): p. 509-512.
23. Barthélemy, M., *Spatial networks.* Physics Reports, 2011. **499**(1-3): p. 1-101.
24. Newman, M., *The structure and function of complex networks.* SIAM, 2003. **45**(2): p. 167-256.
25. Paik, K. and P. Kumar, *Power-Law Behavior in Geometric Characteristics of Full Binary Trees.* Journal of Statistical Physics, 2011. **142**(4): p. 862-878.
26. Rinaldo, A., et al., *Evolution and selection of river networks: statics, dynamics, and complexity.* Proc Natl Acad Sci U S A, 2014. **111**(7): p. 2417-24.
27. Weisbrod, G.R., A., *Economic Impact of Public Transportation Investment*, APTA, Editor. 2009, TCRP Project J-11, Task 7, TRasit Cooperative Research Program: APTA.
28. Carrico, N., et al., *Prioritization of rehabilitation interventions for urban water assets using multiple criteria decision-aid methods.* Water Sci Technol, 2012. **66**(5): p. 1007-14.
29. Watts, D.J.S., S.H., *Collective Dynamics of 'Small-Worlds' Networks.* Nature, 1998. **393**: p. 440-442.
30. Dorogovtsev, S.N., A.V. Goltsev, and J.F. Mendes, *Pseudofractal scale-free web.* Phys Rev E Stat Nonlin Soft Matter Phys, 2002. **65**(6 Pt 2): p. 066122.
31. Noh, J.D., *Exact scaling properties of a hierarchical network model.* Phys Rev E Stat Nonlin Soft Matter Phys, 2003. **67**(4 Pt 2): p. 045103.
32. Staff, A.A.o.S.H.a.T.O., *A Policy on Geometric Design of Highways and Streets*. 6 ed. 2011: American Association of State Highway and Transportation Officials.
33. Mair, M., W. Rauch, and R. Sitzenfrei, *Improving Incomplete Water Distribution System Data.* Procedia Engineering, 2014. **70**: p. 1055-1062.
34. Mair, M.S., R.; Moderl, M.; Rauch, W., *Identifying Multi Utility Network Similarities*, in *World Environmental and Water Resources Congress 2012: Crossing Boundaries*, ASCE, Editor. 2012. p. 3147-3153.
35. Blumensaat, F., M. Wolfram, and P. Krebs, *Sewer model development under minimum data requirements.* Environmental Earth Sciences, 2011. **65**(5): p. 1427-1437.
36. Roth, C., et al., *A long-time limit for world subway networks.* J R Soc Interface, 2012. **9**(75): p. 2540-50.
37. Managers, G.L.U.M.R.B.o.S.a.P.P.H.a.E., *Recomended Standards fo Wastewater Facilities.pdf*. 2014, Health Reasearch Inc.
38. Rosini, M.D., *Macroscopic Models for Vehicular Flows and Crowd Dynamics: Theory and Applications*. 1 ed. 2013: Springer International Piblishing.
39. Treiber, M.K., A., *Traffic Flow Dynamics: Data, Models and Simulation*. 1 ed. 2013: Springer-Verlag Berlin Heidelberg.
40. Tyagi, V.D., S.; Rajagopal, K.R., *A review of the mathematical models for traffic flow.* International Journal of Advanced Science, Engineering, and Applied MAthematics, 2009. **1**: p. 53-68.
41. Amirat, A., A. Mohamed-Chateauneuf, and K. Chaoui, *Reliability assessment of underground pipelines under the combined effect of active corrosion and residual stress.* International Journal of Pressure Vessels and Piping, 2006. **83**(2): p. 107-117.

Volume 36, Number 3, December 2017 *Decision Analysis Today*

Research

Column Editor: Roshanak Nateghi

Resilient Urban Infrastructure?

P. Suresh C. Rao, Elisabeth Krueger and Christopher J. Klinkhamer
Lyles School of Civil Engineering, Purdue University
West Lafayette, IN 47906 (SureshRao@purdue.edu)

Widespread devastation and attempts at recovery, a humanitarian crisis still unfolding along the tracks of three hurricanes (Harvey, Irma, and Maria), have revealed several important features about community resilience, and raised questions about the role of infrastructure networks, especially in extreme events. Emergency response and recovery efforts rightfully focus on rebuilding the damaged infrastructure to restore critical services. Yet, by failing to also address changes needed in management structures, decision making, and policy instruments that serve as disincentives for change, restoring infrastructure addresses only a part of the recovery to enhance community resilience. How do we then assess the resilience of infrastructure networks and coupled socio-economic systems in these affected communities, and develop decision tools for enhancing urban resilience? We will argue here that technological systems in isolation do not have *inherent resilience*. On the contrary, technological systems are imbued with resilience by coupling with socio-economic systems (institutions), which build, maintain, and repair such systems to provide several critical services.

Let us start with the definitions of resilience of complex systems. We have argued (Park et al., 2013) that resilience is not about what a system/network *has* (a list of attributes; all nouns) but rather what it *does* (all verbs) in response to small or large disturbances. In this sense, fail-safe designs of robust infrastructure networks, informed by risk analyses, lead to increased hardening to offer resistance up to a designed level of stress with known probabilities of occurrence. When external stresses exceed such built-in resistance, or arrive as a "surprise" (unexpected from risk analyses), robust infrastructure often fails with catastrophic consequences; levee failures in New Orleans and overtopped sea walls in Tohoku are classic examples. Such robust systems also have designed redundancy and some flexibility to minimize loss of critical services. However, such robust technological systems do not recover without the intervention of public and private institutions that manage them (e.g., utilities, agencies, etc.) and in extreme cases through collective action within the affected communities.

Ability to marshal financial resources, emergency supplies, technological prowess, coordination among government agencies and utilities are all crucial elements of recovery. Building urban resilience requires tightly coupled technological and socio-economic networks. Washed away bridges, eroded and blocked roads, blown substations, or downed power lines and cell towers, etc., do not self-repair. Thus, infrastructure systems in isolation do not have *inherent r*esilience to recover. What resilience the

infrastructure exhibit is instead endowed by the adaptive capacity of the social-economic systems that depend on the critical services. The ability to *self-organize* in response to crisis is what complex socio-economic systems (and ecosystems) reveals their resilience. Resilience is then an *emergent property* of coupled complex systems/networks and ecosystems.

Along the tracks of the three hurricanes, poorer and isolated communities experienced more severe damages, have limited adaptive capacity because of the confluence of many limiting factors, and will have longer recovery times. In urban communities, we strive to return to the pre-disaster, desirable state (in a normative sense). However, post-Katrina evolution in New Orleans shows that urban recovery trajectories might lead to social transformations, evident in demographic shifts in the city population, persistence of economic and social inequalities and differential rates of recovery in different parts of the city.

Resilience is not only the ability to recover from a single, large disturbance. As the Japanese saying goes "*Nana korobi, yaoki*" ("fall seven times; get up eight times"), resilience is about being prepared for surprises. Long-term persistence in recovering from loss of functions caused by a series of unexpected disturbances is an essential feature. Resilience is also about recovering from a series of chronic, high probability, and low magnitude events, which gradually erode the adaptive capacity of the affected communities, and leads to collapse even in the absence of an extreme event (Klammler et al., 2017).

Resilience is contingent on *memory* of past events, which defines the current state of the system of interest. The relationship between the recurrence period of disturbance events and the social memory of such disturbances determines the preparedness of the affected community. Because the return period of extreme events is large, social memory of lessons learned from such events has to be equally long (inter-generational). On the other hand, because return periods for frequently recurring events are small, the communities are already well adapted to them. However, non-stationarity of disturbances, with changes in the magnitude and frequency probabilities of extreme events, as illustrated by three successive 1 in 500 year floods in Texas or three back-to-back magnitude-4 hurricanes, pose serious challenges to the resilience of affected urban communities.

The challenge then is to measure/monitor adaptive capacity and to manage it in three ways. First, maintain *total* adaptive capacity above some critical level, both at the scale of the individual within the community and at the city scale. This is similar to accumulating total financial assets (say savings account) to ensure economic security. Second, maintain a certain level of *active* adaptive capacity (e.g., accessible cash flow, similar to not overdrawing a checking account). Third, discourage maladaptive practices that erode adaptive capacity or inhibit emergence of resilience.

In the current crisis in Puerto Rico, delivering essential supplies where most needed is limited by logistical challenges from collapse of transport, communication and power infrastructure networks in Puerto Rico (constrained adaptive capacity). The communities coping with such a dire situation for extended periods have to depend on self-help at a neighborhood scale. As admirably demonstrated in Houston, Florida, and Puerto Rico, self-organized large-scale mobilization of resources helped affected communities to survive the aftermath of the hurricanes.

Resilience of communities depends on multiple infrastructure systems/networks that are geospatially co-located and functionally inter-dependent. These networks co-evolve over time as cities grow and as the demands change, and the complexity of inter-dependence increases. For example, failure of power grids

Volume 36, Number 3, December 2017 *Decision Analysis Today*

leads to problems in treating and pumping potable water through distribution networks, traffic jams from loss of traffic signals and other traffic management systems, loss of communication networks, and inability to provide critical medical assistance. Again, in Puerto Rico, such cascading failures have severely limited the communities' ability to cope and recover from the hurricanes.

We proposed (Park et al., 2013) that resilience of complex systems is also a *recursive process.* The Adaptive Cycle for resilience in coupled social and technological systems comprises of four essential steps. *Sensing* requires monitoring of the system states (e.g., Big Data) for diagnosing shortcomings. "Sensing" does not eliminate variability, instead it increases awareness of *people* to changes to their environment. *Learning*, based on analysis of monitoring data and other related information (e.g., machine learning and other analytical tools), allows recognition of spatial and temporal patterns. A part of "learning" is maintaining community memory of past events and lessons learned from events that had occurred in different places.

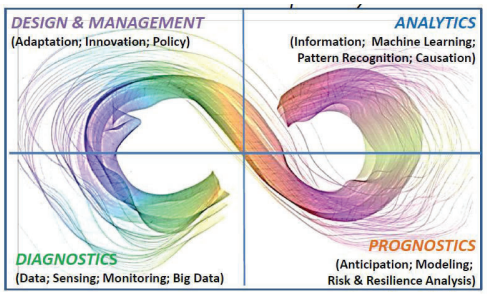

Figure 1. Resilience as a recursive process. Mobius strip image from: https://gizmo.com/tag/mobius-strip

Anticipating, based on data-model integration, helps develop forecasting ability of impending vulnerabilities. Communities fine-tuned to long-term variations develop appropriate adaptive strategies, but are not well prepared to deal with surprises (stochastic shocks). For extreme events like hurricanes, sophisticated monitoring and advanced models do provide few days of lead-time for preparation. Failure to predict the erratic trajectories of the Hurricanes Harvey and Irma show how even sophisticated models are unable to predict the outcomes of feedbacks on large-scale behavior of complex systems. However, large events like earthquakes and tsunamis or flash floods require quick response if robust infrastructure fails.

Adapting is needed for maintaining a desirable regime, by coping with disturbances and improving system elements, such as design and management practices, or by transforming system structures (e.g., network topology and flows) in order to maintain and improve functions. Anticipation and adaptation also determine the preparedness of the communities. Kreibich et al (2017) examined impacts of successive floods, and found that the damage from the second flood event was significantly lower. Increase in awareness (learning), better preparedness (anticipation), and improved emergency response (management) all contributed to effective reduction in flood vulnerabilities and facilitated adaptation. Based on analyses (data analytics) multiple case studies, they argue for a shift from reactive to anticipatory flood risk management.

Our recent work (Krueger et al., 2017; Klinkhamer et al., 2017; Yang et al., 2017; Zischg et al., 2017) on urban water infrastructure networks in several cities shows that in spite of the obvious differences in structure (layouts of pipe, road, and river networks) among these urban networks, their functional topologies based on flows have striking similarities. These results are in agreement with analyses of internet and neural networks. With increasing size, as the population and demands grow, the network functional topology converges to become increasingly self-similar. That is, neighborhood variations in

infrastructure networks reflect local constraints and engineering design requirements, but larger, city-scale features overwhelm such differences, and urban network topology is surprisingly similar to naturally evolved networks (e.g., rivers). Where deviations from this "natural design" occur, operational difficulties are likely in managing infrastructure networks. We should learn from these observations that while engineered systems allow maintaining certain desired functions, natural systems provide blueprints of how to approach engineering design. Cities are integral components of regional, national, global networks of other cities; as such, resilience of any one city has significant implications to many other cities embedded in the network.

Large cities that build and operate large, complex, interdependent infrastructure networks also develop sophisticated socio-economic networks to maintain and manage the delivery of crucial services to urban citizens. Reliable functioning of these infrastructure networks contributes to their "invisibility." Only failure reveals their inadequacies. In such cities, the user community is largely not engaged in the operations of infrastructure. In fast-developing countries, the existing aging infrastructure is overwhelmed by rapid growth in demands, the lack of coordination among agencies, and limited financial resources to maintain and upgrade. Given such limitations of infrastructure and dysfunctional institutions, household- and community-level adaptive strategies help cope with limited services, and inadequate access to infrastructure.

Like in the case of the recent hurricanes, poorer communities have a lower ability to cope and adapt, restrained by multiple limiting factors, such as the lack of financial capital and access to infrastructure and services. Such examples reveal how inter-dependence between infrastructure and socio-economic systems contributes to or erodes community resilience. Just as there are differences among cities in their adaptive capacity for maintaining resilience, there are similar differences within communities in a city. This contributes to inequities in the ability of communities to cope with extreme events, and contributes to persistent patterns of unequal spatial resilience within and among cities. In Puerto Rico, recovering slowly from the ravages of Hurricane Maria, only ~30% of the population has power (unlikely to meet the promised 90% recovery by end of the year), and 70% have water but must boil to drink. However, economic inequalities that existed before Maria were exacerbated and evident in the great disparities in the recovery of different communities.

Resilience of coupled technological-engineered systems/networks is also about avoiding "traps". Significant limitations of resources (i.e., adaptive capacity) to cope with and upgrade infrastructure and improve institutions drives some communities into "Poverty Traps" where provision of critical services is inadequate, unreliable, and/or access is limited. Without help from external agencies, these communities cannot recover. The other extreme is a "Rigidity Trap", where the sunk costs of robust-yet-fragile infrastructure are large enough to scuttle efforts in reducing vulnerabilities from extreme events. Increasing adaptive capacity and improved access to infrastructure are essential to escape from poverty traps. Instead of hardening infrastructure to be robust, introducing flexibility, diversity, and some decentralization of infrastructure helps avoid rigidity traps. In socio-ecological systems, increased robustness to decrease system state variance works in the short-term, but builds up hidden vulnerabilities and can lead to catastrophic failures (Ishtiaque et al., 2017). Such trade-offs must be carefully evaluated in technological-social systems as well. Improved social connectivity and broader engagement in governance enhances overall community resilience.

Lack of methodical knowledge and integrated modeling of loss/recovery of critical services derived from coupled engineered and social systems, and failure to maintain appropriate interdependencies between these coupled urban systems - especially for coping with chronic and extreme events - can have serious consequences. Examples include failure to maintain adequate adaptive capacity, poor understanding of the recovery process, misallocation of resources; longer recovery times for physical networks and communities, high recovery costs, incremental degradation of system functioning, and misguided policy-making. A recent National Academy Workshop Report (NRC, 2015) concluded that the US does not "currently have a consistent basis for measuring [community] resilience" that includes infrastructure and institutional interdependencies, and as such "making it difficult for communities to monitor improvements or changes in their resilience." The report also emphasizes the need to work with communities and urban managers to identify decision tools and strategies for implementing resilience enhancing approaches.

Complete destruction of the power grid in Puerto Rico gives the reconstruction planners and decision makers the opportunity to consider how best to spend the millions of dollars allocated for reconstruction. Should we rebuild the power-grid back with above ground power lines that are vulnerable for future hurricanes, or to put new power lines below ground? Similarly, should the water supply infrastructure be somewhat decentralized at least for remote and rural locations? How do we alter the regulatory and economic disincentives that encourage counter-productive recovery paths (e.g., insurance support to rebuild in vulnerable areas; further hardening of infrastructure; funding policies for disaster relief)?

The communities ravaged by the hurricanes have an opportunity to restore and rebuild their infrastructure by not returning to pre-hurricane technological systems (perhaps even more hardening); rather, some optimal combination of risk-based resistance and resilience approaches will decrease their vulnerabilities to future disruptions. Restored infrastructure must enable communities to better use and amplify their adaptive capacity. In addition, maintaining the numerous ecosystem services provided by natural systems (see Costanza et al., 2017) is a prerequisite to community resilience, and must not be compromised by a singular focus on either social or technological systems in isolation. Resources needed for urban prosperity and resilience are drawn from distant sources, and urban flows do have adverse impacts on resources at these locations. Cities are integral components of regional, national, global networks of other cities; as such, resilience of any one city has significant implications to many other cities embedded in the network.

Many initiatives around the world exist to make cities resilient, such as the "100 Resilient Cities" initiative (Rockefeller, 2016), the London School of Economics Cities project (LSE, 2016), the C40 Cities (C40, 2016), ICLEI Resilient Cities (ICLEI, 2016), among many others. These initiatives show the urgency and global efforts to develop and operationalize urban resilience (e.g., NRC 2015). However, these projects are currently striving to develop tangible criteria, such as developing urban resilience indices for making cities resilient. Yet, delivering methods to measure and model urban resilience remains a challenge. Operationalizing resilience strategies and developing consistent policy/regulatory frameworks are also challenges (Linkov et al. 2015). It is important to understand how cities can be highly adaptive and resilient in order to maintain essential functions (i.e., demands for critical services are met) even when confronted by catastrophic disasters and multiple changes (de Perez et al., 2015).

Citations

C40. Benefits of Climate Action: Plotting a Global Approach to Measurement. www.c40.og.

Costanza, R., R. de Groot, L. Braat, I. Kubiszewski, L. Fioramonti, P. Sutton, S. Farber, and M. Grasso. 2017. Twenty years of ecosystem services: How far have come and how far do we still need to go? *Ecosystem Services,* 28: 1-18.

De Perez, E.C., M. van Aalst, D. Chetan, B. van den Hurk, et al. 2015. Managing the risk of extreme events in a changing climate: Trends and opportunities in the disaster-related funding landscape. *Working Paper series No. 7,* Red Cross/Red Crescent Climate Centre, The Hague, The Netherlands.

ICLEI, 2017. Resilience Cities Report 2017: Tracking Local Progress on the Resilience Targets; *8th Global Forum on Urban Resilience and Adaptation*, May 4-6, 2017, Bonn, Germany.

Ishtiaque, A., N. Sangwan, and D. Yu. 2017. Robust-yet-fragile nature of partly engineered social-ecological systems: a case study of coastal Bangladesh. *Ecology and Society* 22(3):5.

Klammler, K., P. S. C. Rao, and K. Hatfield. 2017. Modeling dynamic resilience in coupled technological-social systems subjected to stochastic disturbance regimes. *Env. Sys. & Decision*.

Klinkhamer, C., E. Krueger, X. Zhan, F. Blumensaat, S. Ukkusuri, and P. S. C. Rao. 2017 Topological Analyses of Urban Transport and Drainage Networks: A US case study of Geospatial Co-location and Heterogeneity. *Scientific Reports* (in review)

Krueger, E., Klinkhamer, C., Ulrich, C., Zhan, X., Rao, P.S.C., 2017. Generic patterns in the evolution of urban water networks: Evidence from a large Asian city. *Physical Review E*, **95**(3).

Linkov, I., T. Bridges, F. Creutzig, J. Deker, C. Fox-Lent, W. Kroger, et al., 2014. Changing the Resilience Paradigm. *Nature Climate Change*, 4:407-409.

National Research Council. 2015. Developing a Framework for Measuring Community Resilience: Summary of a Workshop. National Academy Press, Washington, DC.

Park, J., T. P. Seager, P. S. C. Rao, M. Convertino, and I. Linkov. 2013. Integrating Risk and Resilience Approaches to Catastrophe Management in Engineering Systems. *Risk Analysis, Vol. 33, No. 3.*

Rockefeller Foundation, 2017. Cities are Taking Action: How 100 Resilient Cities are Building Urban Resilience. Rockefeller Foundation, NY.

Yang, S., K. Paik, G. McGrath, C. Urich, E. Krueger, P. Kumar, and P. S. C. Rao. 2017. Functional topology of evolving urban drainage networks. *Water Resources Research*. (in press).

Zischg, J., C. Klinkhamer; X. Zhan; E. Krueger; S. Ukkusuri; P. S. C. Rao; W. Rauch; and R. Sitzenfrei. 2017. Evolution of Complex Network Topologies in Urban Water Infrastructure, *ASCE World Environmental and Water Resources Congress*.

World Environmental and Water Resources Congress 2017

Evolution of Complex Network Topologies in Urban Water Infrastructure

J. Zischg[1]; C. Klinkhamer[2]; X. Zhan[3]; E. Krueger[4]; S. Ukkusuri[5]; P. S. C. Rao[6]; W. Rauch[7]; and R. Sitzenfrei[8]

[1]Unit of Environmental Engineering, Institute for Infrastructure, Univ. of Innsbruck, Technikerstrasse 13, 6020 Innsbruck, Austria. E-mail: jonatan.zischg@uibk.ac.at
[2]Lyles School of Civil Engineering, Purdue Univ., 550 Stadium Mall Dr., West Lafayette, IN 47907. E-mail: cklinkha@purdue.edu
[3]Lyles School of Civil Engineering, Purdue Univ., 550 Stadium Mall Dr., West Lafayette, IN 47907. E-mail: zhanxianyuan@purdue.edu
[4]Lyles School of Civil Engineering, Purdue Univ., United States & Helmholtz Center for Environmental Research – UFZ, Leipzig, Germany. E-mail: elisabethkrueger@purdue.edu
[5]Lyles School of Civil Engineering, Purdue Univ., 550 Stadium Mall Dr., West Lafayette, IN 47907. E-mail: sukkusur@purdue.edu
[6]Lyles School of Civil Engineering & Agronomy Dept., Purdue Univ., 550 Stadium Mall Dr., West Lafayette, IN 47907. E-mail: sureshrao@purdue.edu
[7]Unit of Environmental Engineering, Institute for Infrastructure, Univ. of Innsbruck, Technikerstrasse 13, 6020 Innsbruck, Austria. E-mail: wolfgang.rauch@uibk.ac.at
[8]Unit of Environmental Engineering, Institute for Infrastructure, Univ. of Innsbruck, Technikerstrasse 13, 6020 Innsbruck, Austria. E-mail: robert.sitzenfrei@uibk.ac.at

Abstract

In this paper, we investigate the historical development of complex network topologies in urban water distribution networks (WDNs) and urban drainage networks (UDNs). The analyses were performed on time-stamped network data of an Alpine case study, which represent the evolution of the town and its infrastructure over the past 106 years. We use the dual representation of the network, where pipes are considered as nodes and intersections as edges, respectively. The functional topologies of the networks are analyzed based on the dual graph, providing insights beyond a conventional graph (primal mapping) analysis. We observe that the WDNs and UDNs show scale-free network characteristics and evolve with consistent patterns over time. However, structural differences between both network types are found in the node degree distributions and the characteristic path lengths, resulting from different functionalities of the systems. Finally, we show the remapping of the dual network characteristics to the spatial map and discuss possibilities for further applications.

Keywords: Complex network analysis, HICN approach, Historical evolution, Network design, Urban drainage, Water distribution.

INTRODUCTION

The field of complex network analysis originated in statistical physics at the end of the 20th century, and is now widespread among numerous disciplines including natural, technical and social sciences. In engineering, the focus of network analysis has shifted away from the traditional perspective of investigating individual components to the exploration of topological properties of the networks, taking a holistic view of the entire system (Blanchard & Volchenkov 2008). Many complex systems can be described in form of a network, with recent increases in computing power making it feasible to investigate the topologies of entire networks consisting of high-resolution data (Strogatz 2001). Examples of these types of investigations range from molecular interaction networks (e.g. protein interactions of cells) and social networks (e.g. communication between humans) to global transportation systems and individual human mobility (Assenov *et al.* 2007; Gonzalez *et al.* 2008; Uhlmann *et al.* 2012). Despite the various types and representations of these networks, important commonalities exist. Most complex networks are neither regular graphs (e.g., perfect grids), nor are they purely hierarchical systems (e.g., trees), but a hybrid of these structures. The analysis of complex networks gives insight to structural morphologies, similarities, recurring patterns and scaling laws (Barabási & Albert 1999). The applications are multifaceted: Identification of central nodes; prediction of future developments and network growth (e.g., information spreading); identification of vulnerabilities to enhance security (Zweig & Zimmermann 2008), and improvement of the network resilience (Sterbenz *et al.* 2013).

Complex network analyses of critical infrastructures, such as water distribution networks (WDNs) and urban drainage networks (UDNs), provide valuable insights beyond the traditional engineering approaches to design and operate systems in a more reliable way, and to help build-up structural resiliency (Yazdani *et al.* 2011). In the past, most structural features in complex networks were investigated based on a conventional graph representation (so-called "primal space"), where pipes or conduits are the edges and their intersections the vertices of a mathematical graph. Conversely, different approaches, based for example on common attribute classification (i.e., road name or pipe size) or intersection continuity (i.e. maximum angle of deflection), consider the network structure in its "dual space", i.e. functional components (e.g. pipes with same diameter) which belong together, represent the vertices and their intersection the edges of the graph (Masucci *et al.* 2014). Further explanations are given in the subsequent section. Unlike the conventional primal representation, dual mapping approaches may also consider the continuity of links (pipes or conduits) over a variety of edges and hierarchy (e.g., pipe diameter; maximum designed flow) for further graph analysis.

Previous studies using the dual mapping approach were mainly performed on street networks (Porta *et al.* 2006; Hu *et al.* 2009; Masucci *et al.* 2014), but an extension to each network type is possible. Krueger et al. (2017, in review) applied the HICN principle for the first time to the water distribution and sewer networks in a large Asian city with 4 million people. The authors found that both network types quickly evolve to become scale-free in space. Klinkhamer et al. (2016, in review) examined the co-location of existing road and drainage networks in a large Midwestern U.S. city, and homoscedasticity of subnets across the city, but did not examine temporal evolution of these networks. Additional studies for comparison and for generalization, considering also the evolution of water infrastructure networks of different cities are needed.

In this paper, we show the results of the dual mapping for a unique dataset of 11 time-stamped water distribution and urban drainage network states of the small Alpine case study of Innsbruck (Austria), as the town and its infrastructure have evolved during the last 106 years and

the population tripled from about 40K to about 130K. We observe that the water distribution and urban drainage networks show scale-free network characteristics under the dual representation, and evolve with consistent patterns over time. With the presented methodology patterns (e.g. vertex connectivity) and trends for the future network development and engineering design are obtained. Furthermore, the reflected structural features, such as the characteristic path length or the backbone of the networks, can be uncovered and remapped to the spatial map, which builds the basis for analyzing disturbances and structural resilience.

METHODS

In this chapter a dual mapping approach, Hierarchical Intersection Continuity Negotiation (HICN), and the investigated topological metrics are presented. A short description of the case study is also given.

HICN Principle of Dual Mapping. The HICN approach emphasizes the functional topology of the network by aggregating components (e.g., pipes, conduits, streets) with identical attributes (e.g., pipe diameter, street name), while also maintaining a certain level of straightness (e.g., street sections) (Masucci *et al.* 2014). After reducing the network complexity with this "generalization model," the aggregated edges are converted into vertices and the intersections are converted into edges. The resulting graph is the so-called "dual" (mapped) representation of the "primal" graph (see Figure 1). In addition to the edge attributes, the angular threshold Θ_{max} is a second criterion used for the generalization model. It defines the maximum exterior convex angle of connected edges being merged (Porta *et al.* 2006).

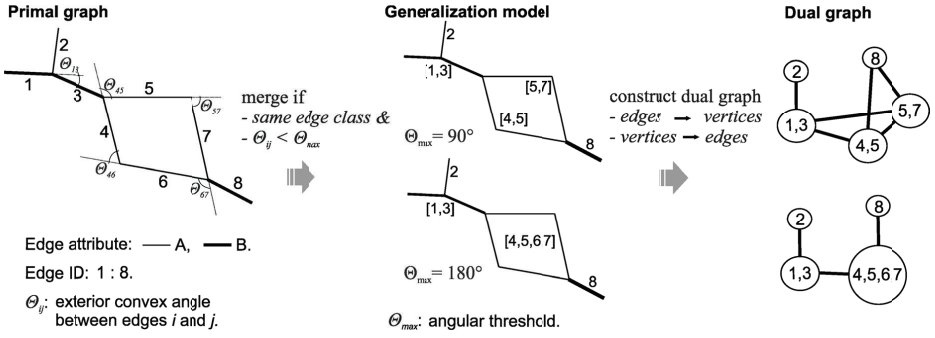

Figure 1: HICN method to construct the dual graph from the primal map. Resulting dual graphs are dependent on the generalization model, here shown with two different angular thresholds Θ_{max}.

The HICN allows for reducing the network complexity of the primal map and considers the hierarchy of network elements (pipes) (e.g., different level of detail of the pipe segments). Identical cohorts of pipes are considered as a single component, the dual node. Take for example the same pipe segment (identical diameter) mapped with differing criteria: On the one hand, it is described with 2 vertices (start vertex + end vertex) and, on the other hand, is described with 6 vertices (start vertex + end vertex + 4 intermediate vertices). The resulting graph characteristics

are significantly different (e.g. mean degree of 1 and 1.67), which shows the important effect of network simplification before the complex network analysis. However, the dual-mapped network still preserves the connectivity information of the original network. With this methodology, the underlying hierarchy of the network can be uncovered.

Connectivity. A significant property of complex networks is the node degree k and its distribution $p(k)$. The degree of a single node i in an undirected network describes the number links intersecting with it. It can be calculated through the network's adjacency matrix A, where the degree of node i is defined by the sum of the i-th row of A. For example, the node degree in social networks represents the number of contacts. The node degree distribution describes the fraction of all nodes with the same degree in the network. While randomly created networks in most cases reveal a symmetrical distribution around the average degree (e.g., Poisson or normal distribution), many natural and engineered networks show scale-free characteristics, following a power-law distribution (see Figure 2). The mean node-degree is defined as $\langle k \rangle = \frac{2e}{n}$, where e is the total number of edges and n is the total number of vertices. In the limits, a mean degree of 2 indicates a tree-like network structure, grid patterns or cyclic structures have mean degrees around 4 (Barthélemy 2011).

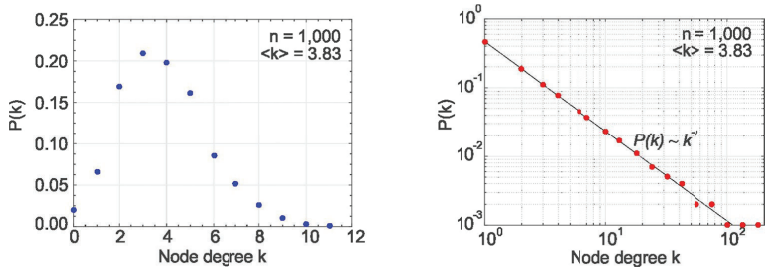

Figure 2: Example of node degree distributions for a randomly connected network (left) and a scale-free network (right). Both hypothetical networks have identical average degrees <k> and number of nodes.

Characteristic path length. Along with the node degree distribution, the characteristic path length <l> (or average path length) is one of the most important and robust measures of network topology. It quantifies the level of integration/segregation throughout the network. In water infrastructure and power grid networks energy losses are dependent on the characteristic path length. It is calculated by the average shortest path distance between all couples of nodes as follows:

$$\langle l \rangle = \frac{1}{n \times (n-1)} \times \sum_{i \neq j} d(v_i, v_j),$$

where n is the number of vertices and $d(v_i, v_j)$ denotes the shortest path between vertex v_i and v_j (Assenov et al. 2007). The probability density function of the path length $p(l)$ can, for example, be considered for the approximation of the travel-time distribution with a nearly consistent distribution of flow velocities.

Case study. For using the HICN dual mapping methodology to explore water network characteristics we utilize available, high-resolution network data for the Alpine city of Innsbruck (Austria). The temporal evolution of the water infrastructure networks is defined through time-stamped system states at 10-year intervals, starting with the year 1910. The city has grown from approximately 40,000 inhabitants in 1910 to 130,894 in 2016. The historical data set describes the expansion of the networks, and includes pipe rehabilitation of the water distribution and urban drainage systems. The detailed description of the network reconstruction for this case study can be found in Sitzenfrei et al. (2015). Figure 3 illustrates the time-stamped networks at four stages in the primal representation. Greater thickness and a darker color of the edges indicate larger pipe diameters.

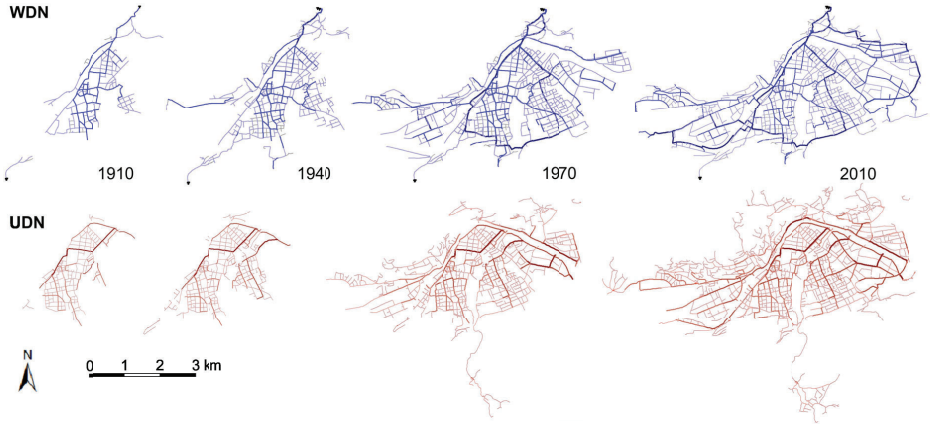

Figure 3: Time-stamped evolution of WDN and UDN of Innsbruck (Austria).

RESULTS

In this section the results of the historical evolution of the WDN and UDN are presented, followed by a sensitivity analysis of the HICN dual mapping. Finally, two examples of remapping the dual network characteristics to the primal network are shown.

Dual mapping. Figure 4 illustrates the application of the HICN dual mapping (Masucci *et al.* 2014) to the historical water infrastructure networks of Innsbruck for the first (year 1910) and last state (year 2010). The dual graphs show the node degree (darker and larger nodes represent central network "hubs" with high node degree). For the application of the HICN method an angular threshold Θ_{max} of 180 degrees is used; i.e., we ignore the curvature of pipe segments. We further discuss the application of the threshold value in the section Sensitivity HICN.

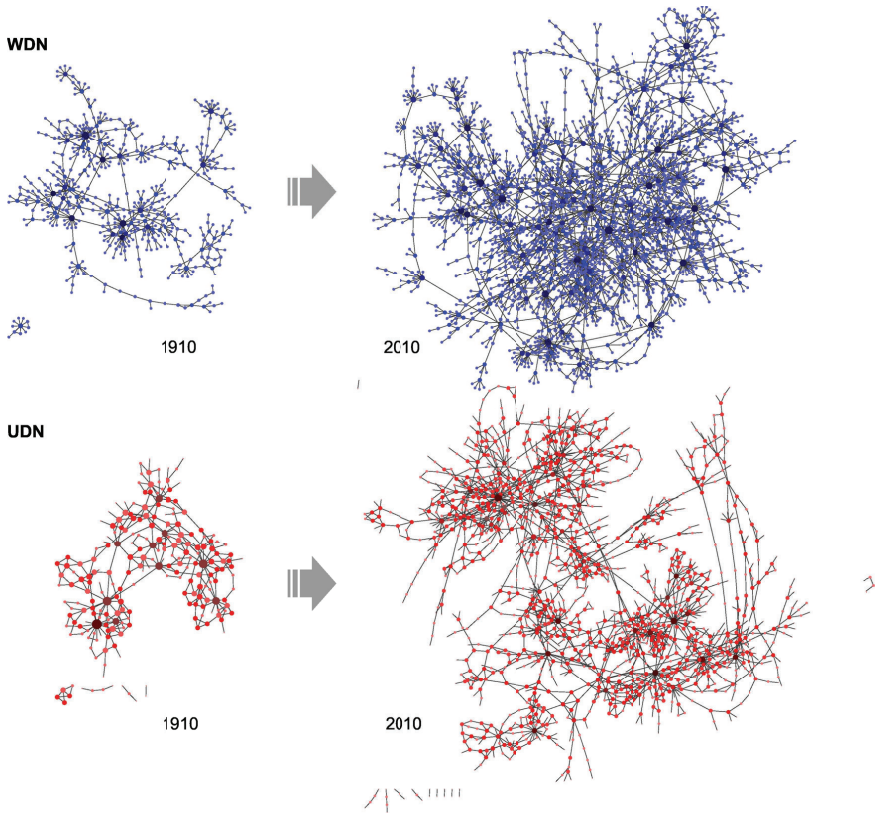

Figure 4: Examples of dual mapped WDNs (top) and UDNs (bottom).

Dual network characteristics. Resulting nodal degree distributions, *p(k)*, for WDNs and UDNs in the dual space are presented in Figure 5, plotted for both network types on log-log axes for the 11 time-stamped states. We observe emergence of a consistent pattern, namely, a truncated power law distribution $p(k) \sim k^{-\gamma}$, $k > k_{min}$, with k_{min} equal to 1 and 2 for WDN and UDN, respectively. For the UDNs larger slopes (mean: 2.7±0.11) and a stronger decrease of the number of leaf nodes (k = 1) are found compared with the WDNs (mean: 2.31±0.12). A possible explanation of the truncation could be the missing house (low-degree) connections for both network types. The exponent γ values fall in the range between 2.08 and 2.49 for WDN and 2.49 and 2.92 for UDN (see Table 1). The goodness of fit is described with the coefficient of determination R^2 and is based on log-log linear regression values (see Table 1).

The truncated power law [Pareto] distribution also indicates that the probability of finding nodes with many connecting links ("hubs") is much lower than nodes with few connections (terminal dual nodes). According to the literature this behavior is typical for scale-free networks, which are dominant in most natural networks. The "scale-free" characteristics, within the

observed range [$k_{min} \leqslant k \leqslant k_{max}$], are also indicated with the significant higher maximum degrees k_{max} (representing a "network hub") compared to the mean degree <k> (Table 1).

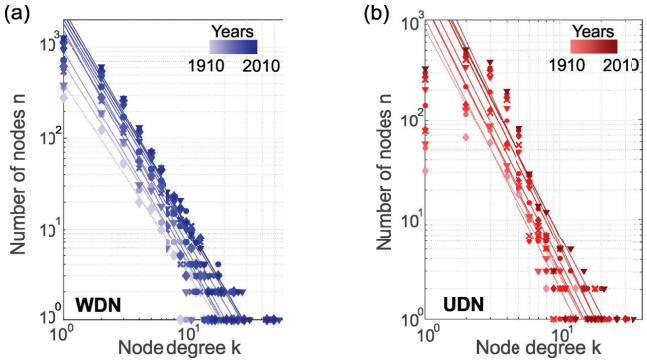

Figure 5: Dual node degree distribution over time of (a) WDN and (b) UDN.

Although for the UDN the maximum degree k_{max} is smaller as for the WDN, the contrary is observed for the mean degree <k>. Reason for that are fewer changes in the conduit diameters, resulting in the aggregation of more conduits and thus having higher connectivity.

Table 1: Topological dual mapped properties over time for the WDN and UDN.

Year	n (dual)		k_{max}		<k>		γ		R^2	
	WDN	UD	WDN	UD	WDN	UD	WDN	UD	WDN	UD
1910	533	223	25	16	2.27	3.19	2.08	2.49	0.994	0.994
1920	741	321	24	19	2.32	2.91	2.18	2.71	0.990	0.991
1930	789	354	24	19	2.33	2.88	2.33	2.60	0.990	0.992
1940	1,081	436	24	19	2.30	2.93	2.49	2.70	0.992	0.999
1950	1,222	462	24	19	2.31	2.93	2.48	2.68	0.990	0.988
1960	1,493	715	47	23	2.34	2.82	2.28	2.72	0.995	0.982
1970	1,921	1,042	55	22	2.34	2.77	2.29	2.77	0.992	0.987
1980	2,150	1,236	50	22	2.35	2.75	2.30	2.92	0.996	0.983
1990	2,294	1,318	50	30	2.36	2.76	2.31	2.76	0.994	0.985
2000	2,439	1,431	50	31	2.36	2.77	2.31	2.66	0.994	0.983
2010	2,550	1,585	50	35	2.36	2.81	2.35	2.71	0.996	0.989
						Mean:	2.31	2.70		
						Coefficient of variation:	0.052	0.041		

Furthermore, change in slopes (γ) reveals that secondary pipes connect more likely to "well-connected" main pipes. The growth of the networks in terms of total number of dual nodes n over time is illustrated in Figure 6 (a). Highest growth rates of the networks are seen in the 1960's and 1970's, which can be partly related to the economy boom and the implementation of the waste water treatment plant (Sitzenfrei *et al.* 2015).

The characteristic path length <l> of the system states is shown in Figure 6 (b). In the dual representation, the path length defines the number of changing pipe attributes (diameter changes) between two dual vertices. We observe that the <l> value is much smaller than the number of vertices, which is an indicator for a "small world" property of the graph, meaning that every

vertex is connected to every other through a very short path. In general, the characteristic path length increases with geographical boundaries. This can be seen in Figure 6 (b): during the 1980's there is a significant increase of the characteristic path length for the UDN. Possible reasons for that are the (tree-like) connections of peripheral zones and neighboring villages to the central wastewater treatment plant. On the other hand, for the WDNs a decrease of <*l*> during the past few years is observed, as a result of the WDN densification and the construction of alternative flow paths (loops) for redundancy purposes. Furthermore, it is remarkable that the characteristic path length of the UDNs at the early stages of the 20th century is lower compared to the WDNs. One reason for that is that the UDN at the historical center of Innsbruck had fewer alterations of conduit diameters (see Figure 3, bottom left), resulting from the coarse design concepts and material limitations at that time. To compare the results with the physical shortest path length (e.g., in km) in the original geographical embedding, the same analysis should be repeated in the primal representation of the network.

Figure 6 (c) presents the slopes γ of the node-degree distributions [*p(k)*] over time. When comparing γ with previous studies in the literature, similar ranges between 2 and 3 are reported (Porta *et al.* 2006). In this study, larger exponents for the UDN compared to those for the WDN are observed for all investigations. Peaks of γ are found during the 1940's and 1950's for the WDN and around 1980 for the UDN. This can be explained with the tree-like expansion of the network to new parts of the city (also indicated with larger characteristic path lengths) and without a strong network densification at those times. During the last part of the 20th century the WDN evolved with a homogeneous pattern, namely a network growth with a slight increase of the power law exponent γ. This could indicate that the WDN is now topologically "mature", i.e., a similar behavior is expected when the network grows further.

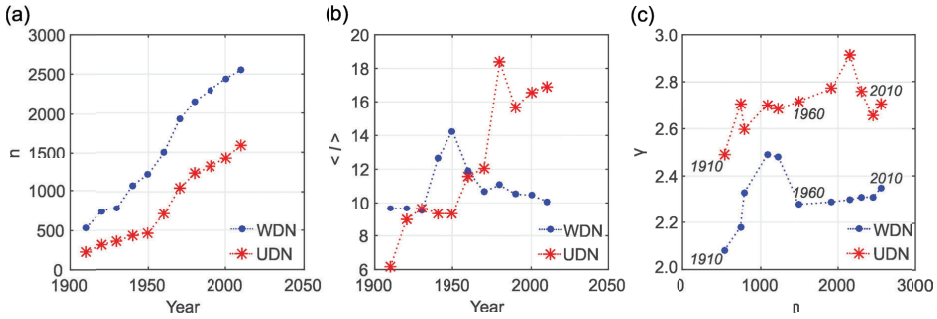

Figure 6: Topological properties of evolving WDN and UDN: (a) Number of vertices *n* over time; (b) characteristic path length *l* over time and (c) power law exponent γ depending on the number of vertices *n*.

Dual Mapping Sensitivity. Here we perform a sensitivity analysis of the angular threshold Θ_{max} used for the HICN approach. For reference the WDN 2010 of Innsbruck is used. We observe that with increasing angular threshold Θ_{max}, more pipes (of the same class) are merged together and therefore the size of the dual graph is reduced. For example, the reference network has 7,604 edges in the primal space, which are generalized to 3,426 and 2,550 dual nodes for angular thresholds of 15 and 180 degrees, respectively. Figure 7 shows the outcome of the sensitivity analysis, where 7 different angular thresholds Θ_{max} from 15 to 180 degrees are investigated. All

resulting node-degree distributions follow truncated power-law distributions, with increasing slope and stronger truncation for lower threshold angles. The results using angular thresholds of 90 and 180 degrees are identical, meaning that no sharp inner angles between connected pipes of the same class are found in the graph. We conclude that for investigating the node degree distribution of the historical networks, the angular threshold Θ_{max} is of minor significance, but must be consistently applied between the types and the states of the networks.

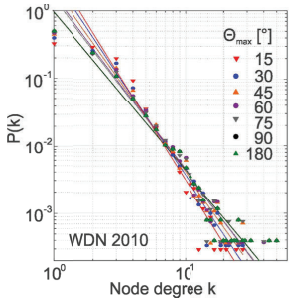

Θ_{max} [°]	n (dual)	Slope γ	R^2
15	3,426	3.13	0.868
30	3,007	2.93	0.907
45	2,803	2.74	0.941
60	2,705	2.57	0.958
75	2,641	2.54	0.973
90	2,550	2.35	0.996
180	2,550	2.35	0.996

Figure 7: Sensitivity of the HICN approach on the node degree distribution of the WDN 2010

Remapping network characteristics from dual to primal space. The results obtained from the dual network analysis can be remapped to the primal map representation. Figure 8 (a) exemplifies the dual degree distribution of the WDN 2010. Dual nodes with high degrees are illustrated with dark blue lines and represent the "backbone" of the network with high connectivity, whereas bright colored lines represent low connection pipes; note that the high-degree nodes do not strongly correlate with larger pipe diameters.

In addition, the average shortest path distance of each dual node to every other node is presented in Figure 8 (b). While in the primal map representation the path length expresses the closeness as a centrality measure of the vertex, in the dual representation the path length defines the number of changing pipe attributes (diameter changes) between two dual vertices. Darker lines indicate longer average shortest paths. As already described, the historical center (definition in Figure 3, top left) has the highest connectivity of the entire system, due to more consistent pipe diameters.

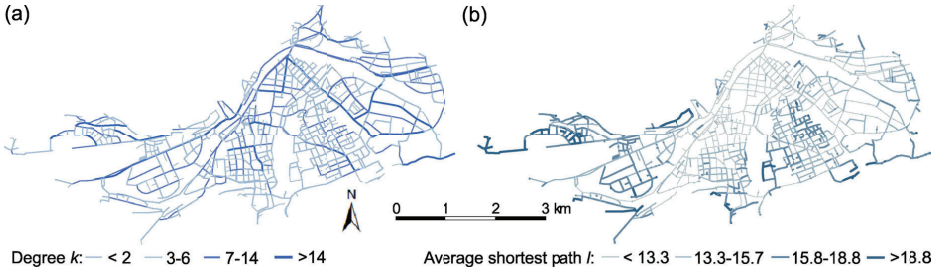

Figure 8: Remapping of dual characteristics to the primal network WDN 2010: (a) dual node degree and (b) dual average shortest path length.

45. Aligning Different Schools of Thought on Resilience of Complex Systems and Networks[i]

David J. Yu[1,*], P. Suresh C. Rao[1,*], Christopher J. Klinkhamer[1], Elisabeth H. Krueger[1,2], Nikhil Sangwan[1], Kyungmin Sung[1]

[1]Purdue University, [2]Helmholtz Centre for Environmental Research - UFZ Germany

Contact: davidyu@purdue.edu, SureshRao@purdue.edu

Keywords: Resilience, Robustness, Adaptability, Transformability, General resilience

Resilience Thinking, Robust Control, Resilience Engineering, and Spatial Resilience

Multiple schools of thought have emerged on how complex systems persist or reorganize in response to change. A first step towards resilience management should be clarifying how these different schools of thought fit together. With this aim, we synthesize the following four concepts: resilience thinking as developed in the fields of ecology and social-ecological systems (SESs) research, resilience engineering as developed in the safety management research of engineered systems, robust control as developed in control theory of feedback systems, and spatial resilience as developed in the fields of geomorphology, landscape ecology, or complex network studies.

Resilience thinking is a cluster of concepts that has been expanded to represent how complex self-organized systems persist or reorganize among multiple regimes of reinforcing processes (or multiple stable attractors or basins of attraction). It focuses on three emergent system-level features: resilience as persistence, adaptability, and transformability (Walker et al., 2004; Folke et al., 2010).

- Resilience is the ability to respond to external (or internal) disturbances while undergoing change so as to still preserve essentially the same functions of the current regime. Resilience can be further classified into specified and general resilience. Specified resilience is specific about "resilience of what to what" (Carpenter et al., 2001). It refers to the capacity of a system to maintain a specific set of functions in relation to a well-defined set of disturbances. General resilience, in contrast, relates to the capacity of a system to deal with all kinds of disturbances, both expected and unexpected ones (Folke et al., 2010). Many resilience studies focus on the aspects of self-organization that generate multiple regimes, thresholds that form the boundaries of these regimes, and how a system may suddenly flip between such regimes from a seemingly small change in a condition (regime shift). Finally, resilience by itself does not address normative considerations; a resilient regime can be either good or bad to human welfare.
- Adaptability is the ability of a system to learn and adjust its responses to changing conditions and continue operating within the current regime. Hence, adaptability

[i] This paper is part of the IRGC Resource Guide on Resilience, available at: https://www.irgc.org/risk-governance/resilience/. Please cite like a book chapter including the following information: IRGC (2016). Resource Guide on Resilience. Lausanne: EPFL International Risk Governance Center. *v29-07-2016*

enhances resilience. Adaptability is aided by structural and functional diversity and redundancy of components, connections, and processes. Loss of such features, either through natural or anthropogenic changes, contributes to decreased adaptability and thus resilience loss.

- Transformability is the ability to create a fundamentally new system when the existing system becomes untenable because of great change. In a complex system with nested or multi-level hierarchy (e.g., households make up neighbourhoods, neighbourhoods comprise districts, districts make up a city, etc.), transformability at a lower level can help the resilience at a higher level. For example, periodic district-level water supply failures and the resulting rehabilitation of pipes in these districts can make the whole city resilient to a major water supply failure. Therefore, it is crucial to understand that multi-level interactions drive the interplay among resilience, adaptability, and transformability. Adaptive cycle and panarchy of nested adaptive cycles are useful heuristics about how such interplays unfold across multiple levels (Allen et al., 2014).

In the field of robust control, robustness relates to the sensitivity of a designed system's performance to a well-defined set of disturbances (Csete & Doyle, 2002). Unlike resilience, aspects of multiple regimes are not explicitly covered by robustness. Robustness represents a degree of resistance relative to a particular set of disturbances with known and anticipated (with some probability) frequency and intensity that are identified through risk analysis. Hence, robustness and specified resilience are analogous when the focus of analysis is on system dynamics in the vicinity of a regime's steady-state. When the focus of analysis is expanded to cover potential regime shifts, robustness and specified resilience mean different things. Further, a fundamental property of all feedback systems is that designed features that confer robustness to certain kinds of disturbances necessarily lead to hidden fragilities to some other set of disturbances (Carlson & Doyle, 2002). This so-called robustness-fragility trade-off has been observed in SESs (Janssen & Anderies, 2007). In coupled engineered-social systems, this debate is focused on balancing fail-safe designs (robustness-based) with safe-fail (resilience-based) design paradigms; that is, there is a need for an integration of both risk and resilience approaches for design and operations of coupled systems (Park et al., 2013).

Safety management engineers have traditionally focused on robustness through risk analysis. They have begun to embrace resilience ideas (Fiksel, 2003), and termed their approach as "resilience engineering." They define resilience as "the intrinsic ability of a system to adjust its functioning prior to, during, or following changes and disturbances, so that it can sustain required operations under both expected and unexpected conditions" (Hollnagel, 2014). This definition is essentially the same as that of general resilience. Hollnagel (2014) outlines four main traits of resilience engineering: the ability to respond to various kinds of disturbances (both familiar and unfamiliar ones), the ability to monitor system states, the ability to learn from the consequences of past decision-making, and the ability to anticipate and proactively adapt to changing conditions. Engineered complex systems, such as urban infrastructure networks, indeed are designed to monitor system state and performance, and re-rout flows of traffic or water, etc. when necessary. Yet, these systems are not inherently resilient, because they do not have the ability to adapt or transform structure and functions through self-organization, as do ecological and social systems/networks. Further, when engineered systems fail, either through long-term erosion of physical structures or suddenly from major shocks, they do not re-emerge or re-organize by themselves; rather, it is the urban communities that use and depend on them that actively invest to repair and rehabilitate the failed infrastructure.

Resilience characterization of a complex system needs to incorporate processes and feedbacks, not only over different time scales but also across the spatial domains of the system. It is important to observe and model changes in spatial heterogeneity (statistical spatial moments), spatial structure and patterns (geo-statistical analyses), flows (of matter, energy, etc.) across gradients and interfaces, connectivity (network topological metrics) among spatial elements, and dispersal (diffusion of matter, information, organisms, etc.). Such spatiotemporal attributes respond dynamically to both internal and external forcing, whether deterministic or stochastic, to maintain local (specific) or overall (general) resilience. Just as cumulative adverse impacts of sequences of internal and external disturbances can lead to either gradual erosion of system functions (performance) over time or experience a sudden collapse, so too do spatial cascades of losses of diversity, patterns, connectivity, and flows lead to propagation of regime shifts across space. Thus, spatial resilience can be understood as the ability to maintain the appropriate combination of spatial attributes required to enable emergence of asymmetries, heterogeneity, patterns, connectivity, flows, and feedbacks (Allen et al., 2016). Spatial resilience is linked to the "preservation of a system's structure", which does not necessarily refer to the spatial layout of a system, but rather the "functional map" and topology of the system. Such functional mapping of urban infrastructure networks has been suggested by several authors (Porta et al., 2006; Masucci et al., 2014).

Strategies for Resilience Improvement

How do these schools of thought fit together? How can we use them in concert as instruments for resilience management of coupled complex systems? It is important to realize that resilience and robustness are not conflicting concepts as shown in Figure 1. When the time scale of analysis is in the units of decades or longer, resilience may be more fitting because it incorporates aspects such as adaptability and transformability that begin to matter in such longer time scales (Anderies et al., 2013). When the time scale is shorter (i.e., in the units of few hours or days) and system boundaries are more narrowly defined, robustness (resistance) may be more fitting because it explicitly deals with the sensitivity of a system output to a well-defined set of disturbances. In a similar manner, when specificity or predictability of key outputs and system dynamics is high, risk analysis can still be useful and planned adaptation or deliberate transformation can be possible. When the opposite is true, learning-by-doing may be necessary and unplanned adaptation or forced transformation is more likely. Hence, resilience and robustness are complementary concepts—the choice between the two concepts ultimately depends on the nature of the spatial boundary, time-scale, and specificity or predictability of key variables that one is considering. However, continuously applying robustness as the sole basis for ensuring persistent performance is dangerous: It can lead to catastrophic failures when another type of hazard co-occurs, as illustrated by the examples of Park et al. (2013) and the notion of robustness-fragility trade-offs.

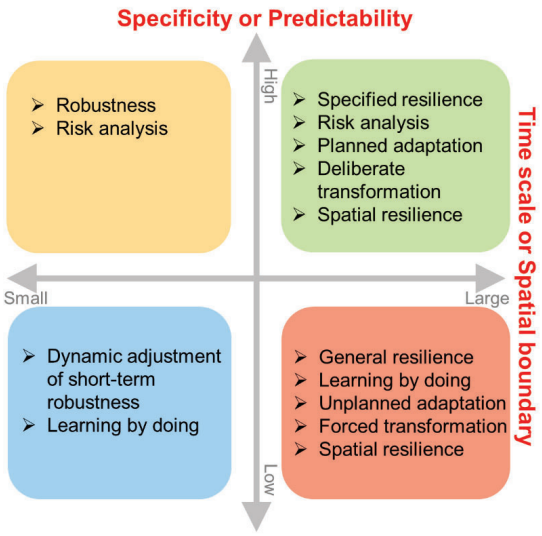

Figure 1: Relevance of the resilience-related concepts discussed along four analytical dimensions (time scale, spatial boundary, specificity of key variables, and predictability).

In the short term, robustness can be achieved by deciding which disturbances will be controlled and which ones will be tolerated at a particular point in time. Robustness ideas facilitate this process by forcing analysts to consider a precise system boundary and output measure and potential robustness-fragility trade-offs associated with design choices. When predictability is low and the time scale is longer, general resilience can be achieved by taking short-term and local robustness to the global scale with dynamically changing conditions and disturbances. This requires moving from the idea of protecting the system from failure ("fail-safe"), which is achievable only to expected risks, to embracing the potential of failure and creating a "safe-fail" environment in the event of unknown or unexpected shocks (Park et al., 2013). Implementation of this dynamic adjustment requires learning-by-doing, i.e., an iterative cycle of experimentation, monitoring, learning, and adaptation (Hollnagel, 2014; Yu et al., 2016). Similarly, resilience engineering scholars suggest that resilience ideas do not replace the conventional risk-based engineering approach. The basic idea is that risk analysis alone is insufficient for dealing with irreducible uncertainties associated with complex systems and thus should be accompanied by improved adaptability. Hence, practitioners should use robustness (through risk analysis) and general resilience (through learning-by-doing and dynamic adaptation) in concert to operationalize resilience management.

Quantifying Resilience

Quantifying resilience has received increasing attention in recent years, both from systems and networks modeling and composite indicators construction perspectives (Angeler & Allen, 2016), and is moving beyond earlier work defining terminology, concepts, and conceptual frameworks (Park et al., 2013; Ayyub, 2014). More recent attempts at quantifying resilience of technological systems were

based on performance recovery from a single shock, or used an aggregate measure (average level of service provision) computed from system responses to multiple events over multiple years (Ganin et al., 2016).

New modeling approaches are based on either systems analyses perspectives or complex network analyses based on graph theory and acknowledge increasing vulnerability to unexpected shocks, or combinations of series of chronic, low-intensity and infrequent acute shocks (Moore et al., 2015; Klammler et al., 2016). Two key state variables of interest, aggregated at the system or network level, are: (1) the "system performance" ("functions", e.g., ecological or infrastructure or social services) and (2) "adaptive capacity", which defines the ability of the system to cope with disturbances, recover from losses, learn from, and improve the process. While it is easy to monitor system performance, it has been much more challenging to quantify and monitor "adaptive capacity"; this gap remains the focus of current and future research efforts.

Klammler et al. (2016) developed a model to quantify resilience using multiple metrics of coupled systems performance under a stochastic disturbance regime. Here, resilience is modeled as a dynamic and emergent property of the coupled system with respect to regime shifts between a desirable regime (full service) and limited service conditions or complete system collapse. They also showed that resilience is a non-stationary (i.e., memory- or path-dependent) and emergent phenomenon under stresses, contingent on initial conditions, and the nature of the stochastic disturbance regime. However, lack of required long-term data for engineering system (infrastructure) performance under a series of stochastic shock (i.e., disturbances of varying frequency and intensity), and how to measure and monitor the dynamics of social system's "adaptive capacity" remains a major obstacle to model testing and applications

Representation of the systems of interest as interdependent networks has also been examined. Examples include engineered and natural networks (e.g., river) and engineered networks (e.g., roads, pipes, power) and social networks (e.g., communities) in urban settings. Recent work (Newman, 2006; Barzel & Barabasi, 2013) has shown that many engineered and natural networks have topological similarities in that they all exhibit distinct features of functional self-similarity and scale-independence. Such networks have few well-connected critical nodes (hubs) and a large number poorly connected (terminal) nodes. Such networks are known to be vulnerable to structural fragmentation, and functional disruptions with the loss of only a few hubs, but robust to the loss of other less-connected nodes (Barabasi, 2016). Interdependent networks generally tend to be less robust, and more likely to be vulnerable to cascading failures initiated in other networks. Several quantitative measures of network topology, interconnectedness, and resilience have been recently proposed (Gao et al., 2016).

Closure

Despite continued advances in understanding and quantifying resilience, accurately measuring resilience remains an ongoing challenge, often only possible after system failure has already occurred and the recovery is underway. As a result, the design and management of engineered systems follow fail-safe strategies rooted in robustness and risk analysis. These strategies, however, often fail to recognize the importance of people, i.e., social capacity in imbuing resilience within an engineering system that is otherwise designed, built and operated on robustness, resistance, and redundancy,

but does not inherently has resilience (as in adaptation and transformation) (Klammler et al., 2016). Recognizing the community's contributions to adaptive capacity should be a principal component of any future quantitative measure of coupled systems resilience.

Annotated Bibliography

Allen, C. R., Angeler, D. G., Garmestani, A. S., Gunderson, L. H., & Holling, C. S. (2014). Panarchy: Theory and Application. Ecosystems 17(4):578–589.
The article reviews the panarchy theory which has been used in various field, especially in complex systems. Also, it emphasizes the needs for testing hypothesis, regarding quantifying and measuring panarchy, to support the theory.

Angeler, D. G, & Allen, C. R, (2016). Quantifying Resilience (Editorial). Journal of Applied Ecology, 53: 617-624.
The article provides an overview of current work on resilience, its quantification, and knowledge gaps in the field.

Anderies, J. M., Ostrom, E., Folke, C., & Walker, B. (2013). Aligning Key Concepts for Global Change Policy: Robustness, Resilience, and Sustainability. Ecology and Society 18(2):8.
Authors look closely at three similar and hence often confounding concepts of global change policy: robustness, resilience and sustainability. This paper provides explicit definitions of these concepts and highlights the similarities, distinctions and linkages between them. It points out their relevance at different time-scales and how they complement each other in different contexts.

Ayyub, B. M. (2013). Systems resilience for multi-hazard environments: definition, metrics, and valuation for decision-making. Risk Analysis, 34(2):340-355.
In this article, a resilience definition is provided that meets a set of requirements with clear relationships to the metrics of the relevant abstract notions of reliability and risk.

Barabasi, A. (2016). Network Science. Cambridge University Press.
This book provides a comprehensive overview of the present state of network science. Modular in design, the book includes sections on network evolution, robustness, and spreading phenomena, among other topics integral to network science and graph theory.

Barzel, B., & Barabasi, A. (2013). Universality in Network Dynamics. Nature Physics 9:673-681.
The authors develop a theory of the effects of perturbations to the dynamics of complex systems, and predicts several archetypes of universality in complex social and biological systems. Predictions of system response to perturbations are provided and supported by experimental data.

Carlson, J. M., & Doyle, J. (2002). Complexity and robustness. Proceedings of the National Academy of Sciences of the United States of America 99 Suppl 1:2538–45.
This paper contrasts two different perspectives on complexity: Highly Optimized Tolerance (HOT) and Self-Organized Criticality (SOC). HOT framework considers the complex systems to

have highly structured, self-dissimilar internal configurations and robust-yet-fragile external behaviour.

Carpenter, S., Walker, B., Anderies, J. M., & Abel, N. (2001). From Metaphor to Measurement: Resilience of What to What? Ecosystems 4(8):765–781.
The article actually measures "which variable is resilient to which disturbance" in two different social-ecological systems. It is found that the adaptive capacity is evolved by novelty or learning.

Csete, M. E., & Doyle, J. C. (2002). Reverse engineering of biological complexity. Science (New York, N.Y.) 295(5560):1664–9.
Taking cues from the engineering theory of complexity, authors explore biological complexity and highlight that spiraling complexity, feedback regulation, robustness, fragility and cascading failures are highly intertwined. This work also illustrates how fragility is conserved in complex systems through feedback interconnection resulting in robustness-fragility tradeoffs.

Fiksel, J. (2003). Designing resilient, sustainable systems. Environmental Science & Technology 37:5330–5339.
To develop truly sustainable industrial product and design systems, the author proposes a broader systems thinking with explicit consideration of resilience in the core engineering systems as well as the larger systems in which they are embedded. A design protocol incorporating the related systems and their resilience is also presented in the paper.

Folke, C., Carpenter, S. R., Walker, B., Scheffer, M., & Chapin, T. (2010). Resilience Thinking: Integrating Resilience, Adaptability and Transformability. Ecology And Society 15(4):20.
Folke et al. define and discuss three concepts-resilience, adaptability and transformability-which are central to resilience thinking of SES. Concepts such as adaptability and transformability are needed to enhance the SES resilience and better manage these intertwined systems across multiple scales. Authors also contrast general resilience vs specified resilience, and forced vs deliberate transformations in this work.

Ganin. A.A, Massaro, E., Gutland, A., Steen, N., Keister, J., Kott, A., Mangoubi, R., & Linkov, I. (2016) Operational resilience: concepts, design, and analysis. Scientific Reports, 6, 19540.
The authors propose quantitative measures of engineering resilience using two types of modes: 1) multi-level directed acyclic graphs, and 2) interdependent coupled networks. It evaluates the critical functionality as a source of information on system resilience and robustness over time.

Gao, J., Barzel, B., Barabasi, A. (2016). Universal Resilience Patterns in Complex Networks. Nature 530:307-312.
Authors develop a framework for assessing the resilience of complex systems while separating the roles of dynamics and topology, revealing characteristics that can either enhance or diminish resilience.

Hollnagel, E. (2014). Resilience engineering and the built environment. Building Research & Information 42(2):221–228.
The paper defines the resilience of engineered systems and discusses various strategies for improving the resilience of such systems.

Janssen, M., &Anderies, J. (2007). Robustness trade-offs in social-ecological systems. International Journal of the Commons, 1(1):43–65.
The article explains the concept of robustness in social-ecological systems, and provides a framework for robustness-fragility trade-offs with examples. It argues that absolute robustness doesn't exist: a system can only be robust to specific disturbances.

Klammler, H., Rao, P. S. C. R., & Hatfield, K. (2016). Resilience of Urban Communities: Coupled Dynamics of Infrastructure and Institutions. Submitted.
The article presents a systems model of the interdependence between urban technological systems (infrastructure) and socio-economic systems (institutions). Each system is characterized by a single state variable - service deficit resulting from insufficient infrastructure services to meet customer demands, and adaptive capacity of the institutions to maintain services. Resilience is identified as an emergent property of the system in response to stochastic shocks, and with respect to regime shifts between a desirable regime, limited service conditions or complete system collapse.

Masucci, A.P., Stanilov, K., & Batty, M. (2014). Exploring the evolution of London's street network in the information space : A dual approach. Phys. Rev. E - Stat. Nonlinear, Soft Matter Phys. 012805, 1–7. doi:10.1103/PhysRevE.89.012805
New approach to map urban streets based on hierarchies of streets, which emphasize the functional traits of the network.

Moore, C., Grewar, J., & Cumming, G. S. (2015). Quantifying Network Resilience: comparison before and after a major perturbation shows strengths and limitations of network metrics. Journal of Applied Ecology 53:636-645.
Authors explore the resilience of social-ecological systems using network theory as an analytical tool, with a focus on systems that, although reorganized following perturbation show no obvious resilience features such as learning or adaptation.

Newman, M. E. J. (2006). Networks—An Introduction. Oxford University Press.
A comprehensive review of network science across multiple disciplines touching on the basics of network science and graph theory, as well as detailed explanations for phenomena such as cascading failures based on percolation theory and the dynamics of complex networks.

Park, J., Seager, T., & Rao, P. S. C. (2011). Lessons in risk- versus resilience-based design and management. Integrated Environmental Assessment and Management, 7(3), 396-399.
This study calls for a new resilience-based design and management paradigm that draws upon the ecological analogues of diversity and adaptation in response to low-probability and high-consequence disruptions.

Park, J., Seager, T. P., Rao, P. S. C., & Linkov, I. (2013). Integrating risk and resilience approaches to catastrophe management in engineered systems. Risk Analysis, 33(3), 356-367.
The authors describe resilience analysis as complementary to risk analysis with important implications for the adaptive management of complex, coupled engineering systems. Resilience is defined as an emergent property resulting from a recursive process of sensing, anticipation, learning, and adaptation.

Porta, S., Crucitti, P., Latora, V., (2006). The network analysis of urban streets : A dual approach. Physica A 369, 853–866. doi:10.1016/j.physa.2005.12.063
Authors introduce an information-based for mapping the topologies of urban street networks.

Walker, B., Holling, C. S., Carpenter, S. R., & Kinzig, A. (2004). Resilience, Adaptability and Transformability in Social-ecological Systems. Ecology And Society 9(2):5.
The article explains future trajectories of social-ecological systems (SESs) are determined by an interplay of their resilience, adaptability, and the transformability.

Yu, D. J., Shin, H. C., Pérez, I., Anderies, J. M., & Janssen, M. A. (2016). Learning for resilience-based management: Generating hypotheses from a behavioral study. Global Environmental Change 37:69–78.
The article emphasizes that learning enhances adaptive capacity for resilience. Authors examined how learning is encouraged for resilience by analysing empirical data from a behavioral experiment on SES.

Complex network analysis of water distribution systems in their dual representation using isolation valve information

Jonatan Zischg[1], Julian D. Reyes-Silva[2], Christopher Klinkhamer[3], Elisabeth Krueger[4], Peter Krebs[5], P. Suresh C. Rao[6], and Robert Sitzenfrei[7]

[1]Unit of Environmental Engineering, Institute for Infrastructure, University of Innsbruck, Technikerstrasse 13, 6020 Innsbruck, Austria; e-mail: jonatan.zischg@uibk.ac.at

[2]Institute for Urban Water Management, Department of Hydrosciences, TU Dresden, Bergstraße 66, 01069 Dresden, Germany; e-mail: julian_david.reyes_silva@tu-dresden.de

[3]Lyles School of Civil Engineering & Agronomy Department, Purdue University, 550 Stadium Mall Drive, West Lafayette, IN 47907, United States & KERAMIDA Inc., 401 N College Ave, Indianapolis, IN, United States; e-mail: cklinkha@purdue.edu

[4]Lyles School of Civil Engineering, Purdue University, United States & Helmholtz Center for Environmental Research – UFZ, Permoserstr. 15, 04318 Leipzig, Germany; e-mail: elisabeth.krueger@ufz.de

[5]Institute for Urban Water Management, Department of Hydrosciences, TU Dresden, Bergstraße 66, 01069 Dresden, Germany; e-mail: peter.krebs@tu-dresden.de

[6]Lyles School of Civil Engineering & Agronomy Department, Purdue University, 550 Stadium Mall Drive, West Lafayette, IN 47907, United States; e-mail: sureshrao@purdue.edu

[7]Unit of Environmental Engineering, Institute for Infrastructure, University of Innsbruck, Technikerstrasse 13, 6020 Innsbruck, Austria; e-mail: robert.sitzenfrei@uibk.ac.at

ABSTRACT

In the event of a disruption of operation, parts of the water distribution networks (WDNs) must be temporarily disconnected from the supply source by the closure of isolation valves to allow pipe repair. For cost reasons, however, the number of such valves is usually limited, requiring strategies for their optimal placement. In this paper we combine graph theoretical approaches with reliability analysis by using the WDN topology and isolation valve information. A novel methodology for the assessment of valve placement strategies is developed, in which we investigate WDNs in their information space by means of complex network analysis. Unlike traditional approaches, we use the dual representation of the network, where WDN segments (i.e., a set of pipes) are considered as nodes and isolation valves as edges. With the developed algorithm, the WDNs are analyzed on the basis of the dual graph, providing new insights beyond a conventional graph (primal mapping) analysis. The method is applied to two real-world systems, to identify different patterns with respect to the probability density functions of (dual) node properties: node-degree *P(k)*, aggregated pipe length *P(l)*, and demand *P(d)*. Additional complex network metrics, such as the characteristic path length, degree correlation, and modularity are investigated and discussed. The observed topological differences also reflect the availability of financial resources and the different types of water supply of the systems.

The implications of the results allow for a novel assessment of WDN reliability and robustness in the event of disruption and network isolation.

Keywords: Disruption, dual graph, graph theory, network isolation, water supply.

INTRODUCTION

Water supply has to fulfil the users' needs for reliable water quality and sufficient quantity. In the event of an intended or unexpected disruption of operations, parts of the water distribution networks (WDNs) must be temporarily disconnected from the supply source to allow maintenance and pipe repairs. This is done by closing spatially distributed shut-off devices, such as isolation valves. In the literature, the isolated part of the WDN is often referred to as WDN segment (Jun 2005), WDN section or isolation zone. In the following we use the term WDN segment.

Isolation valves in WDNs are used to stop the flow (e.g., for maintenance or safety reasons), but can also be used to provide a flow logic, e.g. flow paths can be selected for the control of pressure zone boundaries or district metered areas (Walski *et al*. 2001). Isolation valves are the most commonly used valves in WDNs, which are infrequently operated in an on-off mode, and often ranked in the lower order of importance in WDN modeling. To emphasize the importance of isolation valves, take the example of a necessary isolation in a highly meshed system, considered as reliable and robust. However, the system can be highly vulnerable even to small disruptions that affect large WDN parts, if isolation valves are lacking, inappropriately placed, or non-functional. In the worst case the entire network must be isolated by disconnecting the source node(s). The basic concept of WDN isolation is illustrated in Figure 1, where inflow and outflow at the WDN segment are prevented by valve closure. For cost and maintenance reasons, however, the number of such valves is limited, so that usually not every pipe can be isolated individually. As such, a group of pipes (i.e., the WDN segments) must be isolated at once. Given this constraint, it is sought to minimize the negative effects on the supply by placing the available number of valves in the most useful locations.

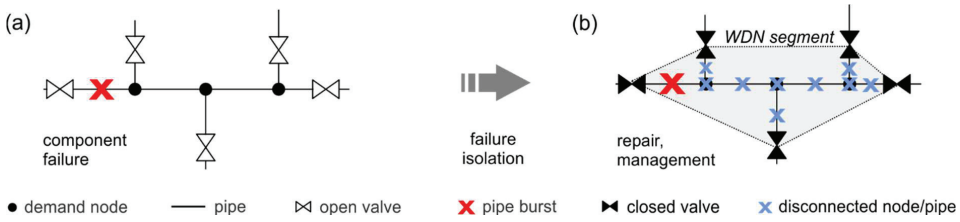

Figure 1: Component failure and the isolation process to allow for repair. (a) Open valves in normal operation condition when a failure is detected; and (b) closed valves to isolate the failure and the entire WDN segment.

In the last decades the topics of robustness, redundancy, vulnerability, and resilient design when experiencing planned or unplanned disruption were investigated in detail and extensively discussed in the literature on WDN modeling (see e.g., Farmani *et al*. 2005; Prasad

& Park 2004; Diao *et al*. 2016). Conversely, the optimal placement of isolation valves in combination with the network topology has received relatively little attention. More than two decades ago, however, Walski (1993) emphasized the importance of isolation valves when investigating WDN reliability. Since then several studies on segment identification, optimal valve placement, and valve shutdowns have been conducted (see e.g., Alvisi *et al*. 2011; Giustolisi & Savic 2010; Giustolisi *et al*. 2014; Choi *et al*. 2018). More recent research has considered WDNs as mathematical graphs and used metrics from complex network analysis to describe network topological reliability and robustness (see e.g., Agathokleous *et al*. 2017; Hwang & Lansey 2017; Ulusoy *et al*. 2018; Yazdani & Jeffrey 2012; Zeng *et al*. 2017; Zischg *et al*. 2018).

In this paper, we combine graph theoretical approaches with reliability analysis by using the WDN topology and isolation valve information. A novel methodology for the assessment of valve placement strategies in WDNs is developed, in which the network is represented in its "information space" (dual mapping) and described as a mathematical graph, where the nodes are the WDN segments and the links are the isolation valves (Jun 2005). To create the dual graph, we use a breadth-first search algorithm with the primal network topology and isolation valve positions as input information. In addition, the dual graph is assessed with various metrics from complex network theory. These include, for example, dual node-degree distribution (Zischg *et al*. 2019), modularity (Newman 2006), and assortativity (Newman 2002). The results obtained can be re-mapped from the "information space" to the georeferenced map to better identify, interpret and visualize the results. The methodology is tested and then applied to medium-sized real-world WDNs with more than 10,000 (primal) network nodes. Structural differences between the investigated WDNs are reflected in the node-degree distribution, the size distribution of WDN segments in terms of aggregated pipe length and demand, the node-degree correlation, and the community structure within the network. These results provide new insights into the complexity of WDNs in the event of pipe disruptions, with implications for reliable and robust network design.

MATERIALS AND METHODS

In this chapter we present the dual mapping approach, the investigated topological complex network metrics, and give a short description of the case studies used for model application.

Dual Mapping. In contrast to the conventional WDN representation (primal graph), dual graphs consider a set of pipes as (dual) vertices, and their intersection as (dual) edges. In the first process of the dual graph creation, parts of the WDN are aggregated based on functional equalities/similarities. In Zischg *et al*. (2017) and Krueger *et al*. (2017) dual graphs were created by using pipe diameter for the aggregation criterion to resemble the functional topology of the network under regular operation conditions.

This work focuses on abnormal operation conditions and therefore we use the WDN segments, i.e., parts of the network that can be isolated by surrounding valves, as the vertices and the isolation valves as the edges of the graph. In doing so, WDN components with the same functionality in the case of WDN isolation are considered.

Figure 2 shows the concept of the dual graph creation for an illustrative example. In Figure 2a it can be seen that based on a given distribution of 8 isolation valves (V_1 - V_8), the primal mapped WDN can be divided into 6 WDN segments (S1 - S6), consisting of aggregated pipes (including operational valves/pumps) and junctions (including source nodes). When considering all those WDN segments as "super-nodes" (Figure 2b), the connections among them are the isolation valves. The resulting dual graph is shown in Figure 2c. For this example, the maximum (dual) node-degree is at node S3 (k_{max} = 5), i.e., in the event of a pipe break in S3, five isolation valves must be closed to temporarily isolate the segment from the water supply and to enable repair. In general, the resulting dual graph is an undirected multigraph where two nodes are connected by more than one edge. Such a multi-edge is present between S2 and S3 in Figure 2c. An interpretation of those attributes is given in the results and discussion section.

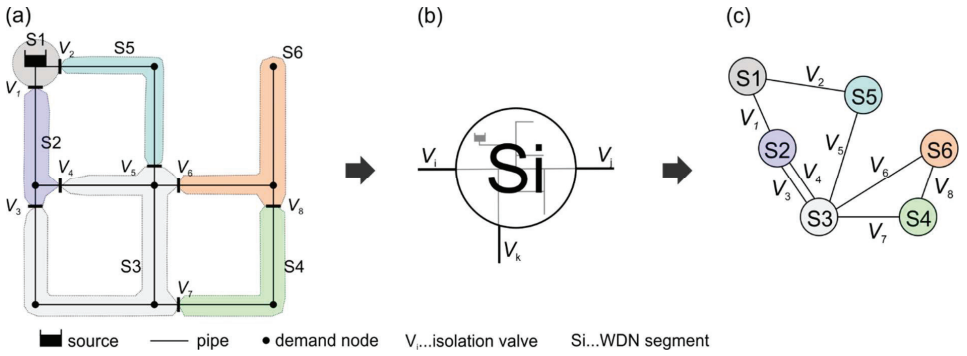

Figure 2: From primal to dual graph: (a) segments of a WDN in primal mapping; (b) network aggregation (pipe length, water demand) to a "super-node"; and (c) construction of a dual graph, on which statistical and graph theoretical analyses are performed.

Here, the starting point for the dual graph creation is a hydraulic EPANET model as an input file without including household connections (Rossman 2000). Since isolation valve data are often available as point feature sets (e.g. as GIS shp-file with point features), the aim is to map this information to the junctions. If in the initial model there is no junction at the position of the isolation valve, the nearest pipe (within a tolerance of 1cm) is split and a new junction is created to represent the isolation valve. Otherwise it is rejected (e.g. due to different level of detail). The information regarding whether a junction is an isolation valve or not is then written to the [TAGS] section of the input file. The algorithm for creating the dual graph is described in terms of a pseudocode in Table 1. The primal edges are all pipes, control valves (e.g. flow control or pressure reducing valves) and pumps, whereas the primal vertices are all junctions, reservoirs and tanks. The process contains the breadth-first search algorithm (Kozen 1992) for identifying the WDN segments, that subsequently form the dual vertices/nodes. This approach results in a reduction of the network's level of detail, because WDN segments generally consist of more than a single pipe.

Table 1: Proposed pseudocode in 4 steps for the dual graph creation.

Step 1: Put all primal edges into the unused edge set E_N and let the used edge set be $E_U = \emptyset$.

Step 2: If $E_N \neq \emptyset$, take a primal edge e_P from E_N; create a candidate dual edge $e_{CD} = e_P$; otherwise go to Step 4.

Step 3: Grow e_{CD} by recursively performing the following until e_{CD} cannot be extended further by using the breadth-first search algorithm (Kozen 1992):

i. inspect the two end points of e_{CD}. For each of the end points, check if neighbour edges $e_i \in E_N$ exist, where $i = 1, 2, ...n_{eCD}$ is the index of all such edges.

ii. Aggregate e_{CD} and e_i if their connecting point is no isolation valve.

iii. If e_{CD} and e_i can be aggregated, then $e_{CD} = e_{CD} \cup \{e_i\}$, $E_N \setminus e_i$, $E_U = E_U \cup \{e_i\}$.

iv. If neither end point of e_{CD} can continue to grow, then $v_D = e_{CD}$ and assign it a unique dual vertex ID. Return to Step 2.

Step 4: Construct the dual graph. Let the dual vertices in the dual graph be all the dual vertices v_D. Construct a dual edge e_{Dij} between two dual vertices v_{Di} (represented as a set of primal edges) and v_{Dj} (represented as another set of primal edges), if they contain primal edges that intersect each other (i.e. share the identical primal vertex). Check this for all combinations of dual vertex pairs.

Network topology. Networks can be analyzed with a variety of metrics to identify, among others, complex patterns, scaling laws and hierarchical structures. Here we briefly describe the most commonly used metrics, which we also analyze by using the Matlab toolbox provided by Narula *et al.* (2017) in the subsequent sections. For more detailed information, we refer the reader to the respective references. The *degree k* of a node describes the number of its connections. Among significant properties of complex networks is the *node-degree distribution P(k)*, which provides information about the occurrence probability of nodes with a certain number of connections. If this probability follows, for example, a [Pareto] power law function $P(k) \sim k^{-\gamma}$, the network is considered scale-free. Such characteristics can be observed, for example, in most natural but also engineered networks (Yang *et al*. 2017). Other important statistical moments of the network connectivity are the *mean (node) degree* $\langle k \rangle$; the *dispersion index D* (describing the variance around the mean) and the *mode* of the distribution (most frequent *k*). The *characteristic path length* $\langle l \rangle$ is calculated by the average shortest path distance between all couples of nodes, whereas the *network diameter* is defined as the longest of those shortest paths (Barthélemy 2011).

Networks with identical node-degree distributions can be significantly different in their node-degree correlation. For example, positive degree correlations are observed in the dating networks of celebrities (assortative mixing). Conversely, hubs (high degree nodes) in protein networks avoid other hubs and preferably connect to nodes that are not similar to them (disassortative mixing) (Barabási 2018). As such, *assortativity* describes the tendency of nodes to connect to nodes with similar attributes. Although the attributes for comparison can be different, in many cases the correlation between node-degrees is used. Here we use the degree correlation coefficient *r* to describe the degree correlations between WDN segments, where $r >$

0 describes assortative mixing, $r = 0$ neutral mixing, and $r < 0$ disassortative mixing. In general r ranges from $[-1 \leq r \leq +1]$ (Newman 2002).

Modularity is a metric to quantify "community structure", i.e. the degree to which the network can be sub-divided into groups by maximizing the number of edges within groups (intracommunity edges), while minimizing the (intercommunity) edges between groups. The factor Q $[-1 \leq Q \leq +1]$ quantifies the quality of graph sub-division (Newman 2006). A value of 0 indicates that the number of intracommunity edges is no more than random, while $Q = 1$ indicates the absence of intercommunity edges. Usually, $Q \geq 0.3$ indicates the presence of significant communities within the network (Clauset *et al*. 2004). To calculate Q we use the procedure described in Rubinov and Sporns (2010) to identify groups of WDN segments that can easily be isolated through a small number of edge disconnections. For the calculation of Q and r, the multigraph is converted to a simple graph in which only one edge can exist between a vertex pair.

Case studies. For application of the methodology we use high-resolution WDN data for an Asian and a European city. Both networks have more than 10,000 primal nodes and similar total pipe length of approximately 300 km without considering house connections. While the former case study is situated in a developing country with low financial resources and intermittent piped water supply due to limited water resources caused by strong population growth, the latter is located in an industrial nation with continuous piped water supply. Details about the case studies, their primal mapped networks and remapped dual characteristics cannot be shown for security reasons. Additionally, for comparison purpose a third case study located in Canada (referred to as American WDN) of approximately the same size as the other WDNs is taken from the literature (Jun 2005).

RESULTS AND DISCUSSION

In this section we present the results of dual graph creation and the subsequent complex network analyses for the two case studies. Following the comparison of the network topology, we discuss the potential of the methodology and future direction of this work.

Dual Mapping. After creating the dual graph, which includes an algorithm for WDN segment identification, various attributes obtained from the dual network can be remapped to the primal map (their geospatial embedding) for a better visualization of the results. This remapping of dual characteristics to the primal map can be done for every dual node ($\triangleq$ WDN segment) attribute, such as the node-degree or the node ID. In Figure 3, an example of the latter case is shown for two excerpts of the investigated WDNs. The black dots represent the locations of the isolation valves, and the color-coded lines show the pipes belonging to a specific dual node ID, a unique WDN segment.

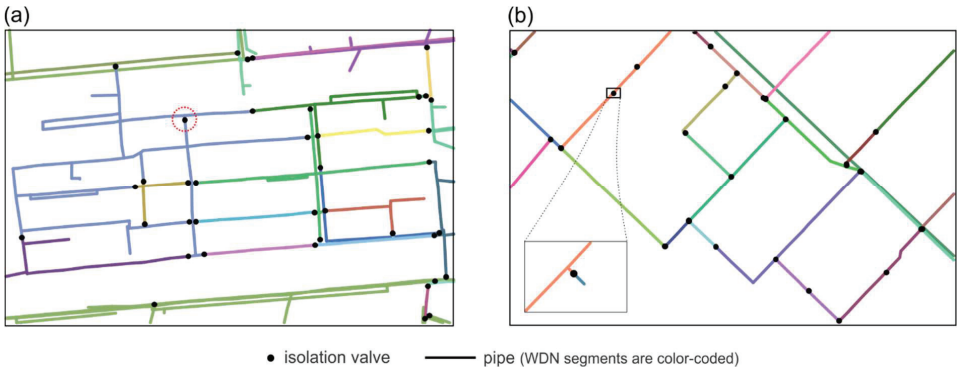

Figure 3: Excerpt from the WDNs showing the isolation valves and the dual nodes (≙ WDN segments) in primal mapping: (a) Asian case study and (b) European case study. The red dotted circle indicates the presence of one "ineffective" valve.

In Figure 4 the dual graphs of the entire WDNs are illustrated, where the nodes are the WDN segments and the links are the isolation valves. The size of the nodes is proportional to their degree (k ranging from 1 to 37) and thus the number of connections between WDN segments. The network shown in Figure 4a is more than 10 times smaller (number of nodes) than the network in Figure 4b, although in primal representation they have about the same size in terms of total pipe length. The reason for this discrepancy is the higher valve density of 20.4 valves per km for the European case study, compared to 1.86 valves per km for the Asian case study. One explanation for this large difference may be the intermittent water supply for the latter case, where the system is used only on chosen days and is disconnected from the water sources at all other times, making a pipe repair possible during intermittence.

Network topology. Table 2 lists the basic characteristics of both dual networks and compares them to another case study known from literature (see Jun 2005). The mean pipe length per WDN segment is 800 m, 53 m, and 230 m and the number of valves is 577, 5,891 and 1,720 for the Asian, European and American case study, respectively. One would expect that the number of isolation valves is identical to the number of dual links, however this holds true only if all valves are "regular" in the primal network (see Figure 5a). This is not the case for both investigated case studies as seen in Table 2. More details are found in the subsequent paragraphs.

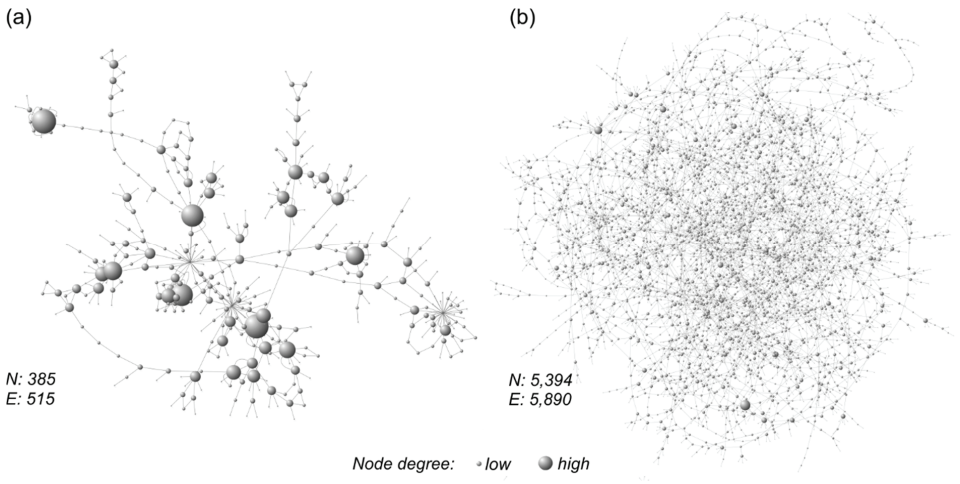

Figure 4: Topology of the dual graphs: (a) Asian case study and (b) European case study.

The statistics also include the number of ineffective valves, i.e. valves whose closure has no isolation effect due to flow redundancy (see Figure 5d and Figure 3a). With the methodology presented, such a valve can be easily identified by analysing a dual vertex (represented as a set of primal edges) that contains an intersection of primal edges (i.e. share the identical primal vertex) and, at the same time, is an isolation valve. The ineffective valves account for approximately 10% and 0.05% for the Asian and European WDN, respectively. Possible reasons for that might be the uncontrolled creation of cycles without considering appropriate isolation valves or errors in the data. The existence of multi-edges indicates that two neighbouring WDN segments have more than one isolation valve separating each other (see, e.g. S2 and S3 in Figure 2).

Table 2: Calculated attributes of the dual networks.

	Asian WDN	European WDN	American WDN[3]
Number (dual) nodes	385	5,394	1,166
Number (dual) links	515	5,890	1,580
Number isolation valves	577	5,891	1,720
Number of "ineffective" valves[4]	58	3	-
Percentage of multi-edges (%)	8.3	0.05	-
Percentage of valves with $k = 2$ (%)[4]	97.9	99.3	-
Valve density (valves/km)	1.86	20.4	6.24
Mean demand per segment (l/s)	1.05 (≈ 0.26%)[1]	0.045 (≈0.02%)[2]	-
Maximum demand per segment (l/s)	43.2 (≈ 11%)[1]	1.914 (≈ 0.8%)[2]	0.9%
Mean pipe length per segment (m)	800 (≈ 0.26%)	53 (≈ 0.02%)	230 (≈ 0.08%)
Maximum pipe length per segment (m)	28,400 (≈ 9%)	2,741 (≈ 1%)	-

[1]based on the peak (design) demand; [2]based on the yearly average demand; [3]for comparison purpose (Jun 2005); [4]according to Figure 5.

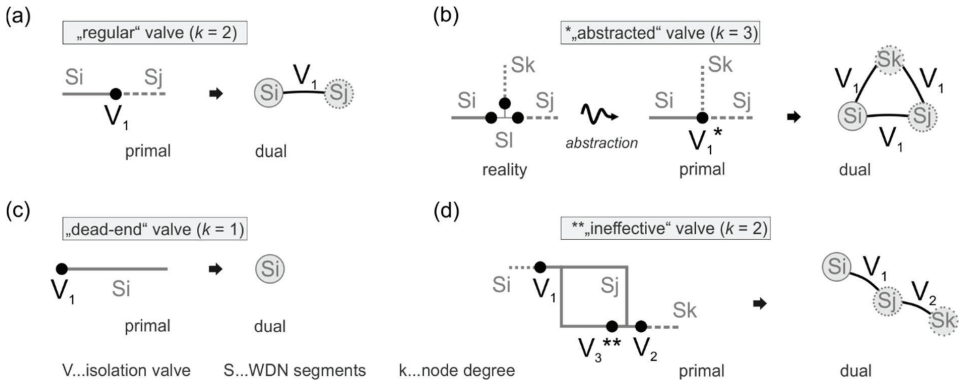

Figure 5: Possible locations of isolation valves in primal and dual representation separated by the black arrows: (a) valve with $k = 2$ dividing two WDN segments defined as the "regular" case; (b) valve located at a T-connection ($k = 3$) which represents an abstraction of 3 valves of $k = 2$; (c) isolation valve located at a "dead-end" node ($k = 1$) and thus not dividing two segments; and (d) existence of an ineffective valve ($k = 2$) located within a cycle, whose closure leads has no effect on the segment isolation.

As already mentioned, isolation valves are considered as nodes in primal and edges in the dual graph representation. However, several combinations of valve configurations exist, which are shown in Figure 5. The most frequent valve type, and thus referred to as "regular" valve is illustrated in Figure 5a. The valve (black dot) has a degree $k = 2$ and separates exactly two WDN segments. However, valve V_3** in Figure 5d also has $k = 2$, but it does not separate two segments. Therefore, it indicates an "ineffective" valve. These two types account for approximately 98 - 99% of the investigated WDN (see Table 2). In some cases, a group of valves (e.g. at a T-connection) is abstracted to one single valve V_1* in the primal network (e.g. data error), resulting in a degree of 3 (see Figure 5b). In this case, the number of "abstracted" valves is not identical to the number of dual edges. This is also the case for a "dead-end" valve, as presented in Figure 5c.

The results of the topological analysis of the two case studies are presented in Figure 6, Table 3 and Table 4. When comparing the probability density functions (PDFs) of WDN segment length *P(l)* (Figure 6a), demand *P(d)* (Figure 6b), and node-degree *P(k)* (Figure 6c) of both dual networks, we observe heavier-tailed distributions for the Asian case study with high dispersions around the mean. We tested the truncated power-law hypothesis $P(x) \sim x^{-\gamma}$, $x_{min} \leq x \leq x_{max}$, for all PDFs according to the method suggested by Clauset *et al.* (2009). We found that the power-law hypothesis is a plausible approximation for the *P(d)* and *P(k)* for the Asian WDN, and for the *P(l)* of the European WDN (see Table 3). Although the hypothesis is rejected for the remaining distributions, significant differences in the scaling factors γ (slopes of the tail) are observed by visual inspection. While for the Asian WDN γ is always smaller than 2.75, for the European WDN the slopes of the distribution are greater than 3.30. One can argue that with the frontal truncation of the power function, data points are neglected, however for the reliability and robustness analysis the tails of the distributions are of particular interest, i.e. the WDN segments characterized with high length, demand and degree ("network hubs"). While the size of the hubs is an indicator for failure probability, directly

affected demand, and effort for segment isolation by valve closure, we argue that the slopes of the PDFs are a direct indicator for the global robustness of the WDN. By introducing new isolation valves, hubs (dual nodes) can be split and the negative effects of the isolation reduced.

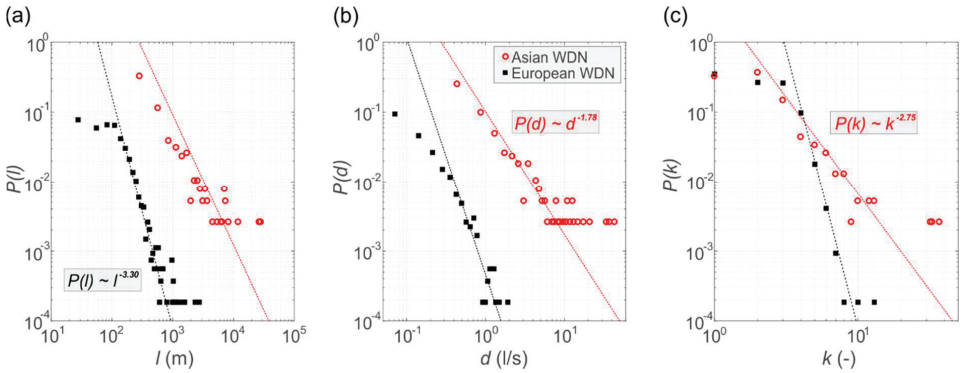

Figure 6: PDF comparison of the two dual WDNs: (a) pipe length distribution per segment *P(l)*; (b) demand distribution per segment *P(d)*; and (c) (dual) node-degree distribution of the segments *P(k)*.

Table 3 also shows the results of the power-law hypothesis test, according to the methodology proposed by Clauset *et al*. (2009). It includes the lower bound to the power-law behavior x_{min}, the power law exponent γ, and the goodness-of-fit represented by the *p-value*. When $p \geq 0.1$, the power law hypothesis is a plausible fit to the data in the observed range [$x_{min} \leq x \leq x_{max}$]. At this point it has to be mentioned that power-law fitting is still in a state of ongoing research and a method to strictly distinguish between power-law and power-law-like distributions has not yet been agreed upon (Corral & González 2018).

Table 3: Analysis of the power-law hypothesis testing (Clauset *et al*. 2009).

	Asian WDN			European WDN		
Distribution of:	x_{min}	γ	*p-value*[1]	x_{min}	γ	*p-value*[1]
Segment length *P(l)*	286 m	1.87	0.010	164 m	3.30	**0.995**
Segment demand *P(d)*	0.413 l/s	1.78	**0.128**	0.321 l/s	3.37	0.040
Segment degree *P(k)*	2	2.75	**0.431**	4	7.86	0.000

[1]Goodness-of-fit: For p ≥ 0.1 the power law hypothesis $P(x) \sim x^{-\gamma}$ is accepted within the range [$x_{min} \leq x$] and shown in bold.

Additional statistical moments of the node-degree distribution, such as the average degree $\langle k \rangle$, maximum degree k_{max}, mode, and dispersion index are listed in Table 4. For example, in case of a pipe failure in the Asian WDN, on average, $\langle k \rangle = 2.45$ valves have to be closed for a successful isolation, while for the European case 2.18.

Moreover, Table 4 shows that both networks reveal a disassortative mixing of the nodes (r = -0.18 and -0.37), meaning that nodes of similar degree tend to "avoid" a connection with each other (i.e. are more likely connected to nodes with other degrees). This topological attribute can be beneficial in case of valve failure (no dual edge disconnection possible), if the

neighboring node is also affected and its adjacent valves must be identified and closed in addition. Similar positive effects on the isolation of larger WDN parts (a group of dual nodes) are expected for a modular structure ($Q \geq 0.3$) of the network. Both networks reveal a such a modular structure with $Q = 0.383$ and $Q = 0.420$ for the Asian and European WDN, respectively. In the case of a larger disruption where several WDN sections are affected, such "modules" can be isolated by disconnecting only a few edges. Those edges, however, represent vulnerable components which have to be maintained frequently. The characteristic path length $<l>$ and the network diameter indicate the efficiency of information or mass transport on a network. In the case of a potential water contamination a fast dispersion is undesirable. For the European WDN, for example, the (contaminated) water particle has to pass on average 40 WDN segments to reach all the other segments. This gives a large number of opportunities for isolation, compared to the Asian WDN with $<l> = 8.86$.

Table 4: Topologies of the dual networks.

	Asian WDN	European WDN
Average (dual) node-degree $<k>$	2.45	2.18
Maximum degree k_{max}	37	13
Node-degree dispersion index D	4.25	0.58
Mode of $P(k)$	2	1
Assortativity r	-0.18	-0.37
Modularity Q[1]	0.383	0.420
Characteristic path length $<l>$	8.86	40.88
Network diameter	22	112

[1]100 iteration steps (Rubinov and Sporns 2010).

The results obtained from the dual network and the subsequent analysis provide new insights regarding WDN reliability and robustness. Moreover, the dual graph builds the basis for future WDN failure analysis and for improving system robustness through additional placement of isolation valves.

Future work should address failure cascades of dual nodes (pipe failures), dual edges (valve failures), and possible combinations thereof. Furthermore, a performance comparison between the type of failure analysis presented here and hydraulic simulations is needed for identifying synergies for a new level of WDN robustness analysis. It is expected that complex network analysis can increase the efficiency of hydraulic failure analysis (e.g. reduction of computational costs). For example, Figure 7a illustrates network failures in dual graph representation and Figure 7b presents four levels of consequences of a single pipe/valve failure on the WDN performance. With complex network analysis the failure analysis can be performed with regard to the level of unintended isolation, whereas hydraulic simulations are necessary for the analysis of pressure changes and potential supply deficit in the remaining network.

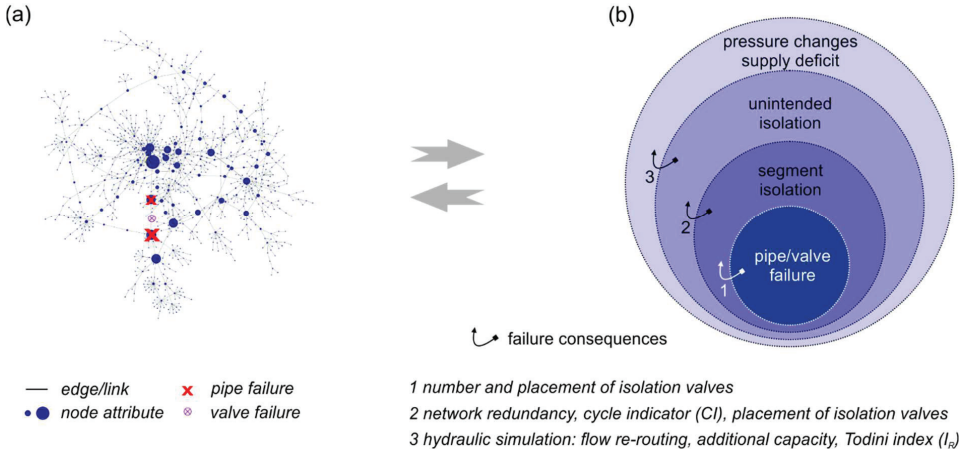

Figure 7: Component failure in the dual graph representation and the effect on WDN function: (a) various failure mechanisms (e.g. pipe break and/or valve malfunctioning) and (b) the different levels of failure consequences to the water supply. Adjusted from Jun (2005).

SUMMARY AND CONCLUSIONS

The high resolution data sets of two WDNs were investigated in their dual representation based on the location of isolation valves. The dual graph consists of dual nodes, representing the WDN segments (or super-nodes), and dual edges, representing the isolation valves. The analysis of the functional topology was performed using metrics known from complex network analysis. The results showed that the probability density functions of the dual nodes describing WDN segment length, demand and degree, are heavy tailed and in half of the cases can be approximated with truncated power law distributions $P(x) \sim x^{-\gamma}$, $x_{min} \leq x \leq x_{max}$.

- Structural differences of the networks are seen in the power-law exponent, γ, ranging from 1.78 to 3.30 for the accepted data fits. A larger exponent, γ, is expected to be more beneficial for minimizing failure resulting from isolation. This can be achieved by the splitting of network hubs.
- The differences in valve densities and resulting dual network size of both case studies can possibly be attributed to lower financial investment and intermittent water supply of the Asian case study, where WDN failures can be repaired during intermittence.
- In the Asian WDN, 10% of the isolation valves are identified as ineffective, i.e. their closure has no effect on segment isolation, since alternative flow routing is possible. Activation of such valves would require the installation of additional valves, thus reducing WDN segment size.
- The characteristic path length $<l>$ of the European WDN is almost 5 times higher than for the Asian WDN, which is considered to be beneficial when preventing undesired mass flow, e.g. the isolation of contaminated water.

- Both WDNs reveal a disassortative mixing behavior of the node-degrees, which means that nodes of similar degree generally avoid a connection with each other. This can have a positive effect when an isolation valve fails requiring both segments to be isolated.
- Both WDNs reveal significant modular sub-structures ($Q \geq 0.3$) which can be considered advantageous when isolating modules of the WDN (groups of dual nodes) by disconnecting only a few dual edges.

Future investigations should focus on a deeper assessment of WDN disruptions, considering unintended isolation, failure cascades of pipes, valves and combinations thereof. Additionally, the results from complex network analysis should be compared to hydraulic failure analysis, to identify synergies for providing a new method of WDN robustness assessment. For comparison purposes, future studies should include the investigation of many other WDNs with different climatic, geographical and topological characteristics.

ACKNOWLEDGEMENTS

This work was initiated at the Summer Synthesis Workshop on Network Functional Dynamics, held at TU Dresden, Germany, during summer 2017. The research was partly funded by the Austrian Research Promotion Agency (FFG) within the research project ORONET (project number: 858557) and the Austrian Science Fund (FWF): P 31104-N29. The presented work was also partly conducted under the framework of the International Research Training Group "Resilient Complex Water Networks". It is supported by TU Dresden's Institutional Strategy. TU Dresden's Institutional Strategy is funded by the Excellence Initiative of the German Federal and State Governments. The authors would also like to thank the German Academic Exchange Service (DAAD), the Federal Ministry of Education and Research (BMBF), and the TU Dresden's Institutional Strategy by the Excellence Initiative of the German Federal and State Governments for their funding in the framework of the group2group exchange for academic talents (great!ipid4all). This research was also funded, in part, by the US NSF RIPS Type 2 Collaborative Research Project (Award# 1441188) "Resilience Simulation of Water, Power, and Road Networks". The authors would also like to thank HydroPraxis for the provision of PCSWMM in the Europe University Grant Program.

REFERENCES

Agathokleous A., Christodoulou C. and Christodoulou S. E. (2017). Topological Robustness and Vulnerability Assessment of Water Distribution Networks. Water Resources Management 31(12), 4007-4021.

Alvisi S., Creaco E. and Franchini M. (2011). Segment identification in water distribution systems. Urban Water Journal 8(4), 203-217.

Barabási A.-L. (2018). Network Science. http://networksciencebook.com/ (accessed 18.12.2018).

Barthélemy M. (2011). Spatial networks. Physics Reports 499(1), 1-101.

Choi H. Y., Jung D., Jun H. and Kim H. J. (2018). Improving Water Distribution Systems Robustness through Optimal Valve Installation. Water 10(9).

Clauset A., Newman M. E. J. and Moore C. (2004). Finding community structure in very large networks. Physical Review E 70(6), 066111.

Clauset A., Shalizi C. and Newman M. (2009). Power-Law Distributions in Empirical Data. SIAM Review 51(4), 661-703.

Corral Á. and González Á. (2018). Power-law distributions in geoscience revisited. In: ArXiv e-prints.

Diao K., Sweetapple C., Farmani R., Fu G., Ward S. and Butler D. (2016). Global resilience analysis of water distribution systems. Water research 106, 383-393.

Farmani R., Walters Godfrey A. and Savic Dragan A. (2005). Trade-off between Total Cost and Reliability for Anytown Water Distribution Network. Journal of Water Resources Planning and Management 131(3), 161-171.

Giustolisi O., Berardi L. and Laucelli D. (2014). Optimal Water Distribution Network Design Accounting for Valve Shutdowns. Journal of Water Resources Planning and Management 140(3), 277-287.

Giustolisi O. and Savic D. (2010). Identification of segments and optimal isolation valve system design in water distribution networks. Urban Water Journal 7(1), 1-15.

Hwang H. and Lansey K. (2017). Water Distribution System Classification Using System Characteristics and Graph-Theory Metrics. Journal of Water Resources Planning and Management 143(12), 04017071.

Jun H. (2005). Strategic valve locations in a water distribution system. PhD, Department of Civil Engineering, Virginia Polytechnic Institute and State University, Blacksburg, Virginia.

Krueger E., Klinkhamer C., Urich C., Zhan X. and Rao P. S. C. (2017). Generic patterns in the evolution of urban water networks: Evidence from a large Asian city. Physical Review E 95(3), 032312.

Kozen D.C. (1992) Depth-First and Breadth-First Search. In: The Design and Analysis of Algorithms. Texts and Monographs in Computer Science. Springer, New York, NY.

Narula V., Zippo A. G., Muscoloni A., Biella G. E. M. and Cannistraci C. V. (2017). Can local-community-paradigm and epitopological learning enhance our understanding of how local brain connectivity is able to process, learn and memorize chronic pain? Applied Network Science 2(1), 28.

Newman M. E. J. (2002). Assortative Mixing in Networks. Physical review letters 89(20), 208701.

Newman M. E. J. (2006). Finding community structure in networks using the eigenvectors of matrices. Physical Review E 74(3), 036104.

Prasad T. D. and Park N.-S. (2004). Multiobjective Genetic Algorithms for Design of Water Distribution Networks. Journal of Water Resources Planning and Management 130(1), 73-82.

Rossman L. A. (2000). The EPANET Programmer's Toolkit for Analysis of Water Distribution Systems. In: WRPMD'99, pp. 1-10.

Rubinov M. and Sporns O. (2010). Complex network measures of brain connectivity: Uses and interpretations. NeuroImage 52(3), 1059-1069.

Ulusoy A.-J., Stoianov I. and Chazerain A. (2018). Hydraulically informed graph theoretic measure of link criticality for the resilience analysis of water distribution networks. Applied Network Science 3(1), 31.

Walski T. M. (1993). Water distribution valve topology for reliability analysis. Reliability Engineering & System Safety 42(1), 21-27.

Walski, Thomas M.; Chase, Donald V.; and Savic, Dragan A. (2001). Water Distribution Modeling. Haestad Methods Inc., Heastad Press, Waterbury, USA.

Yang S., Paik K., McGrath G. S., Urich C., Krueger E., Kumar P. and Rao P. S. C. (2017). Functional Topology of Evolving Urban Drainage Networks. Water Resources Research 53(11), 8966-8979.

Yazdani A. and Jeffrey P. (2012). Applying Network Theory to Quantify the Redundancy and Structural Robustness of Water Distribution Systems. Journal of Water Resources Planning and Management 138(2), 153-161.

Zeng F., Li X. and Li K. (2017). Modeling complexity in engineered infrastructure system: Water distribution network as an example. Chaos: An Interdisciplinary Journal of Nonlinear Science 27(2), 023105.

Zischg J., Klinkhamer C., Zhan X., Krueger E., Ukkusuri S., Rao P. S. C., Rauch W. and Sitzenfrei R. (2017). Evolution of Complex Network Topologies in Urban Water Infrastructure. In: World Environmental and Water Resources Congress 2017, pp. 648-659.

Zischg J., Rauch W. and Sitzenfrei R. (2018). Morphogenesis of Urban Water Distribution Networks: A Spatiotemporal Planning Approach for Cost-Efficient and Reliable Supply. Entropy 20(9).

Zischg J., Klinkhamer C., Zhan X., Rao, P.S.C, and Sitzenfrei R. (2019). A Century of Topological Co-Evolution of Complex Infrastructure Networks in an Alpine City. Complexity, Article ID 2096749, 16 pages.

VITA

VITA

Chris Klinkhamer received a B.S. in Natural Resources and Environmental Science and an M.S. in Toxicology through the Ecological Science and Engineering Interdisciplinary Graduate Program at Purdue University. He has published in Chemosphere, Physical Review, Environmental Toxicology and Chemistry, and Complexity and has submitted manuscripts currently under review to multiple journals. He has applied concepts derived from a diverse interdisciplinary background to topics ranging from the Deepwater Horizon Oil Spill to the resilience of urban infrastructure.